Fall 1-1-2015

Topographical Differences in Stress Vulnerability in Experimental Parkinson's Disease

Jessica M. Posimo

TOPOGRAPHICAL DIFFERENCES IN STRESS VULNERABILITY IN EXPERIMENTAL PARKINSON'S DISEASE

A Dissertation

Submitted to the Graduate School of Pharmaceutical Sciences

Mylan School of Pharmacy

Duquesne University

In partial fulfillment of the requirements for

the degree of Doctor of Philosophy

By

Jessica M. Posimo

December 2015

TOPOGRAPHICAL DIFFERENCES IN STRESS VULNERABILITY

IN EXPERIMENTAL PARKINSON'S DISEASE

By

Jessica M. Posimo

Approved October 12th 2015

Rehana K. Leak, Ph.D. Assistant Professor of Pharmacology Graduate School of Pharmaceutical Sciences Duquesne University, Pittsburgh, PA	Jane E. Cavanaugh, Ph.D. Associate Professor of Pharmacology Graduate School of Pharmaceutical Sciences Duquesne University, Pittsburgh, PA
David A. Johnson, Ph.D. Division Head of Pharmaceutical Sciences and Associate Professor of Pharmacology and Toxicology Graduate School of Pharmaceutical Sciences Duquesne University, Pittsburgh, PA	Lauren A. O'Donnell, Ph.D. Assistant Professor of Pharmacology Graduate School of Pharmaceutical Sciences Duquesne University, Pittsburgh, PA
J. Patrick Card, Ph.D. Professor of Neuroscience Center for Neuroscience University of Pittsburgh, Pittsburgh, PA	James K. Drennen, III, Ph.D. Associate Dean and Associate Professor of Pharmaceutics Graduate School of Pharmaceutical Sciences Duquesne University, Pittsburgh, PA

ABSTRACT

TOPOGRAPHICAL DIFFERENCES IN STRESS VULNERABILITY IN EXPERIMENTAL PARKINSON'S DISEASE

By

Jessica M. Posimo

December 2015

Dissertation supervised by Dr. Rehana K. Leak

Parkinson's disease is characterized by the progressive spread of protein misfolding stress, or proteotoxicity, across the brain. During this protracted process, the allocortex of the temporal lobe develops protein inclusions before the neocortex in the frontal and parietal lobes. In the present study we tested the hypothesis that the staged appearance of proteotoxicity in allocortex followed by neocortex is the result of intrinsic vulnerability differences. We microdissected the neocortex and multiple subregions of the allocortex from rat brains and plated the primary neo- and allocortical neurons for parallel *in vitro* studies. Cells were then exposed to a number of Parkinson's disease-mimicking toxins and cellular viability was measured by three independent and unbiased assays that we have validated as linear and highly sensitive. As expected, neocortex was more resistant to loss of proteasomal degradation of proteins than three allocortical subregions: entorhinal cortex, piriform cortex, and hippocampus. Neocortex was also

more resistant to α-synucleinopathy than hippocampal allocortex. Entorhinal allocortex exhibited lower protein degradative activity than neocortex and greater stress-induced increases in misfolded proteins. Entorhinal allocortex also expressed higher stress-sensitive changes in heat shock proteins (Hsps) such as Hsp70 and Hsc70, suggesting that allocortex needs to rely more on chaperone defenses. In support of this hypothesis, simultaneous loss of Hsp70/Hsc70 and proteasome activity was far more toxic in allocortex than neocortex, whereas facilitation of Hsp70/Hsc70 activity was protective only in neocortex. Neocortex exhibited higher levels of the antioxidants glutathione and ceruloplasmin, and loss of glutathione synthesis rendered neocortex as vulnerable to proteotoxicity as allocortex. Consistent with these observations, allocortex was protected against proteotoxicity by facilitating glutathione synthesis with N-acetyl cysteine. Finally, as aging is a natural model of protein misfolding stress, the levels of select heat shock proteins, proteasome subunits, and glutathione were examined in neocortex and allocortex *in vivo* as a function of age. Our findings suggest that the cerebral cortex is more heterogenous than previous *in vitro* studies of this brain region have acknowledged and that the staged appearance of protein inclusions in Parkinson's disease is at least partly determined by topographic differences in intrinsic vulnerability to protein misfolding stress.

DEDICATION

This dissertation is dedicated to my parents, Andrea and Joseph Posimo, who have provided endless love, support, and encouragement.

ACKNOWLEDGEMENT

I thank my advisor, Dr. Rehana Leak, for encouraging me to pursue my Ph.D. and for continuously supporting me throughout my time here at Duquesne University. I would also like to thank my committee members, Dr. Jane Cavanaugh, Dr. David Johnson, Dr. Patrick Card, Dr. Surratt, and Dr. O'Donnell for their guidance and advice.

I thank Dr. Peter Wipf and Dr. Jeffrey Brodsky from the University of Pittsburgh for their generosity in providing the Hsp70 modulators for my studies. I would like to thank Dr. Virginia Lee and Dr. Kelvin Luk from the University of Pennsylvania for generating the synuclein fibrils used in my project. I would also like to acknowledge the assistance of Denise Butler-Buccilli and Christine Close in maintaining the animal colonies.

I thank all of the graduate students, faculty, and administrative staff in the Graduate School of Pharmaceutical Sciences. I would especially like to thank my fellow graduate student, Amanda Gleixner, for always providing scientific and personal support, encouragement, and friendship.

Finally, I thank my family and friends, especially my fiancée, Michael Blenk, whose love and support made all of this possible.

TABLE OF CONTENTS

Page

LIST OF FIGURES

Page

Introduction

The Impact of Parkinson's Disease

Parkinson's disease is the second most common neurodegenerative disorder after Alzheimer's disease. It has a mean age of onset of approximately 60 years and affects about 1 million people in the United States and 4 million people worldwide (Shehadeh et al., 2010). Age is the major risk factor for Parkinson's disease as its prevalence rises from 1% in those over 60 years of age to 4% of the population in those over 80 (D. T. Dexter & Jenner, 2013). Parkinson's disease is more prevalent in men than in women with reports of ratios ranging from 1.1:1 to 3:1 (Schrag, Ben-Shlomo, & Quinn, 2000). The socioeconomic impact of the disease can be high with a cost per patient per year of approximately $10,000 in the United States. Indeed, the total economic burden of Parkinson's disease has been estimated at $23 billion (Huse et al., 2005; Whetten-Goldstein, Sloan, Kulas, Cutson, & Schenkman, 1997). Expenses associated with inpatient care and nursing homes account for the majority of this cost rather than medication-related costs (Huse et al., 2005).

The clinical diagnosis of Parkinson's disease is based on the identification of impaired motor function with symptoms of bradykinesia, rigidity, resting tremor, and/or postural instability. These motor symptoms reflect the loss of dopaminergic neurons in the substantia nigra pars compacta (SNpc) and subsequent decrease in dopamine levels in the striatum. Identification of the hallmark motor symptoms and a positive response to dopaminergic medications help to solidify the clinical diagnosis of Parkinson's disease. Recently, Parkinson's disease has been hypothesized to be an even more complex, systemic illness than previously thought, involving both motor and non-motor symptoms such as depression, sleep disturbance, sensory abnormalities, autonomic dysfunction, and cognitive decline (Langston, 2006). Non-

motor symptoms of the disorder usually antedate motor symptoms by many years (Koller, 1992). Autonomic dysfunction and an impairment in or loss of olfaction are frequently reported years before motor symptoms are manifest (Hawkes, Shephard, & Daniel, 1997). At the very end stages of Parkinson's disease, progressive cognitive decline begins to devastate patients and their families (Dubois & Pillon, 1997). Non-motor symptoms are thought to affect all patients but are poorly diagnosed despite being a major determinant of disease outcome, decreased function and quality of life, and forcing entry into long-term care (Chaudhuri, Healy, Schapira, & Excellence, 2006; D. T. Dexter & Jenner, 2013; Schenkman, Wei Zhu, Cutson, & Whetten-Goldstein, 2001). Furthermore, the etiology of non-motor symptoms remains poorly researched compared to the motor deficits (D. T. Dexter & Jenner, 2013). Nevertheless, recent breakthroughs have established that Parkinson's disease affects both the peripheral and central nervous systems, progresses systematically over time, affects movement in mid-to-late stages, and impairs cognition in end stages (Jellinger, 2011).

Patterns of Neurodegeneration

Parkinson's Disease Staging

In 2003, the German neuroanatomist Heiko Braak and his colleagues proposed that Parkinson's disease could be categorized into six distinct stages based on histopathology, now known as Braak stages 1-6 (H. Braak, Del Tredici, Rüb, et al., 2003). Braak staging was based on the neuroanatomical distribution of proteinaceous inclusions in postmortem idiopathic Parkinson's diseased brains. The signature histopathological lesions of the disorder include eosinophilic inclusions within the cytoplasm or in dendritic and axonal processes. These inclusions are termed Lewy bodies and Lewy neurites, after Fritz Heinrich Lewy, who first reported these pathological markers in 1912 (Goedert, Spillantini, Del Tredici, & Braak, 2013).

These hallmark inclusion bodies can develop as spindle or thread-like Lewy neurites in cellular processes or globular Lewy bodies in neuronal perikarya (Pollanen, Dickson, & Bergeron, 1993). The major component of these lesions is the normally presynaptic protein α-synuclein, which misfolds and aggregates in all or nearly all Parkinson's disease cases (Baba et al., 1998; Duda, Lee, & Trojanowski, 2000). Histological studies of the pathology in familial forms of Parkinson's disease are somewhat limited in scope, but it nevertheless recognized that all or nearly all patients with Parkinson's disease exhibit loss of nigral dopamine neurons and Lewy pathology in this brain region (Farrer et al., 2001; Mori et al., 1998). Thus, Lewy bodies and Lewy neurites are present in both sporadic and familiar forms of Parkinson's disease, consistent with their centrality to the disease process (Poulopoulos, Levy, & Alcalay, 2012).

According to the Braak staging theory, new regions are progressively affected by Lewy pathology with each successive stage, while the pathology increases in severity in previously affected brain regions (Fig. 1)(H. Braak, Del Tredici, Rüb, et al., 2003; Luk & Lee, 2014). In stage 1, the medulla oblongata develops lesions in the dorsal IX/X motor nucleus and/or the intermediate reticular zone as well as anterior olfactory structures such as the anterior olfactory nucleus and olfactory bulb mitral cells (Daniel & Hawkes, 1992). This pathology is exacerbated in stage 2 and the pontine tegmentum becomes gradually involved, with Lewy bodies appearing in the caudal raphe nuclei, gigantocellular reticular nucleus, and coeruleus-subcoeruleus complex. In stage 3, lesions finally develop in the midbrain, particularly the melanin-laden neurons of the SNpc while the severity of the previously developing lesions increases in magnitude. Additionally, the second sector of the Ammon's horn in the large hippocampal formation also begins to develop long Lewy neurites at this middle stage (H. Braak, Del Tredici, Rüb, et al., 2003).

The cerebral cortex is responsible for higher-order executive function, learning, and memory, and Lewy bodies and Lewy neurites in this structure are therefore correlated with symptoms of dementia and cognitive decline (Harding & Halliday, 2001; Hurtig et al., 2000; Mattila, Rinne, Helenius, Dickson, & Röyttä, 2000). Cortical involvement begins at Braak stage 4 and is confined to the temporal mesocortex, specifically the transentorhinal region, and the limbic allocortex. There is continued marked devastation in the melano-neurons of the SNpc as well as the anterior olfactory nucleus at this stage. Specifically, Lewy-bearing inclusions increase in number and there is significant loss of neurons in the posterior region of the SNpc. Lesions also begin affecting the central nuclei of the amygdala and specific subnuclei of the thalamus at mid to end stages. In stage 5, lesions progress into high order sensory association areas of the neocortex and prefrontal cortex while all previously affected subcortical and mesocortical structures exhibit even more severe pathology. At the final stage 6, nearly the entire neocortex is involved, including first order sensory association areas and premotor areas with occasional mild changes in primary sensory areas and the primary motor field (H. Braak, Del Tredici, Rüb, et al., 2003). Thus, the primary sensorimotor neocortex is the last cortical subregion to be affected by the disease process whereas the entorhinal allocortex is the first.

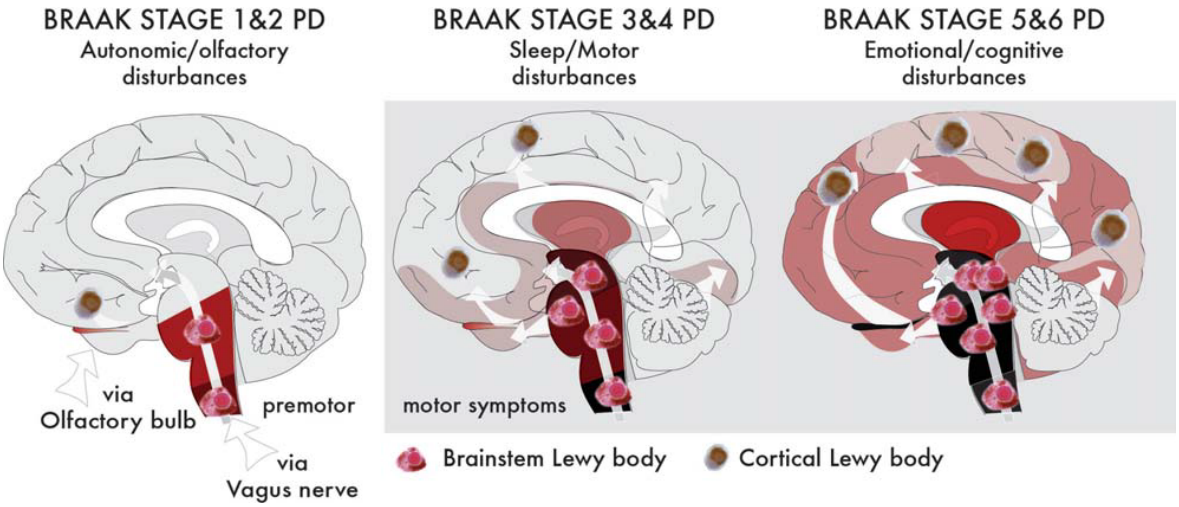

Figure 1. Caudo-rostral progression of Lewy bodies in the brain in Parkinson's disease. Reprinted from "Milestones in Parkinson's disease—Clinical and pathologic features," by G. Halliday, A. Lees, and M. Stern, 2011, *Movement Disorders, 26,* p. 1015-1021. Copyright 2011 by John Wiley and Sons. Reprinted with permission.

Alzheimer's Disease Staging

Similar to Parkinson's disease, Alzheimer's disease is also thought to spread across multiple brain regions, although postmortem studies of Alzheimer's patients have mostly focused upon neurodegeneration in the cerebral cortex. In both disorders, the temporal mesocortex and allocortex seem to be the nucleation site for the spread of protein aggregations in the telencephalon, while the neocortex is affected last (H. Braak, Rüb, Schultz, & Del Tredici, 2006). However, in Alzheimer's disease, the major component of the intraneuronal aggregations–known as neurofibrillary tangles–is the microtubule-associated protein tau (E. Braak, Braak, & Mandelkow, 1994).

Braak staged Alzheimer's disease based on the regional distribution of neurofibrillary tangles. In stages I and II, meso- and allocortical regions such as the transentorhinal and entorhinal cortices exhibit tau pathology, followed by involvement of the hippocampus. In stages III-IV, there is exacerbation of pathology in the entorhinal cortex and commencement of pathology in higher order neocortical areas of the temporal lobe. Finally, in end stages V-VI,

neocortical involvement becomes more severe and encroaches on primary sensorimotor areas of the frontal and parietal neocortex (H. Braak, Rüb, et al., 2006). This staging scheme has been correlated with intellectual status (Bancher, Braak, Fischer, & Jellinger, 1993). In addition, the degeneration of the entorhinal cortex in Alzheimer's disease has been correlated to a severe decline in both memory and executive function (Albert, 1996; Gómez-Isla et al., 1997; Kordower et al., 2001). It is worth noting that amyloid formation begins in the neocortex in Alzheimer's disease, but that total plaque numbers do not correlate to disease severity or loss of neurons (Gómez-Isla et al., 1997; Ingelsson et al., 2004; Josephs et al., 2008; Thal, Rüb, Orantes, & Braak, 2002). In addition, atrophy in the cerebral cortex follows the progression of tau pathology, not of amyloid formations (Arriagada, Growdon, Hedley-Whyte, & Hyman, 1992; Josephs et al., 2008).

The Spreading of Lewy Bodies in Parkinson's Disease

As mentioned previously, the main component of Lewy bodies is the protein α-synuclein, a 14 kDa protein consisting of 140 amino acids that interacts with highly curved phospholipid membranes, such as presynaptic vesicles. α-synuclein appears to play a dynamic role in vesicle trafficking during neurotransmitter release, though its exact function is still a matter of some debate (Recasens & Dehay, 2014). There are six known missense mutations in the gene encoding α-synuclein that have been found to mandate the onset of autosomal-dominant forms of Parkinson's disease (Appel-Cresswell et al., 2013; Athanassiadou et al., 1999; Krüger et al., 1998; Lesage et al., 2013; Polymeropoulos et al., 1997; Zarranz et al., 2004). Additionally, overexpression of α-synuclein due to gene duplication or triplication has been identified as a cause of some forms of familial Parkinson's disease (Goedert et al., 2013). Furthermore, the most important genetic risk factor for idiopathic Parkinson's disease is sequence variation in the

regulatory region of the gene encoding for α-synuclein, as identified by a genome-wide association study (Krüger et al., 1999). These findings highlight the importance of α-synuclein for Lewy body disorders.

α-synuclein is a natively unfolded protein, having no defined structure in aqueous solution. However, under pathological conditions, such as oxidative stress, gene mutations, or following post-translational modifications (such as phosphorylation, ubiquitination, or truncation), it can adopt an oligomeric or fibrillar conformation, which can elicit aggregation and Lewy body formation (Recasens & Dehay, 2014). Growing bodies of evidence indicate that the soluble pathogenic form of α-synuclein may self-propagate and spread progressively between interconnected brain regions via cell-to-cell transmission, similar to the prion hypothesis in Creutzfeld-Jacob disease. This idea of transmissibility is supported by Braak's six-stage scheme of Parkinson's disease progression, which maps the spread of Lewy body pathology in a caudo-rostral topographical manner (H. Braak, Del Tredici, Rüb, et al., 2003). In two independent studies, embryonic mesencephalic neurons were grafted into the striatum of Parkinson's patients. Remarkably, after a number of years, patients developed α-synuclein-positive Lewy bodies in the grafted neurons, indicating a host-to-graft transmission of synucleinopathy in the human brain (Kordower, Chu, Hauser, Freeman, & Olanow, 2008; Li et al., 2008). A potential mechanism for this transmission could be the release of fibrillized or oligomeric α-synuclein by exocytosis or necrosis into the extracellular milieu. Neighboring neurons might take up α-synuclein through endocytotic pathways. Once inside the cell, misfolded a-synuclein might act as a template, promoting the misfolding of neighboring synuclein molecules, ultimately leading to further Lewy body formation (Brundin, Li, Holton, Lindvall, & Revesz, 2008).

Recent *in vitro* studies have shown that synthetic recombinant preformed α-synuclein fibrils can act as a seed to induce endogenous soluble α-synuclein to misfold into insoluble hyper-phosphorylated and ubiquitinated pathologic species (Luk et al., 2009; Volpicelli-Daley et al., 2011b). Disruption of synaptic function, neuronal excitability and connectivity, and eventual neuronal death follows α-synuclein aggregation formation in the recipient cells. *In vivo* studies have also shown α-synuclein can spread via cell-to-cell transmission (Luk, Kehm, Zhang, et al., 2012). Hansen and colleagues demonstrated host-to-graft transfer of α-synuclein, as grafted fetal post-mitotic dopaminergic neurons exhibited human α-synuclein immunoreactivity 6 months after transplantation into the striatum of mice overexpressing human α-synuclein (Hansen et al., 2011). In addition, intracerebral injections of synthetic recombinant preformed α-synuclein fibrils or brain homogenates from aged α-synuclein transgenic mice into the neocortex and striatum of young asymptomatic transgenic mice have been shown to induce widespread Parkinson's disease-like pathology and reduce the lifespan of the mice (Luk, Kehm, Zhang, et al., 2012). These findings were recently reproduced by Mougenot and colleagues, who showed that injections of brain homogenates from symptomatic α-synuclein transgenic mice into the brains of younger, healthy transgenic mice subsequently reduced their lifespan and accelerated the clinical signs of paralysis characteristic of this mouse model (Mougenot et al., 2012). Finally, injection of α-synuclein fibrils into wild type mice has also been shown to induce pathological spreading of α-synuclein (Luk & Lee, 2014).

The studies outlined above all support Braak's hypothesis that the pattern of spread of Lewy pathology from allocortex to neocortex may be explained by an insult traveling across the cortex in a transneuronal fashion. In addition to transneuronal spread across interconnected brain regions, we believe that selective regional vulnerabilities may also play a role in determining

which brain regions are first seized into developing protein misfolding stress and exhibiting Lewy formations.

Selective Vulnerability in Parkinson's Disease

As mentioned above, Parkinson's disease is characterized by the severe loss of nigrostriatal dopamine neurons and the formation of α-synuclein-laden protein aggregations termed Lewy bodies in many brain regions. By end stages of the disease, 80-95% of neurons in the ventral tier (nigrosome 1) of the SNpc degenerate, whereas more dorsally and medially situated dopamine neurons are mostly spared from cell death (Damier, Hirsch, Agid, & Graybiel, 1999). The reason for this differential susceptibility is unknown. Cells of the dorsal tier are innervated by dorsal striatal afferents from the caudate nucleus whereas ventral tier cells receive projections from the caudate nucleus and putamen (Haber, Fudge, & McFarland, 2000). Thus, it is possible that susceptibility is influenced by variations in neuronal afferent and efferent projections. Differential receptor expression in these areas may also play a role in determining selective vulnerability to neurodegeneration. The dopamine type 2 (D_2) receptor is one of the most abundant receptors in the SNpc (Hurd, Suzuki, & Sedvall, 2001). Binding of this receptor results in an efflux of potassium and the subsequent inhibition of neuronal activity and reduced dopamine release (Luján, Maylie, & Adelman, 2009). In the more vulnerable ventral tier of the SNpc, higher levels of D_2 receptor mRNA have been reported than in the dorsal tier in postmortem studies of the human brain (Hurd, Pristupa, Herman, Niznik, & Kleinman, 1994). Furthermore, SNpc neurons utilize L-type voltage-gated Ca^{2+} channels to drive the firing of action potentials (Nedergaard, Flatman, & Engberg, 1993). This lies in contrast to ventral tegmental area neurons, which use Na^{+} based ion channels (Puopolo, Raviola, & Bean, 2007). Thus, SNpc neurons exhibit higher levels of intracellular Ca^{2+} than ventral tegmental area

neurons. In addition, there is a scarcity of calcium binding proteins in the SNpc, with calbindin being absent and paravalbumin and calretinin only sparsely expressed within subregions of the SNpc (McRitchie, Hardman, & Halliday, 1996). These observations are important because a high Ca^{2+} microenvironment is thought to increase mitochondrial metabolic activity and subsequent production of reactive oxygen species, thereby increasing stress vulnerability.

Many decades ago, Parkinson's disease was shown to involve a dramatic increase in iron in the SNpc (Double et al., 2008). Increased iron levels are known to catalyze the production of reactive oxygen species through Fenton chemistry (Rhodes & Ritz, 2008) and may promote α-synuclein fibrillization, which is strongly linked to Lewy body formation (Uversky, Li, & Fink, 2001). The major cellular iron transport mechanism is dependent upon the protein transferrin, including melanotransferrin and lactotransferrin, which shuttle iron in and out of cells. Immunoreactivity for lactotransferrin is higher in the ventral tier of the SNpc in Parkinson's disease (Faucheux et al., 1995). These findings suggest that the ventral tier of the SNpc has a greater capacity to engage in iron flux. Therefore, regional differences in iron transport mechanisms may also play a role in the selective vulnerability of SNpc neurons in Parkinson's disease.

Finally, antioxidant and neurotransmitter systems may also contribute to the enhanced susceptibility of SNpc neurons to neurodegeneration in Parkinson's disease. In one microarray study, a number of glutathione-related genes were shown to be downregulated in the vulnerable ventrolateral SNpc in the human brain (Duke, Moran, Pearce, & Graeber, 2007). Studies in human and non-human primates further show that levels of the dopamine transporter are higher in neurons of the more vulnerable ventral tier than other SNpc subregions (González-Hernández, Barroso-Chinea, De La Cruz Muros, Del Mar Pérez-Delgado, & Rodríguez, 2004). Thus, this

region may experience higher levels of oxidative stress due to enhanced dopamine reuptake from the synapse and subsequent metabolism.

The studies described above sought to examine the selective vulnerability of the SNpc in Parkinson's disease. In contrast, our studies are the first to examine topographical vulnerability differences between the least resistant cortical region, the entorhinal cortex, and the most resistant cortical region, the primary sensorimotor neocortex. Specifically, we investigated differences in endogenous defensive proteins as well as protein degradation pathways in these cortical subregions.

Protein Degradation Pathways

Molecular chaperones regulate the folding, disaggregation, degradation, and trafficking of protein substrates within the cell (Fig. 2) (Kim, Hipp, Bracher, Hayer-Hartl, & Hartl, 2013). They are highly conserved and can be broadly grouped into Hsp70, Hsp90, DNAJ/Hsp40, chaperonin/Hsp60, and small heat shock protein families (Haslbeck, Franzmann, Weinfurtner, & Buchner, 2005; Kim et al., 2013). Members of the Hsp70 and Hsp90 families are the best studied and require ATP hydrolysis for chaperone activity (Kim et al., 2013). In contrast, small heat shock proteins, such as Hsp27, influence protein folding in an ATP-independent manner by forming oligomeric cages that trap misfolded proteins, preventing them from aggregating, and creating a reservoir of substrates for Hsp70 (Haslbeck et al., 2005). The chaperonin Hsp60 is formed by two large hexameric ring complexes that encapsulate the substrate protein into a central cavity so that folding can be unimpaired by aggregation (Kim et al., 2013).

Client specificity and the functionality of Hsp70 and Hsp90 are strongly influenced by interactions with a range of co-chaperones (Taipale et al., 2014). Hsp90 associates with a number of co-chaperones while Hsp70 is principally regulated by Hsp40, which stimulates its ATPase

activity (Kampinga & Craig, 2010; Taipale, Jarosz, & Lindquist, 2010). In addition, the co-chaperones Hsc70/Hsp70 organizing protein (Hop) and Hsc70-interacting protein (Hip) can bind together the Hsp70 and Hsp90 machinery and stabilize the ADP-bound state of the chaperones that have a high affinity for substrate proteins (Hohfeld, Minami, & Hartl, 1995; Taipale et al., 2010). On the other hand, recruitment of the co-chaperones C-terminus of Hsc70-interacting protein (CHIP) and Bcl2-associated athanogene 1 (BAG1) redirects Hsp70 and Hsp90 client proteins to the proteasome for degradation (Connell et al., 2001; Demand, Alberti, Patterson, & Hohfeld, 2001). Thus, chaperones can act alone or in concert with different co-chaperones to refold or eliminate misfolded proteins through the proteasome.

The 26S proteasome consists of a 19S/PA700 regulatory cap and a 20S proteolytic core and is the primary protein degradation system in the cell (Coux, Tanaka, & Goldberg, 1996). The 19S/PA700 cap recognizes ubiquitylated substrates, removes ubiquitin chains, and unfolds the substrate to facilitate entry into the 20S core, where it is degraded into short peptides (Fig. 2). This process is initiated by the addition of polyubiquitin chains to distinct lysine residues on misfolded proteins through a series of enzymatic steps (Finley, 2009). The following enzymes permit the targeted and selective degradation of substrates: E1 (ubiquitin-activating enzyme), E2 (ubiquitin-conjugating enzyme), and E3 (ubiquitin ligase) (Richly et al., 2005). E1 hydrolyzes ATP and forms a link between ubiquitin and itself, E2 receives ubiquitin from E1, and E3 binds both E2 and ubiquitin and transfers the ubiquitin to a specific lysine residues on the substrate (Richly et al., 2005). Misfolded proteins with K48-linked ubiquitin chains are then directed to the proteasome by chaperone-co-chaperone complexes. In contrast, K63-linkages promote inclusion formation and facilitate preferential clearance of inclusions *via* autophagy (Tan et al.,

2008). The process of ubiquitylation of substrates and their subsequent degradation through the proteasome is termed the ubiquitin proteasome system.

The second protein degradation system, autophagy, is known to complement the ubiquitin proteasome system by degrading misfolded proteins as well as larger protein complexes or dysfunctional organelles through the action of lysosomes (Yang & Klionsky, 2010). Autophagy consists of three distinct forms: macroautophagy, microautophagy, and chaperone-mediated autophagy (Yang & Klionsky, 2010). Macroautophagy is the best studied and entails the sequestration of cytosolic substrates by a double membrane structure termed an autophagosome (Fig. 2) (Yang & Klionsky, 2010). The autophagosome then fuses with the lysosome and the contents are released for degradation. Microautophagy is the process of invagination of the lysosomal membrane and direct engulfment of cytosolic material (Yang & Klionsky, 2010). Finally, chaperone-mediated autophagy involves the Hsc70-mediated delivery of specific pentapeptide sequence (KFERQ)-bearing substrates, such as the hallmark Parkinson's disease protein α-synuclein. These substrates are directed to the lysosome and translocated across the lysosomal membrane through the LAMP2A receptor (Fig. 2) (Kaushik & Cuervo, 2012; Yang & Klionsky, 2010).

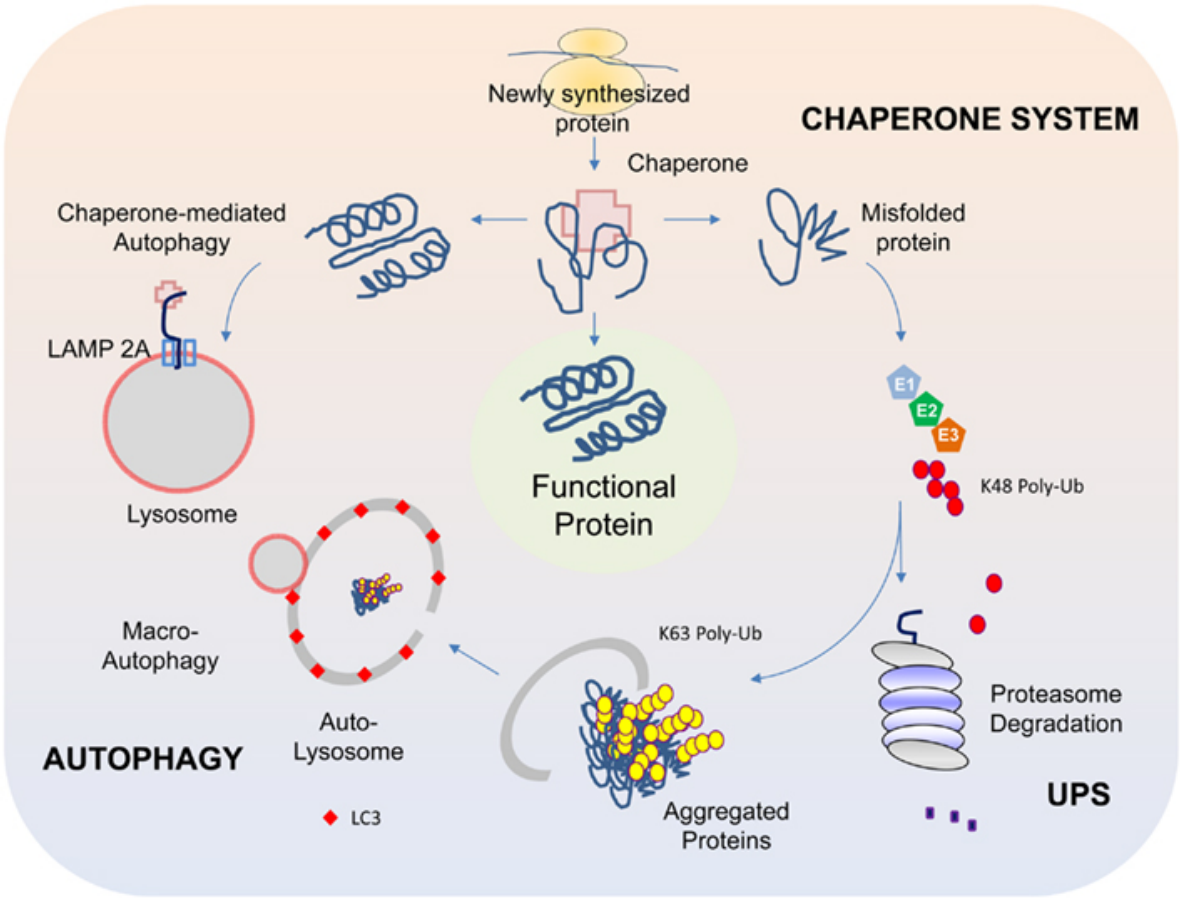

Figure 2. Protein degradation pathways in the cell. Reprinted from "Molecular events underlying Parkinson's disease – an interwoven tapestry," by K. L. Lim and C. W. Zhang, 2013, *Frontiers in Neurology, **4**:33*. Copyright 2013 by Lim and Zhang. Reprinted with permission.

Neurodegenerative Mechanisms in Parkinson's disease

Accumulation of Misfolded Proteins

All neurodegenerative disorders are characterized by the presence of intracellular aggregates, strongly suggesting ubiquitin proteasome system and autophagic dysfunction in these conditions. In Parkinson's disease, the protein α-synuclein is especially prone to misfolding, causing a loss of its functional conformation. This misfolding exposes β sheet stretches prone to protein-protein interactions, thereby leading to the eventual formation of detergent-insoluble protein aggregations (Saxena & Caroni, 2011). The predominant modification of α-synuclein in

Lewy bodies is its selective and extensive phosphorylation at Ser129 (pSer129) (Anderson et al., 2006; Fujiwara et al., 2002; Waxman & Giasson, 2008). It remains controversial whether the conformational changes and accumulation of this protein promote disease through a toxic gain or loss of function. Nevertheless, it is generally assumed that the smaller oligomer or protofibrillar form of this protein is responsible for cell toxicity, although the exact pathogenic mechanism still remains elusive. Mutant α-synuclein is known to induce the formation of filaments that bind and decrease the proteolytic activity of the 20S core particle of the proteasome (Lindersson et al., 2004). Heat shock proteins, such as Hsp/Hsc70, Hsp40, Hsp90, and small heat shock proteins can also be sequestered in aggregations as a consequence of failing to refold the misfolded protein to its native conformation, further negatively affecting protein homeostasis (Auluck, Chan, Trojanowski, Lee, & Bonini, 2002; Saxena & Caroni, 2011). The accumulation of ubiquitinated proteins, heat shock proteins, misfolded synuclein, and components of the ubiquitin proteasome system within Lewy bodies suggest that ubiquitin proteasome system dysfunction is strongly linked with the pathogenesis of Parkinson's disease (Ii, Ito, Tanaka, & Hirano, 1997; Lennox, Lowe, Morrell, Landon, & Mayer, 1989; McNaught, Shashidharan, Perl, Jenner, & Olanow, 2002; Schlossmacher et al., 2002).

Deficits in ubiquitin-proteasome activity further contribute to the loss of protein homeostasis in neurodegenerative diseases. For example, reductions in proteasome activity and levels of proteasomal subunits have been reported in the SNpc of sporadic Parkinson's disease patients (McNaught, Belizaire, Isacson, Jenner, & Olanow, 2003; McNaught & Jenner, 2001; Tofaris, Razzaq, Ghetti, Lilley, & Spillantini, 2003). However, the strongest evidence regarding the role of the ubiquitin proteasome system in Parkinson's disease can be found in studies showing that genetic mutations in components of this pathway cause dopaminergic

neurodegeneration. For example, autosomal recessive loss-of-function mutations in parkin, an E3 ligase, are an established cause of familial Parkinson's disease (Imai, Soda, & Takahashi, 2000; Shimura et al., 2000). In addition, the gene encoding ubiquitin carboxy-terminal hydrolase L1, which hydrolyses ubiquitin chains to free ubiquitin monomers, has been implicated in familial Parkinson's disease (Leroy et al., 1998).

Complimenting these genetic data, pharmacological studies have shown that injections of proteasome inhibitors into rats cause parkinsonian features, including Lewy body-like aggregates (Fornai et al., 2003; McNaught, Perl, Brownell, & Olanow, 2004; W. Xie et al., 2010). In addition, proteasome inhibitors have been found to cause relatively selective degeneration of cultured dopamine neurons and formation of ubiquitin and α-synuclein positive inclusions (McNaught, Mytilineou, et al., 2002; Petrucelli et al., 2002; Rideout, Lang-Rollin, Savalle, & Stefanis, 2005; Sun et al., 2006). Specifically, the peptide aldehyde proteasome inhibitor MG132 has been found to induce degeneration in the SNpc and to deplete dopamine levels in both cell culture and animal models (Sun et al., 2006). Thus, proteasome inhibition recapitulates many of the important behavioral and biochemical features of the disease, making it a useful tool for studying the pathogenesis of Parkinson's disease or for testing neuroprotective therapies.

Dysfunction in the autophagy-lysosomal pathway can also contribute to loss of protein homeostasis in neurodegenerative diseases. Neuron specific autophagy gene knockout mice have been found to develop intraneuronal aggregates and neurodegeneration (Hara et al., 2006; Komatsu et al., 2006). In addition, overexpression of α-synuclein impairs autophagy in mammalian cells and mice by inhibiting autophagosome formation (Winslow et al., 2010). Mutant α-synuclein may also impair chaperone-mediated autophagy by blocking the

translocation of substrates into the lysosome through the LAMP2A receptor (Cuervo, Stefanis, Fredenburg, Lansbury, & Sulzer, 2004; Martinez-Vicente et al., 2008).

Oxidative Stress

Reactive oxygen species are prevalent in the brain as the metabolism of excitatory amino acids and neurotransmitters causes high levels of these toxic byproducts (Uttara, Singh, Zamboni, & Mahajan, 2009). Mitochondrial dysfunction, protein misfolding, and dysregulation of the ubiquitin proteasome system can also contribute to the production of reactive oxygen species (Double, Reyes, Werry, & Halliday, 2010). Neurons are especially sensitive to free radicals as they are post-mitotic cells with an abundance of unsaturated lipids, which are particularly vulnerable to peroxidation and oxidative modification (Uttara et al., 2009). Additionally, the brain is especially susceptible to reactive oxygen species as it has lower levels of antioxidant defenses compared to other tissues, such as the liver.

Oxidative stress is a common feature in neurodegenerative diseases and refers to an imbalance in the levels of reactive oxygen species and antioxidants. Reactive oxygen species can cause protein and DNA damage in addition to lipid peroxidation and are typically kept in check through antioxidant defenses such as glutathione, superoxide dismutases, catalases, and other mechanisms. Increased levels of oxidatively damaged proteins are present in the SNpc in Parkinson's disease (Alam et al., 1997; Yoritaka et al., 1996). In addition, reactive oxygen species-related damage leads to a dysregulation of intracellular calcium signaling pathways. This can lead to cell death through downstream excitotoxic effects such as the activation of glutamate receptors and apoptosis in Parkinson's disease (Uttara et al., 2009). Chronic oxidative stress can also interfere with autophagy, causing incomplete degradation of lysosomal cargo and thereby forming cross-linked products, such as lipofuscin, further impairing lysosomal function (Cuervo

et al., 2005; Kiffin, Bandyopadhyay, & Cuervo, 2006; Terman & Brunk, 2004). Toxic products can then leak from the destabilized lysosomal membrane, thereby causing the release of lysosomal enzymes into the cytosol, a frequently observed event in dying neurons (Kiffin et al., 2006; Terman & Brunk, 2004).

The link between oxidative stress and neurodegeneration is also supported by toxin models, such as the herbicide paraquat, which can elicit dopaminergic degeneration and the motor deficits associated with Parkinson's disease. Paraquat is a structural analog of 1-methyl-4-phenylpyridinium (MPP+), another parkinsonism-inducing toxin (Langston, Ballard, Tetrud, & Irwin, 1983). Paraquat belongs to the class of redox cycling compounds capable of causing mitochondrial damage and increasing levels of reactive oxygen species such as the superoxide free radical (Castello, Drechsel, & Patel, 2007; Jenner, 2003). Epidemiological studies have suggested an association between chronic exposure to pesticides, particularly paraquat, and an increased risk for developing Parkinson's disease (Gorell, Johnson, Rybicki, Peterson, & Richardson, 1998; Hertzman, Wiens, Bowering, Snow, & Calne, 1990; Liou et al., 1996; Semchuk, Love, & Lee, 1993). Moreover, *in vivo* studies have shown that chronic administration of paraquat in mice or rats causes a decrease in the number of dopaminergic neurons in the SNpc and striatal levels of dopamine (McCormack et al., 2002; Shimizu et al., 2003; Thiruchelvam et al., 2003).

Protective Molecules Implicated in Protection Against Parkinson's Disease

Glutathione

Glutathione is a tripeptide containing glutamate, cysteine, and glycine. It is the most abundant nonprotein thiol in cells and participates in many important biological processes (Dickinson & Forman, 2002; Zeevalk, Razmpour, & Bernard, 2008). Glutathione is synthesized

in both neurons and glia and detoxifies oxidants and electrophiles (Dickinson & Forman, 2002; Dringen, 2000; Griffith, 1999). Oxidative stress emerges when the redox equilibrium favors higher levels of reactive oxygen species and lower glutathione levels, resulting in a decreased reducing environment within the cell (Genestra, 2007).

As mentioned earlier, neurodegenerative disorders such as Parkinson's disease are characterized by oxidative stress. In Parkinson's disease, the SNpc exhibits increased levels of lipid peroxidation, iron content, and decreased glutathione levels (D. T. Dexter et al., 1991; D. T. Dexter et al., 1989; D. T. Dexter et al., 1994; Perry, Godin, & Hansen, 1982). Although a 30-40% decrease of glutathione levels has been detected in this condition, there is no corresponding rise in oxidized glutathione levels (Sian, Dexter, Lees, Daniel, Jenner, et al., 1994; Sofic, Lange, Jellinger, & Riederer, 1992). Notably, the degree of disease severity has been correlated with the extent of glutathione loss (Riederer et al., 1989).

Ceruloplasmin

Ceruloplasmin is a multi-copper enzyme ferroxidase found in a free, secreted form as well as a bound glycosylphosphatidylinositol (GPI)-anchored form in astrocytes in the central nervous system (Roeser, Lee, Nacht, & Cartwright, 1970). Ceruloplasmin is essential in iron homeostasis and has potent antioxidant activity (Ayton et al., 2013; Harris, Durley, Man, & Gitlin, 1999; Roeser et al., 1970). This multicopper ferroxidase facilitates cellular iron export by oxidizing toxic ferrous iron to ferric iron at the cell surface for incorporation into the iron transporter transferrin, thereby reducing the production of reactive oxygen species through the harmful Fenton reaction (Hellman & Gitlin, 2002). Ceruloplasmin ferroxidase activity also increases the stability of the iron export transporter, ferroportin, on the cell membrane (De

Domenico et al., 2007). As one might expected, many studies have supported a protective role for ceruloplasmin in neurodegenerative diseases (Texel, Xu, & Harris, 2008).

Defects in ceruloplasmin activity have been linked with brain iron accumulation and neurodegenerative lesions (Jeong & David, 2003). In addition, individuals carrying one mutant ceruloplasmin allele are at increased risk for Parkinson's disease (Hochstrasser et al., 2004). There is a significant loss of ceruloplasmin ferroxidase activity in the cerebrospinal fluid, serum, and SNpc in Parkinson's disease (Boll, Alcaraz-Zubeldia, Montes, & Rios, 2008; Boll, Sotelo, Otero, Alcaraz-Zubeldia, & Rios, 1999; Jin et al., 2011; Olivieri et al., 2011; Torsdottir, Kristinsson, Snaedal, Sveinbjornsdottir, et al., 2010; Torsdottir, Sveinbjornsdottir, Kristinsson, Snaedal, & Johannesson, 2006). Low serum ceruloplasmin levels correlate with an early age of onset of Parkinson's disease and with iron deposits in the SNpc (Bharucha, Friedman, Vincent, & Ross, 2008; Martinez-Hernandez et al., 2011). Iron deposits can promote conformational changes in α-synuclein, thereby contributing to Lewy body formation and to the pathogenesis of Parkinson's disease (Graham, Paley, Grünewald, Hoggard, & Griffiths, 2000). Thus, iron chelation, such as with the drug deferiprone, has potential as a therapeutic strategy for Parkinson's disease (Molina-Holgado, Gaeta, Francis, Williams, & Hider, 2008). This is consistent with the observation that iron homeostasis disorders present clinically with parkinsonian symptoms (Crichton, Dexter, & Ward, 2011). For example, aceruloplasminemia–a rare genetic disorder in which mutations abolish functional ceruloplasmin–presents with parkinsonism as well as cognitive loss and cerebellar and retinal degeneration (McNeill, Pandolfo, Kuhn, Shang, & Miyajima, 2008).

In addition to the clinical studies mentioned above, ceruloplasmin has been found to mitigate pathology in experimental Parkinson's disease (Hineno, Kaneko, Yoshida, & Ikeda,

2011; Kaneko, Hineno, Yoshida, & Ikeda, 2008). Ceruloplasmin knockout mice exhibit neuronal loss in the SNpc that can be mitigated with iron chelation (Ayton et al., 2014). Furthermore, ceruloplasmin mitigates neurodegeneration induced in mice by the dopaminergic neurotoxin MPTP and blunts the toxic accumulation of iron in the SNpc (Ayton et al., 2014).

Aging and Parkinson's Disease

Based on numerous epidemiological studies, aging is acknowledged as the greatest risk factor for Parkinson's disease (Bennett et al., 1996; Morens et al., 1996; Tanner & Goldman, 1996). However, studies have shown that the neurochemical and morphological changes associated with aging are distinct from the pathological patterns evident in Parkinson's disease (Fearnley & Lees, 1991; Gibb & Lees, 1991; Kish, Shannak, Rajput, Deck, & Hornykiewicz, 1992). For example, aging humans exhibit little or no loss of SNpc dopaminergic neurons, a hallmark characteristic of Parkinson's disease (Alladi et al., 2009; Kubis et al., 2000). A lack of age-related dopaminergic neuron loss has also been verified in the non-human primate brain, although expression of the phenotypic marker tyrosine hydroxylase may be lowered with aging (McCormack et al., 2004).

The activity of the ubiquitin proteasome system and autophagy decreases with age in almost every tissue in old organisms (Cuervo et al., 2005). Moreover, small heat shock proteins and the constitutive Hsc70 are elevated but induction of Hsp70 is impaired in the aging brain (Fargnoli, Kunisada, Fornace, Schneider, & Holbrook, 1990; Schultz et al., 2001; Sóti & Csermely, 2000). This dysfunction may play a role in the failure of the intracellular quality control systems observed in neurodegenerative disorders with age.

Increased levels of oxidative stress are a cornerstone of the aging process and neurodegenerative disease. Oxidative stress increases with age in part due to a widening

imbalance between the antioxidant defense system and oxidants in the cell, which progresses exponentially in the last trimester of life (Agarwal & Sohal, 1994). Glutathione content decreases with age in many tissues from different animal species though the mechanism is unclear (Liu, Wang, Shenvi, Hagen, & Liu, 2004). In addition, dysfunctional mitochondria generate increasing levels of reactive oxygen species with age (Brunk & Terman, 2002a, 2002b). These dysfunctional organelles are removed from the cell through the lysosomal system, generating high levels of the autofluorescent pigment lipofuscin (Brunk & Terman, 2002b). Lipofuscin, also known as the "age pigment", accumulates in many brain regions during aging and is thought to reflect increasing age-related mitochondrial damage and subsequent lysosomal degredation (Terman & Brunk, 1998; Terman, Gustafsson, & Brunk, 2006). It is important to note that Braak reported that the allocortex develops lipofuscin pigments at a faster rate than the neocortex (H. Braak, Del Tredici, Schultz, & Braak, 2000; H. Braak, Rub, Schultz, & Del Tredici, 2006). During aging, serum ceruloplasmin expressed greater oxidative modifications that induce conformational changes, thereby reducing the functionality of the ferroxidase in older animals (Musci, Bonaccorsi di Patti, Fagiolo, & Calabrese, 1993). Thus, the reduction in ceruloplasmin activity in the cerebrospinal fluid in Parkinson's disease may reflect increased protein aging and elevated levels of oxidative stress. In sum, the studies discussed here all provide evidence for a strong link between aging and the pathogenesis of Parkinson's disease.

In conclusion, Parkinson's disease is an age-related disorder characterized by protein misfolding, oxidative stress, and the staged appearance of Lewy pathology across various brain regions. The staged appearance of protein inclusions may be attributable to the spread of synucleinopathy across neuroanatomical circuitry as well as selective vulnerability differences. These latter two possibilities are not mutually exclusive and probably converge to determine

whether or not a given cell will develop protein inclusions and perhaps degenerate. The major goal of the present study was to determine whether two large brain areas, the allocortex of the temporal lobe and the neocortex of the frontal and parietal lobes exhibit intrinsic vulnerability differences that parallel the staged appearance of protein inclusions in allocortex followed by neocortex. If this hypothesis were supported, it would be consistent with the notion that selective vulnerability plays an important role in the topographical appearance of Lewy pathology in Parkinson's disease and would contribute a new model for the study of intrinsic vulnerability differences in experimental Parkinson's disease. Furthermore, the identification of factors that mediate selective vulnerability differences might accelerate the discovery of new targets and/or treatments for Parkinson's disease.

Materials and Methods

Animals

Animal use was approved by the Duquesne University Institutional Animal Care and Use Committee and carried out in accordance with the principles outlined in the *NIH Guide for the Care and Use of Laboratory Animals*. Female Sprague Dawley rats were fed *ad libitum* and singly housed in a room maintained at a constant temperature with a 12 hr light/dark cycle. Rats were sacrificed at 2-3.9 (n=6), 4-6 (n=6), 8-9 (n=6), 16-18.9 (n=5), and 19-22 (n=6) months of age for the aging study. These rats formed part of an in-house breeding colony designed to generate rat pup tissue for postnatal cultures. Tissue was dissected according to the definitions in the Paxinos rat atlas (Paxinos & Watson, 1998).

Chemicals and antibodies

Primary and secondary antibodies are listed in supplementary tables in the Appendix**.** Omission of primary antibodies from the assays always resulted in loss of signal. Proteasome inhibitors MG132 (EMD Millipore, Billerica MA, Cat. no. 474790) and PSI (Tocris, Minneapolis, MN, Cat. no. 4045) were stored at – 20 and – 80 ^{o}C, respectively, as 10 mM stock solutions in dimethyl sulfoxide (DMSO). H_2O_2 was purchased from Fisher Scientific (Pittsburgh, PA, Cat. no. H324) and stored at 4^{o}C as an 882 mM stock. The oxidative toxin paraquat (Sigma-Aldrich, St. Louis, MO) was dissolved in PBS (100 mM) and stored at -80 ^{o}C. Hsp70/Hsc70 activity was inhibited with the previously characterized compounds VER155008 (R&D Systems, Minneapolis, MN; Chatterjee et al., 2013; Massey et al., 2010; Saykally et al., 2012; Schlecht et al., 2013) and MAL3-101 (Adam et al., 2014; Braunstein et al., 2011; Hatic, Kane, Saykally, & Citron, 2012; Huryn et al., 2011; Kilpatrick et al., 2013). Hsp70 activity was enhanced with 115-7c (MAL1-271) (Kilpatrick et al., 2013; Wisen et al., 2010). Heme oxygenase 1 was inhibited

with tin protoporphyrin (SnPP) (Drummond & Kappas, 1981). Preformed α-synuclein fibrils (5mg/mL) were made as previously reported (Volpicelli-Daley, Luk, & Lee, 2014b). Fibrils were sonicated in a waterbath for 30 sec at room temperature immediately before use (Fisher Scientific FS6 Ultrasonic Cleaner Model B200).

Primary Cultures

All efforts were made to minimize animal suffering and to reduce the number of animals sacrificed. Animal use was approved by the Duquesne University Institutional Animal Care and Use Committee (protocol number 1006-06), and carried out in accordance with the principles outlined in the *NIH Guide*. Neocortical tissue and tissue from entorhinal allocortex, piriform allocortex, hippocampal allocortex, and olfactory bulb were dissected with microforceps from the brains of postnatal day 1 or 2 Sprague Dawley rats (Charles River, Wilmington, MA) and incubated in 10 Units/mL papain (Sigma-Aldrich, Cat. no. P3125) for 30 min. Following a second incubation in 10% type II-O trypsin inhibitor (Sigma-Aldrich, Cat. no. T9253), cells were triturated in Basal Medium Eagle (Sigma-Aldrich, Cat. no. B1522) containing 10% bovine calf serum (BME/BCS, HyClone Thermo Scientific, Logan, UT, Cat. no. 2151,) supplemented with 35 mM glucose (Sigma-Aldrich, Cat. no. G8769), 1 mM L-glutamine (Gibco, Life Technologies, Cat. no. 25030-081), 50 Units/mL penicillin, and 50 μg/mL streptomycin (Gibco, Life Technologies, Cat. no. 15140-122). Dissociated cells were then seeded in Opti-MEM (Gibco, Life Technologies, Cat. no. 51985-034) supplemented with 20 mM glucose at a plating density of 80,000-100,000 cells/well in 96-well plates or 2.35-3 million cells/well in 6-well plates (Corning Costar, Corning Incorporated, Corning, NY). All plates were precoated with poly-D-lysine (1 μg/mL) and laminin (1.88 μg/mL, BD Biosciences), washed, and dried prior to seeding. After a 2-hour incubation of plated cells in Opti-MEM, a full media change was performed

exchanging Opti-MEM for BME/BCS or Neurobasal-A media (Gibco, Life Technologies) supplemented with 2% v/v serum-free B27 (Gibco, Life Technologies) and 2 mM L-glutamine (Data in Figures 3-9 were from experiments conducted in BME/BCS whereas data in Figures 10-22 were from experiments conducted in Neurobasal-A media). Cells were treated on day-in-vitro 2 (DIV2).

Primary astrocytes were harvested from neocortex and allocortex. For the astrocyte cultures, entorhinal cortex was combined with piriform cortex to generate sufficient astrocytic material. Briefly, tissue was dissociated in Dulbecco's modified eagle medium (Gibco, Life Technologies) supplemented with 10% fetal clone III (Hyclone, Thermo Scientific) and 1% penicillin/streptomycin (Gibco, Life Technologies) after incubation with 0.25% trypsin with EDTA (Invitrogen, Life Technologies). After 7-9 days, cultures were placed overnight on an orbital shaker at 260 rpm. Two to three days later, astrocytes were passaged and seeded onto plates. Astrocyte cultures were treated with toxins on DIV5 and assayed on DIV7.

Validating dissections of neo- and allocortex

In order to visualize the full anatomical extent of our microdissections, we dissected neocortex and allocortex from postnatal day 1 brains and then fixed the dissected brains in 4% paraformaldehyde. Fixed brains were cryoprotected in 30% sucrose in phosphate-buffered saline (PBS) and cut at a thickness of 50 μm in the sagittal plane on a microtome (Thermo Scientific Microm HM 450, Walldorf, Germany). Sections were stained with infrared DRAQ5 (1:2000; BioStatus Limited, Leicestershire, UK) diluted in PBS with 0.3% Triton-X 100 (ACROS, Geel, Belgium) for permeabilization. Washed and dried slides were imaged at 21 μm resolution on an Odyssey Infrared Imager (LI-COR, model number 9201-01).

Toxin and inhibitor treatments

Because these cultures are initiated postnatally, the cortical neurons express high levels of punctate synaptic markers synaptophysin and synaptogyrin 3 already within a few days of culturing (R.K. Leak, unpublished observations). Treatments were begun on DIV2, 48 hours after plating). Cells were treated with 10× stocks of MG132, PSI, paraquat, or H_2O_2 added to BME/BCS III along with 2.5 μM cytosine arabinofuranoside to suppress, but not eliminate, glial proliferation or Neurobasal-A media supplemented with 2% v/v serum-free B27 and 2 mM L-glutamine. Twenty-four hours later (DIV3) fresh media was added. Multiple viability assays were then performed on DIV4 (see below). For inhibition of autophagy, 10× stocks of ammonium chloride (NH_4Cl, 20 mM; Acros Organics, Somerset, NJ) or wortmannin (50 nM; Sigma-Aldrich) were applied in conjunction with MG132 on DIV2 and freshly added on DIV3. N-acetyl cysteine (3 mM; Acros Organics), VER155008, MAL3-101, 115-7c, SnPP, and rapamycin (0.025 - 3.2 μM; Research Products International, Mt. Prospect, IL) were applied with this same protocol. For α-synuclein fibril treatments, cultures were treated with α-synuclein fibrils in a full media exchange on DIV2 and then fixed on DIV9.

Immunocytochemistry and viability assays

In order to gain a comprehensive view of cellular fitness, we used two independent rapid, unbiased assays, one for the neuronal marker MAP2 (see below) and one for ATP. ATP levels were assessed with a modification of the luciferase-based Cell Titer Glo assay (25 μl reagent in 50 μl media; Promega Inc., Madison, WI). Luminescence was measured within 15 minutes on a microplate reader (VICTOR^3 1420 multilabel counter; PerkinElmer, Waltham, MA).

For MAP2 immunocytochemistry, non-specific secondary binding was first minimized by blocking in a fish serum solution (Odyssey Block, LI-COR) diluted 1:1 in phosphate buffered

saline (PBS) with 0.3% Triton-X 100. This was followed by serial incubations in primary antibodies (2 hr or overnight) and secondary antibodies (1 hr) in the Odyssey Block:PBS solution with PBS washes in between steps. Infrared secondary antibody binding (700 and 800 nm) was visualized and quantified with Odyssey software (Version 3.0, LI-COR) on the Odyssey Infrared Imager. Neuronal and astrocyte cultures were stained with Hoechst (10 μg/ml Hoechst 33258, bisBenzimide) in phosphate-buffered saline with 0.3% Triton-X for 15-30 min for blinded cell counts. Astrocytes were also stained with the infrared nuclear stain DRAQ5 (1:10,000, 700 nm; Biostatus, Shepshed, Leicestershire, UK) and assayed on the Odyssey Imager to validate the Hoechst cell count data. In addition, cultures were immunocytochemically stained for the neuronal markers MAP2 and β-tubulin III, the astrocyte marker glial fibrillary acidic protein (GFAP), and/or the synaptic protein synaptophysin in the visible-range and photographed on an epifluorescence microscope for higher resolution images (Advanced Microscopy Group, Model #AMF-4301-US, Bothell, WA). $MAP2^+$ neurons, $GFAP^+$ astrocytes, and/or Hoechst-stained nuclei were then counted by a blinded observer at 20× magnification in a 0.213 mm^2 field of view (three fields per well).

For cultures treated with α-synuclein fibrils, inclusions were visualized by immunostaining for the aggregated form of α-synuclein (pSer129) (Anderson et al., 2006; Fujiwara et al., 2002; Hasegawa et al., 2002; Saito et al., 2003). Images were captured on an epifluorescence microscope as described previously. Hoechst-stained nuclei and α-$synuclein^+$ inclusions were quantified by a blinded observer using ImageJ software (National Institutes of Health, Bethesda, MD). The analyze particles command was used to count and measure objects by scanning the image until the edge of an object was located. The software then outlined the object and displayed the following measurements: particle count, average particle size, and area

fraction. Area fraction refers to the percentage of pixels in the image that have been segmented above background. “Background” was defined at the same level for all microphotographs.

Western immunoblots on in vitro and in vivo lysates

Cultured cells were incubated for 10 min with Cell Lysis Buffer (Cell Signaling, Danvers, MA) supplemented with protease inhibitors (Sigma, Cat. no. P8340) and 10 mM sodium fluoride (Leak, Castro, Jaumotte, Smith, & Zigmond, 2010) 24h after toxin treatments. For cultures treated with α-synuclein fibrils, lysates were collected on DIV9. Scraped cells were sonicated for 20 pulses at 1 sec each (Misonix Inc. Model XL2020 Farmingdale, NY). Protein content in total cell lysates was quantified by the bicinchoninic acid method according to the manufacturer’s instructions (ThermoScientific). Equal amounts of protein (10-30 μg) were then separated on 10% polyacrylamide gels by standard sodium dodecyl sulfate gel electrophoresis and transferred to Immobilon-FL polyvinylidene fluoride membranes (EMD Millipore). Membranes were incubated in the Odyssey Block fish serum solution or 5% milk in Tris buffered saline (TBS) for 30-60 min at room temperature. All membranes were then incubated in primary antibodies in 50% Odyssey block diluted in PBS with 0.1% Tween or 5% bovine serum albumin in TBS overnight at 4^{o}C on a shaker. The following day, blots were washed three times in PBS or TBS and incubated in the appropriate secondary antibody in the same diluent for 1 hour at room temperature. Washed blots were then visualized and quantified on the Odyssey Infrared Imager. All proteins were expressed as a fraction of β-actin, α-tubulin, or GAPDH to control for differences in protein loading across treatment groups. As multiple proteins were probed on the same blots, the identical loading controls are presented twice in some figures.

For *in vivo* immunoblotting, female Sprague-Dawley rats (Charles River) were sacrificed as a group at 2-3.9, 4-6, 8-9, 16-18.9, and 19-22 months of age. Tissue was weighed, sonicated in

the abovementioned Cell Lysis Buffer (20 μL buffer per mg tissue), and standard immunoblotting as described above was then performed.

Proteasome activity

Proteasome activity was assessed 30 min after MG132 treatment on DIV2 according to the manufacturer's instructions (Cayman Chemical Company, Ann Arbor, MI, USA). In this assay, Suc-LLVY-AMC generates a fluorescent product when cleaved by the proteasome. Fluorescent intensity was read at 355 nm excitation and 460 nm emission (VICTOR^3 1420 multilabel counter). Proteasome inhibitors epoxomicin and the tea polyphenol epigallocatechin gallate were used as negative controls during the assay but did not lead to greater loss of proteasome activity than MG132. In addition to negative controls, Jurkat cell lysates were used as a positive control as this cell type exhibits high basal levels of proteasome activity. Nuclear DRAQ5 and MAP2 immunostaining on parallel plates was used to ensure equal protein content across treatment groups.

Glutathione assay

Glutathione levels were measured in neo- and allocortical tissue as a function of age. Dissected tissue was weighed and sonicated in PBS containing 2 mM EDTA (100 μL solution per mg tissue). The manufacturer's instructions for the GSH-Glo assay for reduced glutathione were then followed (Promega Inc. Cat. no. V6911). This luminescent assay is based on conversion of a luciferin derivative into luciferin in the presence of glutathione and is catalyzed by glutathione-S-transferase. Data for each animal were collected in duplicate and expressed as relative luminescence units.

Thioflavin-S Staining

After fixation, hippocampal cultures were stained with 0.05% Thioflavin S (Sigma-Aldrich, St. Louis, MO) in phosphate buffered saline (PBS) at room temperature for 8 minutes and then washed 3 × 10 min with PBS. Images were captured with an epifluorescent microscope as stated above. Hoechst-stained nuclei and Thioflavin S^+ amyloid formations were quantified using ImageJ software as described above, using integrated density (product of area and mean gray value) as the measurement output.

Triton X-100 detergent extraction

Hippocampal cultures were treated with α-synuclein fibrils on DIV2. On DIV9, hippocampal neurons were fixed with 4% paraformaldehyde in the presence of 1% Triton X-100 for 20 min at room temperature followed by 3 × 200 µL PBS washes. Cells were stained with Hoechst and pSer129 antibodies and images were captured with an epifluorescent microscope as described above.

Statistical Analyses

Data are presented as the mean and SEM from 3-6 animals *in vivo* or a minimum of 3 independently run experiments *in vitro*. With the exception of Western blotting, each *in vitro* experimental group was run in three microplate wells, from which data were pooled to yield one average value for that experiment. Data were analyzed by one-, two-, or three-way ANOVA followed by the Bonferroni *post hoc* correction (Graphpad Prism Version 5d or SPSS Version 20, Armonk, NY). For semi-quantitative Western blotting data, the LSD *post hoc* test was employed. For data with only two groups, the two-tailed Student's *t*-test was employed. The Grubb's outlier test was performed once on all the data and bands with fluorescent lint or air

bubbles were excluded from the Western blot analyses. Differences were deemed significant only when $p \leq 0.05$.

Chapter 1

Rationale

All neurodegenerative diseases are characterized by severe disturbances in protein homeostasis, with the rate of formation of misfolded proteins out of balance with their clearance (Uversky, 2009; Walker & LeVine, 2000; Walker, Levine, Mattson, & Jucker, 2006). As a result of loss of protein homeostasis, all neurodegenerative disorders are also characterized by hallmark protein inclusions, such as α-synuclein^{+} Lewy bodies and Lewy neurites in Parkinson's disease. The neuroanatamist Heiko Braak used the distribution of α-synuclein^{+} protein aggregations to categorize Parkinson's disease into 6 distinct stages and hypothesized that the topographical spread of protein inclusions reflects the symptomatic progression of the disease (H. Braak, Del Tredici, Bratzke, Hamm-Clement, Sandmann-Keil, & Rüb, 2002; H. Braak, Del Tredici, Rüb, et al., 2003; Dickson, Uchikado, Fujishiro, & Tsuboi, 2010; Jellinger, 2011). Several studies have found that the presence of cortical inclusions correlates with cognitive impairments in Parkinson's patients (H. Braak, Rub, Jansen Steur, Del Tredici, & de Vos, 2005; Hurtig et al., 2000; Jellinger, 2006). According to the Braak staging scheme, the cortical spread of aggregated α-synuclein begins in the temporal meso- and allocortex whereas the primary sensorimotor regions of the frontal and parietal neocortex are affected only at the very end stages of the disorder. This observation suggests that the allocortex is more vulnerable to protein misfolding stress than the neocortex, ***although this had yet to be tested in an experimental model***. Thus, we developed a novel *in vitro* model of neo- and allocortex, using primary cells from the postnatal rat pup brain and treated these primary cultures in parallel with toxins that elicit protein-misfolding and oxidative stress. First, the primary culture model was characterized and the linearity and reproducibility of all our viability assays was assessed.

Specific Aim 1a: Develop novel neo- and allocortical primary neuron culture models and establish multiple independent viability assays for metabolic fitness and structural integrity.

Results

Characterization of Primary Neo- and Allocortical Cultures

Primary sensorimotor neocortex and entorhinal allocortex were dissected from postnatal day 1 or 2 rat pups and plated at 100,000 cells per well in BME/BCS III media. Cells were treated with 2.5 μM cytosine arabinofuranoside to suppress, but not eliminate, glial proliferation on DIV2. Hoechst staining for nuclei and immunostaining for the neuronal marker MAP2 in neo- and allocortical cultures revealed that the majority of cells present are indeed $MAP2^+$ (Fig. 3C, F). The long stemmed arrows in Figure 3 point to small, condensed nuclei that may be undergoing apoptosis and may therefore no longer express the MAP2 phenotype. The arrowheads point to large, flat nuclei, which may be astrocytic based on staining for GFAP (data not shown) (Fig. 3A, D). Nearly 75% of both neo- and allocortical cultures were found to be $MAP2^+$ (Fig. 3G). However, allocortical cells survived in BME/BCS III media at a higher density than neocortical cells, even though both were initially plated in parallel at the same density. Thus, allocortex had higher MAP2 levels in In-Cell Western analyses, as illustrated in the photomicrograph insert (Fig. 3H, I). In addition, allocortex also exhibited higher levels of ATP because of higher cell density. Photomicrographs of our dissections are illustrated in Figure 3J to show the anatomical boundaries of the areas harvested for study. For this image, postnatal day 1 rat brains were fixed in paraformaldehyde following the fresh tissue dissections, cut in the sagittal plane, and then stained with the nuclear marker DRAQ5 and imaged on an Odyssey imager.

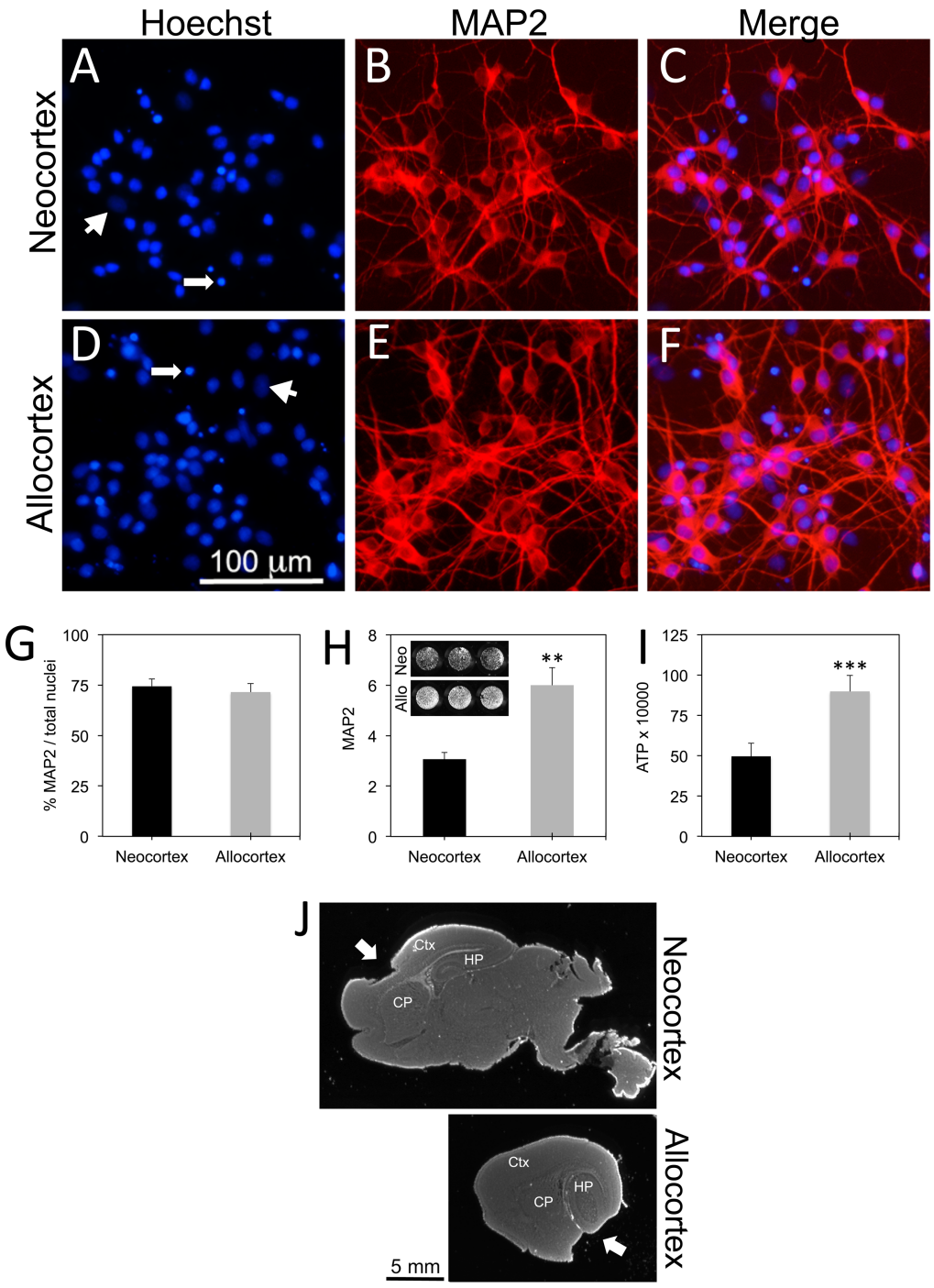

Figure 3. Characterization of in vitro model. **A-F:** Plates were immunostained on DIV4 for the neuronal marker microtubule associated protein 2 (MAP2, shown in red). Nuclei were stained blue with Hoechst. Merged images reveal that the majority of the Hoechst-stained nuclei were neuronal. However, arrowheads point to large nuclei that were possibly glial. Long stemmed arrows point to condensed, potentially apoptotic nuclei that may have lost their neuronal phenotype. **G:** Blind cell counts revealed that nearly 75% of neocortical and allocortical Hoechst-positive cells expressed the MAP2 neuronal phenotype. **H and I:** Basal survival on DIV4 was measured by an infrared In-Cell Western assay for MAP2 and by the Cell Titer Glo assay for ATP. Both assays revealed that allocortex survived *in vitro* conditions at approximately twice the rate of neocortex. A grayscale inset of a representative

infrared MAP2 stain of neo- versus allocortical neurons is included in **H**. Shown are the mean and standard error of the mean of at least 3 independent experiments. ** $p \leq 0.01$ or *** $p \leq 0.001$ by the two tailed *t*-test. **J:** Brains were fixed following tissue dissections, cut in the sagittal plane, and stained for the infrared nuclear marker DRAQ5. Neocortical dissections (arrow) were centered in primary motor and sensory cortex (Ctx), dorsal to hippocampus (HP) and caudoputamen (CP). Allocortical dissections (arrow) were centered much more laterally in the brain ventral to hippocampus in the entorhinal and piriform cortices. Reprinted from "Neocortex and Allocortex Respond Differentially to Cellular Stress *In Vitro* and *In Vivo*," by J. Posimo, A. Titler, H. Choi, A. Unnithan, and R. Leak 2013, *PLoS ONE,* 8(3): e58596. doi:10.1371/journal.pone.0058596. Copyright 2013 by Posimo et al. Reprinted with permission.

Verifying Viability Assay Linearity and Sensitivity in Neo- and Allocortical Cultures

In order to establish multiple independent and unbiased viability assays, rat primary neuronal cultures from the cerebral cortex were stained for the neuronal marker MAP2 (Fig. 4B) and the nuclear and cytoplasmic stain DRAQ5 + Sapphire (Fig. 4A). ATP levels were assessed with the Cell Titer Glo assay (Fig. 4C). Signal strength was then plotted as a function of plating density. The DRAQ5 + Sapphire assay was the least sensitive of all three assays as there was little difference in signal between 100,000 and 200,000 cells per well in the 700 nm channel (Fig. 4A). However, it should be noted that we only plated primary neuronal cells at 100,000 per well for subsequent experiments, a density at which DRAQ5 signal was not saturated. All three assays exhibited a linear correlation between plating density and signal strength, as noted by the R^2 values or the coefficient of determination (two tailed $p \leq 0.05$). Furthermore, changes in luminescence or signal strength were proportional to changes in cell number (ie, 50,000 cells have 50% of the signal of 100,000 cells). These observations demonstrate that the assays are sufficiently sensitive to changes in cell density at the plating densities employed.

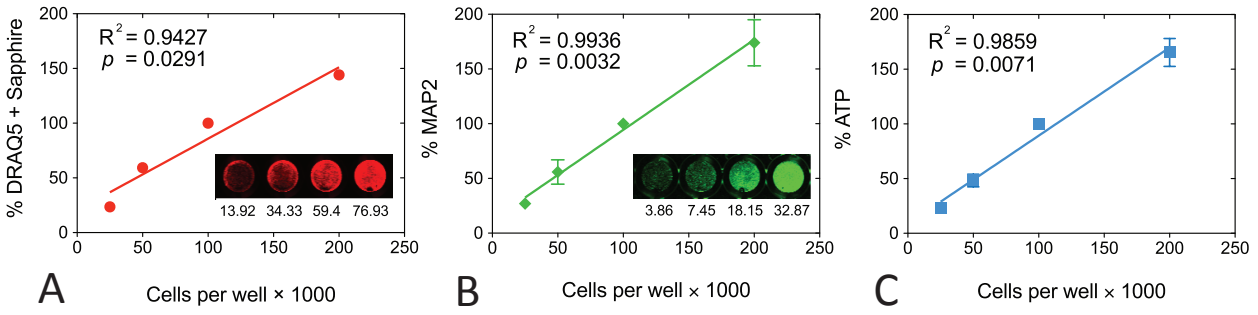

Figure 4: Linearity and sensitivity of viability assays in primary postnatal neurons **(A, B, C).** Signal strength for each assay is plotted as a function of plating density. Insets show representative infrared images of the DRAQ5 + Sapphire (A), or MAP2 (B) stain and raw intensity values are listed for each image. Note that the original infrared images were pseudocolored red (700 nm) or green (800 nm). Each experiment was performed in triplicate wells and repeated 3 times for DRAQ5 + Sapphire, 4 times for MAP2, 4 times for ATP. The data from the 3 wells were averaged for one final value for each experiment. The mean and SEM of these 3-4 final values is shown in the graph. Note that the DRAQ5 + Sapphire values exhibit low standard deviations so that SEM bars are not apparent. The R^2 coefficient of determination and two tailed *p* value assessing the significance of the correlation are also illustrated for each measure. Data were analyzed in Graphpad Prism (Version 6.0). Adapted from "Viability Assays for Cultured Cells," by J. Posimo, A. Unnithan, A. Titler, H. Choi, Y. Jiang, and S. Pulugulla. 2013, *J. Vis. Exp. (83),* e50645, doi:10.3791/50645. Copyright 2014 by Posimo et al. Adapted with permission.

Reproducibility of the Viability Assays

In order to measure the reproducibility of the assays within experiments (intraplate variability), we plotted the raw data from two replicate wells from experiments where cortical neurons were treated with H_2O_2 (Fig. 5A-C). Additionally, in order to measure reproducibility across experiments (interplate variability), we plotted the mean of triplicate wells from two separate plates (Fig 5D-F). The regression analyses illustrate a significant correlation between signal in replicate wells and across independent experiments for every measure. Primary neuronal cultures stained for MAP2 had the highest interplate variability. This might be attributed to the freezing and reuse of the MAP2 antibody or variability in the culturing procedure itself.

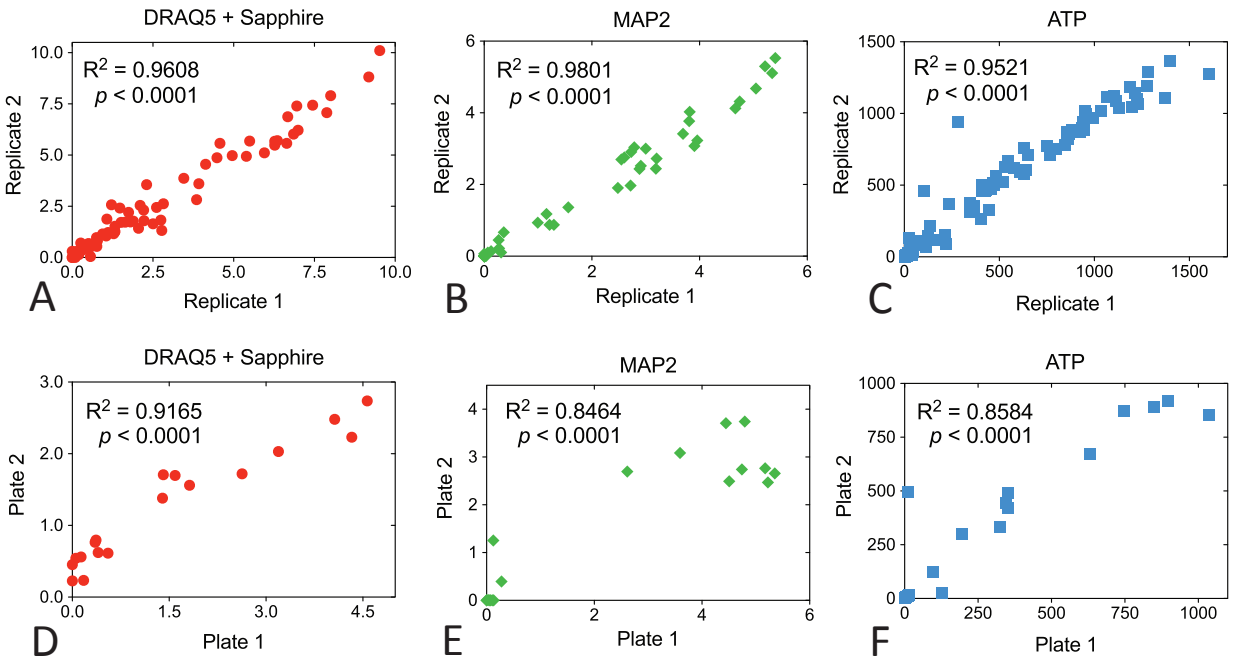

Figure 5: Intra- and inter-experimental variability in viability assays. All individual experiments were run in triplicate wells. Raw data from the second two wells within each group were plotted as replicates 1 and 2 to measure reproducibility within the plates (**A-C**). Data from the same groups in two independent experiments (the mean of the triplicate wells) were plotted as plate 1 and plate 2 to measure reproducibility across plates (**D-F**). The R^2 coefficient of determination and two tailed *p* value assessing the significance of the correlation are also illustrated for each measure. Data were analyzed in Graphpad Prism (Version 6.0). Adapted from "Viability Assays for Cultured Cells," by J. Posimo, A. Unnithan, A. Titler, H. Choi, Y. Jiang, and S. Pulugulla. 2013, *J. Vis. Exp. (83),* e50645, doi:10.3791/50645. Copyright 2014 by Posimo et al. Adapted with permission.

Discussion

Neo- and allocortex were microdissected from postnatal day 1-2 rat pup brains and used for our *in vitro* model. Nearly 75% of neo- and allocortical cells were found to be $MAP2^+$ when plated in BME/BCS III media supplemented with cytosine arabinoside to suppress glial growth. Relative to early embryonic cultures this may seem low, but postnatal studies typically report 50-80% neuronal purity or do not express neurons as a function of total cell numbers (Olivieri et al., 2011; Wang et al., 2006). The remaining large, flat nuclei may be astrocytic as they stain for glial fibrillary acidic protein (data not shown). Astrocyte genesis is known to peak in the early neonatal period (Miller & Gauthier, 2007), so it is not surprising that postnatal cultures have

more astrocytes than embryonic cultures. Glia play an important role in supporting neuronal function and modifying disease processes and are always present *in vivo*. Thus, having some glia present in our cultures is appropriate (Halliday & Stevens, 2011).

One potential caveat in our *in vitro* system was the higher basal survival in allocortical cultures. Higher allocortical cell density might increase the concentration of neuroprotective trophic factors in the extracellular media, leading to an increase in resilience. However, as shown in Specific Aim 1b, we observed opposite results with the oxidative toxin H_2O_2 and the proteasome inhibitor MG132, with allocortex being more vulnerable to MG132 but less vulnerable to H_2O_2, suggesting that cell density *per se* does not drive cell vulnerability in this model. Additionally, we switched to Neurobasal-A media in subsequent experiments, in which neo- and allocortical cultures survived equally well and exhibited similar vulnerabilities to oxidative stress and proteotoxicity.

Another potential caveat of our *in vitro* system was the possibility we had selected specific subpopulations of neo- and allocortical neurons that can survive the culturing process, thereby removing more vulnerable populations and leading to differential stress resistance. However, if this were true, it would be unlikely to observe the same density of $MAP2^+$ cells (expressed as a function of $Hoechst^+$ cell numbers) in neo- and allocortical cultures (Fig. 3G). Nonetheless, further studies to investigate phenotypically distinct subpopulations in these two brain regions *in vitro* and *in vivo* are highly warranted.

After characterizing the *in vitro* model, the linearity and reproducibility of the viability assays were assessed. As expected, the signal from all three viability assays was linearly correlated with plating density. For primary neurons, the DRAQ5+Sapphire stain was the least sensitive measure at high plating densities. Nonetheless, all three assays were well in proportion

to cell number when cultures were plated at 100,000 cells per well or below. As postnatal neurons are not known to replicate, we know that our measurements are not saturated or out of the dynamic range of the assay. Previous work is in agreement with our studies that multiple viability assays are more robust measures of cellular fitness than assays of one feature alone such as cell counts. (Gilbert et al., 2011).

For the vast majority of our studies, these three assays are used as an alternative to manual cell counts of nuclear numbers. Cell counting, when conducted properly and in blinded fashion, is an accurate means of assessing viability. If the ATP and infrared assays fail the linearity test, then manual cell counts are more appropriate. Nevertheless, some caveats of the latter method must be considered. For example, choosing a threshold nuclear diameter to differentiate between a live and dead cell is an arbitrary measurement as it is unknown from nuclear diameter alone when an irreversible apoptotic cascade begins. In comparison, our infrared assays do not depend on a continuous function such as nuclear diameter when making the distinction between live and dead cells. Instead, they avoid this pitfall by treating all cells still attached to the plate after fixation as live and all cells that have washed off as dead.

Manual cell counts also tend to only sample a small fraction of the well, which can lead to sampling bias and high standard deviations of the data. In contrast, our viability assays sample the entire well. This increases sampling size and abolishes the need for subjective decisions. In addition, the photographer must be blinded to the treatment of the cells for manual counts; a requirement that is often not met, as toxin-treated cells typically undergo obvious morphological changes such as atrophy or hypertrophy. Our viability assays do not demand that the investigator remain blinded. Finally, manual cell counts are a more time consuming process that the relatively quick ATP and infrared assays. The incubation period for the ATP assay is approximately fifteen

minutes while the scan on the Odyssey Imager for the infrared assays can be as short as five minutes.

On the other hand, the infrared assays also suffer from limitations. The infrared assays determine IC50s by measuring 50% loss of signal, not 50% loss of cell numbers *per se*. If signal changes in response to treatment because of hypertrophy or atrophy of the dendritic processes, the measurements would not necessarily reflect changes in cell numbers *per se*, although they would still reflect viability. As a result, it is important to immunocytochemically stain the same markers as used in the In-Cell Western and examine the cells by microscropy to determine structural changes upon toxin treatment. If the cytoplasm does change with toxin treatment, the DRAQ5 stain can be used to quantify nuclei to address this confound. However, the DRAQ5 signal will also be subject to changes in nuclear size.

The ATP assay was chosen over other metabolic measures such as the commonly used MTT assay due to its higher sensitivity and greater dynamic range. It has been reported that the ATP assay can detect a lower limit of 1562 cells per well whereas the MTT assay only has a lower limit of 25,000 cells per well (Petty, Sutherland, Hunter, & Cree, 1995). In addition, the ATP assay has a higher signal-to-noise ratio than the MTT assay (Riss & Moravec, 2004). Finally, the ATP assay is less time consuming and more economical than MTT as it has shorter incubation periods and a lower cost. Once again, it is important to bear in mind that metabolic activity may not always parallel cell numbers, especially when cells are exposed to low-level stress, which can cause a hormetic effect, or during necrosis when there is severe loss of ATP output. Therefore, it is critical that ATP measurements are accompanied with the use of a second viability assay.

In conclusion, the limitations of all assays must be borne in mind, whether high-throughput or manual, and multiple assays are always superior to a single assay as they generally afford a more comprehensive view of cellular integrity provided they are performed within the dynamic range of the assay and the instrument.

Specific Aim 1b: Create an *in vitro* model of differential vulnerability of neo- and allocortex and examine the underlying mechanisms. Test the hypothesis that neocortex is less vulnerable to proteotoxic and oxidative stress than allocortex *in vitro.*

Results

Toxicity of MG132 and Hydrogen Peroxide

Our next goal was to contrast neo- and allocortical vulnerability to protein misfolding and oxidative stress. We hypothesized that neocortex would be more resistant to both types of insults, reflecting the topography of neurodegeneration or protein inclusions in Alzheimer's and Parkinson's disease. First, neo- and allocortical cells were treated with various concentrations of the oxidative toxin H_2O_2 and assayed for MAP2 (Fig. 6A, B) and ATP (Fig. 6C). Allocortex was more resistant than neocortex to oxidative stress by both assays. Neo- and allocortex were then treated with the proteasome inhibitors MG132 (Fig. 6D-F) and PSI (Fig. 6G-J) to induce proteotoxic stress. Neocortex was more resistant than allocortex according to both assays and there was a significant statistical interaction between MG132 and brain region by a two-way analysis of variance of the MAP2 data ($p \leq 0.05$, F=2.411). These data support the view that the impact of MG132 on viability depends upon the brain region of origin. As with MG132, the difference in vulnerability of neo- and allocortex to proteotoxic stress was only evident at low concentrations of PSI (Fig. 6G-I) and not at higher concentrations (Fig. 6J). There was also a significant interaction between PSI and brain region, verifying that the topographic origin of the cells in culture determined the toxic response to proteasome inhibition ($p \leq 0.001$, F=13.99 for MAP2, $p \leq 0.001$, F=15.07 for ATP). A third proteasome inhibitor was also used, ALLN, which elicited a similar response, with neocortex being less vulnerable than allocortex (data not shown). Blinded counts of $MAP2^+$ neurons by higher resolution microscopy validated the high-

throughput In-Cell Western assay, as significant neuronal loss after MG132 treatment was only evident in allocortex cultures (Fig. 6K, L). The neuron counts are presented in Figure 6L as the raw numbers in order to illustrate the difference in basal survival in neo- and allocortex. In sum, these data partially supported our hypothesis, as neocortex is less vulnerable than allocortex to proteotoxic stress, but more vulnerable than allocortex to oxidative stress.

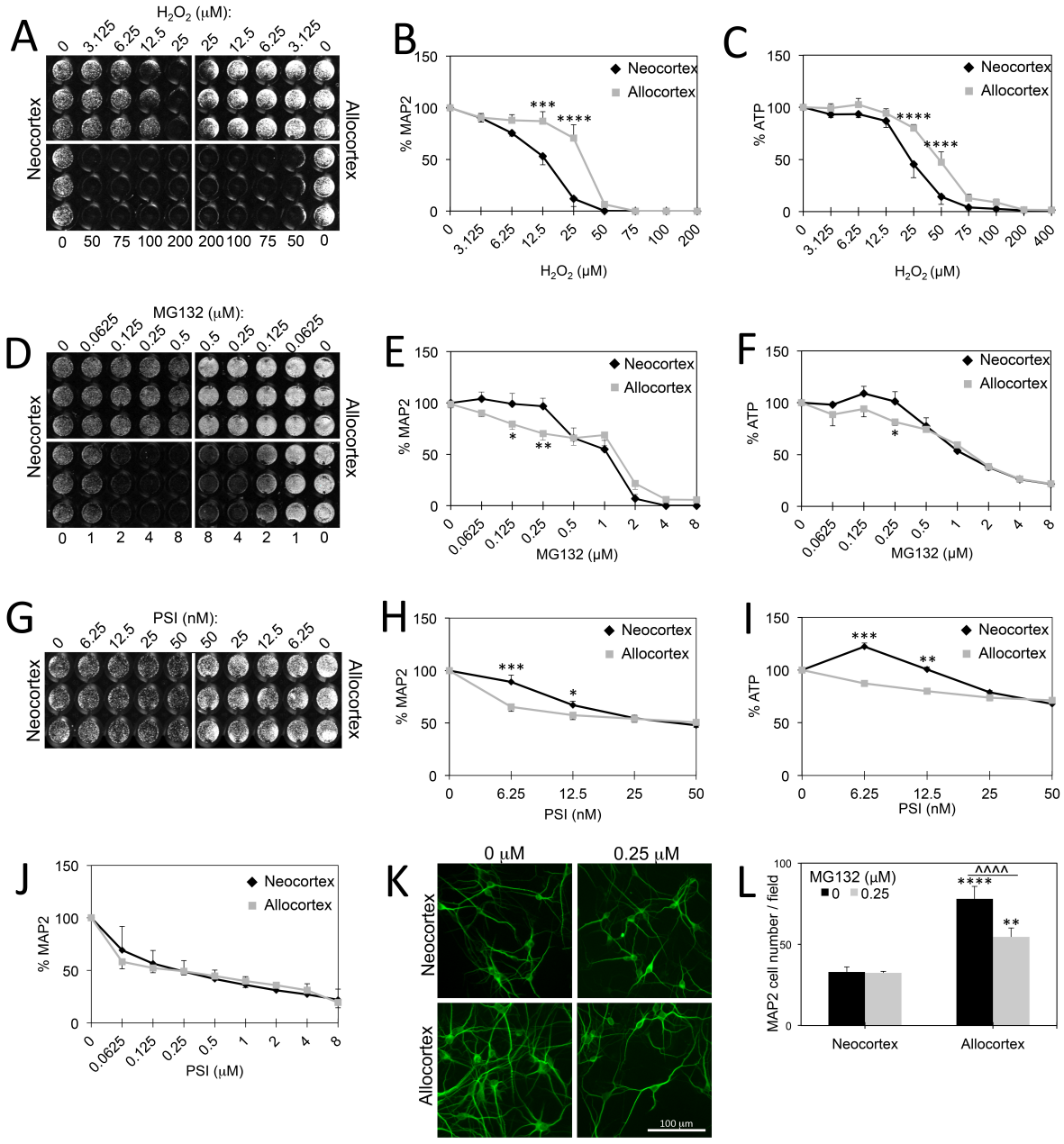

Figure 6. Differential vulnerability of neo- and allocortex to toxins. **A-C**: Neo- and allocortical cultures were treated with indicated concentrations of hydrogen peroxide. Allocortex was more resistant to oxidative stress by both MAP2 (**A and B**) and ATP assays (**C**). **D-F:** Neo- and allocortical cultures were treated with indicated concentrations of MG132 and assayed for MAP2 (**D and E**) and ATP (**F**). Both assays revealed that neocortex was less sensitive to low concentrations of this proteasome inhibitor. **G-I**: Neo- and allocortical cultures were treated with indicated concentrations of PSI and assayed for MAP2 (**G, H, and J**) and ATP (**I**). Allocortex was more vulnerable to low, but not high concentrations of PSI. Shown are the mean and standard error of the mean of at least 3 independent experiments. * $p \leq 0.05$, ** $p \leq 0.01$, *** $p \leq 0.001$, or **** $p \leq 0.0001$ versus neocortex at the same MG132 concentration, Bonferroni *post hoc* correction following two-way ANOVA. **K:** Representative higher resolution photomontage of MAP2 immunostained neocortical and allocortical neurons treated with 0.25 μM MG132 or vehicle (dimethyl sulfoxide, DMSO). **L:** Neurons were counted by a blind observer at 200x magnification in a 0.213 mm^2 field of view (three fields per well). Raw cell counts are shown to illustrate that there were more allocortical neurons under basal conditions. However, allocortical neurons were more vulnerable to 0.25 μM MG132. Shown are the mean and standard error of the mean of four independent experiments. ** $p \leq 0.01$, **** $p \leq 0.0001$ versus neocortex; ^^^^ $p \leq 0.0001$ MG132 versus vehicle (0 μM MG132); Bonferroni *post hoc* correction following two-way ANOVA. Adapted from "Neocortex and Allocortex Respond Differentially to Cellular Stress *In Vitro* and *In Vivo*," by J. Posimo, A. Titler, H. Choi, A. Unnithan, and R. Leak 2013, *PLoS ONE,* 8(3): e58596. doi:10.1371/journal.pone.0058596. Copyright 2013 by Posimo et al. Adapted with permission.

Interaction between Autophagy and the Ubiquitin-proteasome System

In Parkinson's disease and Alzheimer's disease, the more vulnerable allocortical regions are more likely to harbor lipofuscin pigments, lipid residues of failed lysosomal digestion (H. Braak et al., 2000; H. Braak, Rüb, et al., 2006). Thus, we hypothesized that autophagic clearance of cellular debris would be lower in allocortex than neocortex. Two proteins whose levels reflect macroautophagic clearance, Beclin 1 and LC3BII, were not affected by MG132 in neo- or allocortex (Fig. 7A, B). However, when the pan-autophagy inhibitor NH_4Cl was applied, neocortex became as vulnerable as allocortex to 0.25 μM MG132. NH_4Cl is a weak base that neutralizes lysosomal pH, thereby dramatically inhibiting autophagic protease activity (Fuertes, Martin De Llano, Villarroya, Rivett, & Knecht, 2003; Kaushik & Cuervo, 2009; Klionsky, Cuervo, & Seglen, 2007). In addition, no further exacerbation of toxicity was observed with NH_4Cl in allocortex (Fig. 7C). The macroautophagy inhibitor wortmannin was also applied but no enhancement of toxicity was observed in either neo- or allocortex (Fig. 7D). Furthermore, the macroautophagy enhancer rapamycin was applied in the presence or absence of MG132, but no protection against MG132 toxicity was observed (data not shown). These results suggest

neocortex may rely on chaperone-mediated or microautophagy to defend against the proteotoxic stress caused by MG132 treatment but that allocortex does not rely on any form of autophagy to defend against MG132. Repeated attempts were then made to immunostain neo- and allocortical cells or to probe by Western blot the chaperone-mediated autophagy marker lysosome-associated membrane protein type-2a (LAMP2a), but three antibodies were found to be non-specific in our cultures. Moreover, the size of the effect of autophagy inhibition was small, and so we focused instead on the role of the ubiquitin-proteasome system in subsequent experiments.

Ubiquitin is attached to misfolded proteins to target them for proteasomal degradation. There was a significant rise in ubiquitin-conjugated protein levels with MG132 treatment in both neo- and allocortex. However, allocortex had significantly higher ubiquitin-conjugated protein levels than neocortex at both 0.25 μM and 1 μM MG132 (Fig 7E, F). Proteasome activity was also measured to gauge the functional integrity of the ubiquitin-proteasome particles. Neo- and allocortical cells had significantly reduced chymotrypsin-like proteasome activity following treatment with MG132. However, allocortex proteasome activity levels were significantly lower than those of neocortex following treatment with 0.25 μM and 1 μM MG132 (Fig. 7G). In sum, these data suggest that the ubiquitin-proteasome system for degrading damaged proteins is more easily compromised in allocortex than neocortex.

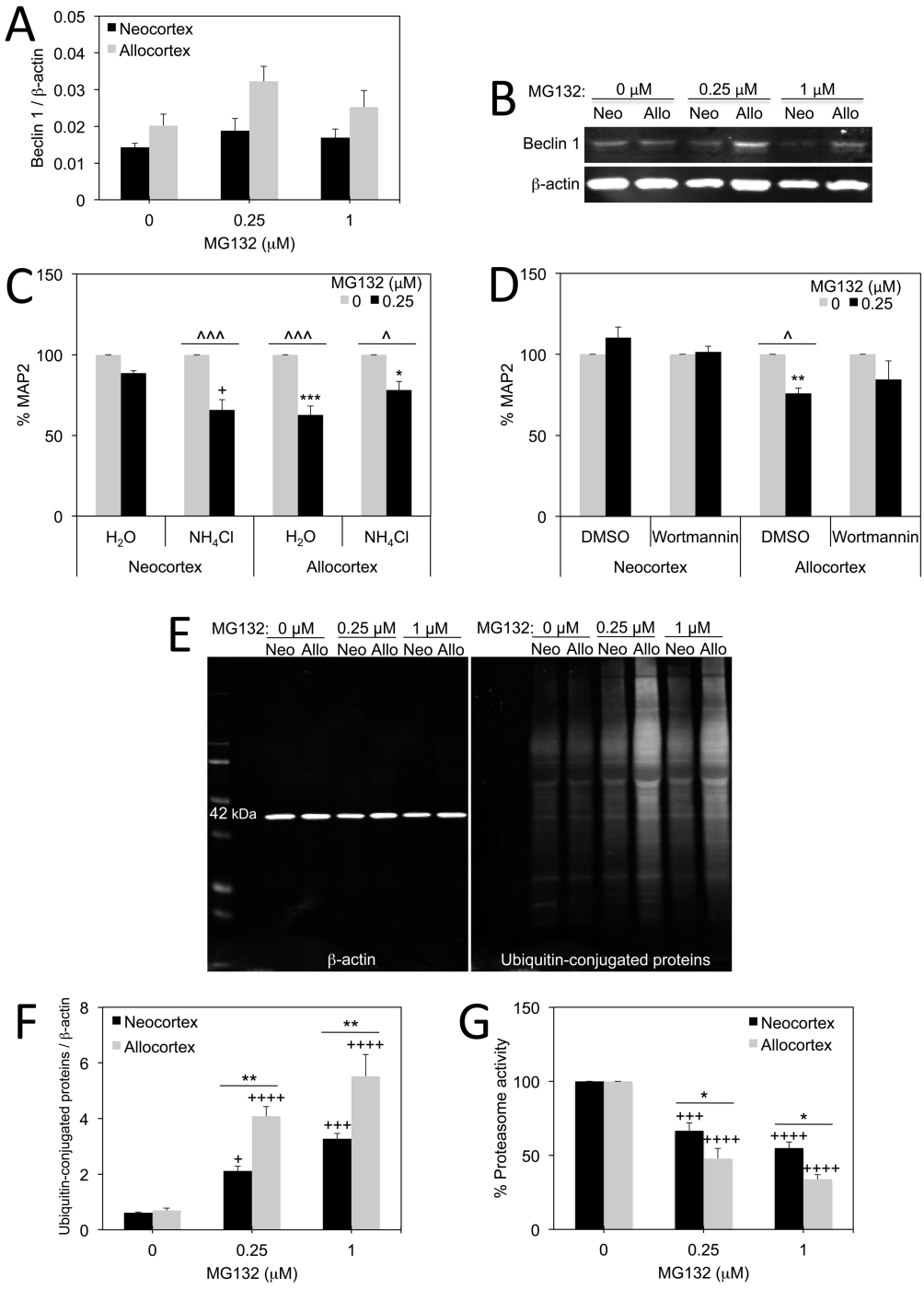

Figure 7. Involvement of autophagic defenses and ubiquitin-proteasome system. **A-B:** Infrared Western immunoblotting for macroautophagy-related molecule Beclin 1 following treatment of neo- and allocortical cultures with 0.25 and 1 μM MG132 is shown. β-actin was used as a loading control. **C-D**: Ammonium chloride (20 mM NH_4Cl) was used to inhibit all forms of autophagy and wortmannin (50 nM) was used to inhibit macroautophagy in neo- and allocortical cultures subjected to vehicle or 0.25 μM MG132. Neocortical neurons became as vulnerable to MG132 as allocortical neurons in response to NH_4Cl. Wortmannin failed to elicit an effect. Shown are the mean and standard error of the mean of at least 3 independent experiments. * $p \leq 0.05$, ** $p \leq 0.01$, *** $p \leq 0.001$ allocortex vs neocortex; ^ $p \leq 0.05$ or ^^^ $p \leq 0.001$ MG132 vs vehicle; + $p \leq 0.05$ NH_4Cl versus vehicle; Bonferroni *post hoc*

correction following two-way ANOVA. **E-F:** Infrared Western immunoblotting for ubiquitin-conjugated proteins revealed that allocortex exhibited higher levels of this measure of proteotoxic stress in response to MG132. **G:** Proteasome activity was measured in the presence or absence of MG132 in a fluorogenic assay. Allocortical proteasomes were more inhibited by MG132 than those from neocortex. Shown are the mean and standard error of the mean of at least 3 independent experiments. For F and G, * $p \leq 0.05$, ** $p \leq 0.01$ allocortex versus neocortex; + $p \leq 0.05$, +++ $p \leq 0.001$, ++++ $p \leq 0.0001$ MG132 versus vehicle (0 μM MG132); Bonferroni *post hoc* correction following two-way ANOVA. Reprinted from "Neocortex and Allocortex Respond Differentially to Cellular Stress *In Vitro* and *In Vivo*," by J. Posimo, A. Titler, H. Choi, A. Unnithan, and R. Leak 2013, *PLoS ONE,* 8(3): e58596. doi:10.1371/journal.pone.0058596. Copyright 2013 by Posimo et al. Reprinted with permission.

Neo/Allocortical Differences in Stress-sensitive Proteins

The activated 26S proteasome is formed when PA700 (the 19S regulator) binds to the 20S proteasome particle. The 20S proteasome particle is activated by the binding of PA28 (the 11S activator) (Pickering et al., 2010; Voges, Zwickl, & Baumeister, 1999). PA700 interacts with the catalytic core in an ATP-dependent manner, thereby providing misfolded proteins access to the core particle. The activated 20S proteasome degrades short peptides and non-ubiquitinated proteins in an ATP-independent manner (Besche, Peth, & Goldberg, 2009; F. Shang & Taylor, 2011; Voges et al., 1999). There was no significant difference in basal levels of the proteasome activators PA28 and PA700 in neo- and allocortex. However, allocortex expressed significantly higher levels of the proteasome regulators PA28 and PA700 than neocortex following MG132 treatment (Fig 8A-C). These findings provide evidence of compensatory changes in allocortex in response to proteotoxic stress, perhaps because it is under more stress than neocortex.

Hsp70 refolds denatured proteins or guides irreparably damaged proteins to the proteasome or lysosome for degradation (Aridon et al., 2011; Kalia, Kalia, & McLean, 2010; Lanneau, Wettstein, Bonniaud, & Garrido, 2010). Hsp70 protects neurons in many experimental models of neurodegeneration (Kalia et al., 2010; Sherman & Goldberg, 2001). For example, Hsp70 offsets apoptosis and ameliorates MPTP, α-synuclein, and β-amyloid toxicities (Dong, Wolfer, Lipp, & Büeler, 2005; Klucken, Shin, Masliah, Hyman, & McLean, 2004; Magrané,

Smith, Walsh, & Querfurth, 2004; Moloney et al., 2014; Nagel et al., 2008). Therefore we examined Hsp70 levels in neo- and allocortex cultures. Treatment with 1 μM MG132 significantly increased neo- and allocortical levels of Hsp70 (Fig. 8D, E). When illustrated as a fold change (allocortex Hsp70 levels as a function of neocortex Hsp70 levels), allocortex was found to express significantly higher levels of Hsp70 than neocortex following treatment with 0.25 μM MG132 (Fig. 8F).

Heme oxygenase 1 (HO1; aka Hsp32) is an inducible enzyme essential for heme catabolism into carbon monoxide and the antioxidant biliverdin (Aztatzi-Santillán, Nares-López, Márquez-Valadez, Aguilera, & Chánez-Cárdenas, 2010; Grochot-Przeczek, Dulak, & Jozkowicz, 2012; Schipper, Song, Zukor, Hascalovici, & Zeligman, 2009; Wu, Ho, & Yet, 2011). In Parkinson's disease, HO1 expression is increased in astrocytes and can be found in Lewy bodies (Schipper, Liberman, & Stopa, 1998). Levels of HO1 were significantly increased in both neo- and allocortex with MG132 treatment (Fig. 8G). However, allocortex had significantly higher HO1 levels following treatment with 1 μM MG132 than neocortex.

Catalase is an enzyme that catalyzes the breakdown of H_2O_2 into water and oxygen. Catalase activity is decreased in the hippocampus of aged humans and in the SNpc of Parkinson's patients (Fahn & Cohen, 1992; Venkateshappa, Harish, Mahadevan, Srinivas Bharath, & Shankar, 2012). Catalase levels rose significantly in allocortex following MG132 treatment and were significantly higher in allo- than neocortex following treatment with 0.25 μM MG132 (Fig. 8I, J).

Ceruloplasmin is a copper chaperone and ferroxidase protein that promotes the transport of iron out of cells and exhibits antioxidant properties (Hineno et al., 2011; Kaneko et al., 2008; Texel et al., 2011). Ceruloplasmin deficient mice are more vulnerable to rotenone and stroke

(Brewer et al., 2010; Capo et al., 2008; Kaneko et al., 2008; Kessler et al., 2006; Squitti, Quattrocchi, Salustri, & Rossini, 2008; Texel et al., 2011). Furthermore, Parkinson's patients exhibit low ceruloplasmin levels in the cerebrospinal fluid and serum while free copper levels are raised (Boll et al., 2008; Torsdottir, Kristinsson, Snaedal, Sveinbjörnsdóttir, et al., 2010). Neocortex exhibited significantly higher levels of the ferroxidase ceruloplasmin basally and following treatment with 0.25 μM MG132 (Fig. 8K, L). The patterns of higher HO1, Hsp70, and catalase expression in allocortex suggest that allocortex has greater need of those defenses in response to MG132 toxicity, whereas the basally higher expression of ceruloplasmin in neocortex suggests that it might have higher antioxidant defenses and superior iron homeostasis. It is also possible that allocortex is more resistant to oxidative stress because of higher catalase expression, although further Western blotting studies are needed to confirm this. Furthermore, in order to confirm the mechanistic role of these proteins, they must be knocked down with RNA interference or inhibited as in Aim 2.

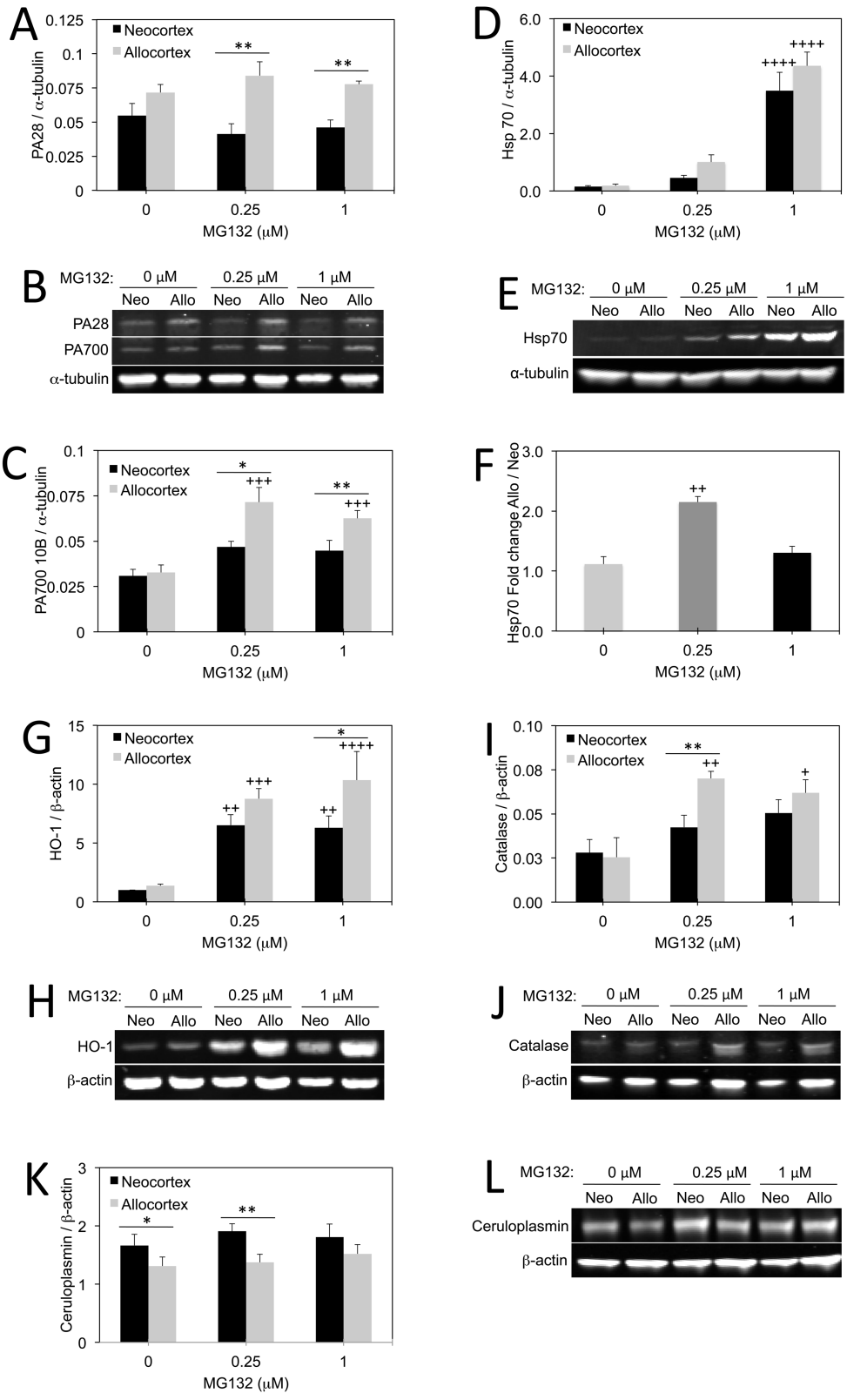

Figure 8. Protein changes in neo- and allocortex in response to proteasome inhibition. **A-G**: Western immunoblotting for PA28 (**A**, **B**), PA700 10B (**B**, **C**), heat shock protein 70 (Hsp70; **D**, **E**, **F**), heme oxygenase 1

(HO-1, also known as Hsp32; **G**, **H**), catalase (**I**, **J**), and ceruloplasmin (**K**, **L**) in neocortical and allocortical cultures treated with indicated concentrations of MG132. Shown are the mean and standard error of the mean of at least 3 independent experiments. * $p \leq 0.05$, ** $p \leq 0.01$ allocortex versus neocortex; + $p \leq 0.05$, ++ $p \leq 0.01$, +++ $p \leq 0.001$, ++++ $p \leq 0.0001$ MG132 versus vehicle; Bonferroni *post hoc* correction following one or two-way ANOVA. Reprinted from "Neocortex and Allocortex Respond Differentially to Cellular Stress *In Vitro* and *In Vivo*," by J. Posimo, A. Titler, H. Choi, A. Unnithan, and R. Leak 2013, *PLoS ONE,* 8(3): e58596. doi:10.1371/journal.pone.0058596. Copyright 2013 by Posimo et al. Reprinted with permission.

Involvement of Glutathione in Defense Against Proteotoxicity

Loss of the ubiquitous tripeptide antioxidant glutathione is one of the earliest pathologies in Parkinson's disease (Martin & Teismann, 2009; Sian, Dexter, Lees, Daniel, Agid, et al., 1994; Sofic et al., 1992; Zeevalk et al., 2008). Thus, we measured glutathione levels in neo- and allocortex in the absence and presence of MG132 exposure. Glutathione levels were significantly higher in neocortex than allocortex, both basally and following 0.25 μM MG132 treatment (Fig. 9A). In order to determine the role of glutathione in the differential vulnerability of neo- and allocortex to MG132-induced proteotoxicity, glutathione levels were decreased with the glutamate cysteine ligase inhibitor buthionine sulfoximine (BSO). MAP2 and glutathione levels were measured in neo- and allocortex after treatment with BSO. BSO was not toxic until concentrations of 50 μM were reached (data not shown). Significant decreases in glutathione were apparent in neocortex with concentrations as low as 3.125 μM BSO (Fig. 9B, C). No significant decrease in glutathione levels was observed in allocortex in response to BSO. Nonetheless, MG132-induced cell loss was exacerbated by BSO in neurons from both regions (Fig. 9D, E). These findings suggest that endogenous antioxidant defenses from glutathione help mitigate proteotoxicity in neocortex.

The thiol N-acetyl cysteine has been shown to improve cognitive function in Alzheimer's disease (Adair, Knoefel, & Morgan, 2001) and is currently undergoing clinical trials in Parkinson's patients (ClinicalTrials.gov Identifier: NCT02212678). N-acetyl cysteine has also

been shown to increase brain and blood glutathione levels in Parkinson's patients (Holmay et al., 2013). Therefore, we tested the hypothesis that N-acetyl cysteine would protect allocortical cells by raising glutathione levels. As expected, treatment with N-acetyl cysteine protected allocortex from MG132 toxicity, rendering it as resilient as neocortex (Fig. 9F, G). These results support the use of N-acetyl cysteine in neurological conditions that affect the allocortex of the telencephalon.

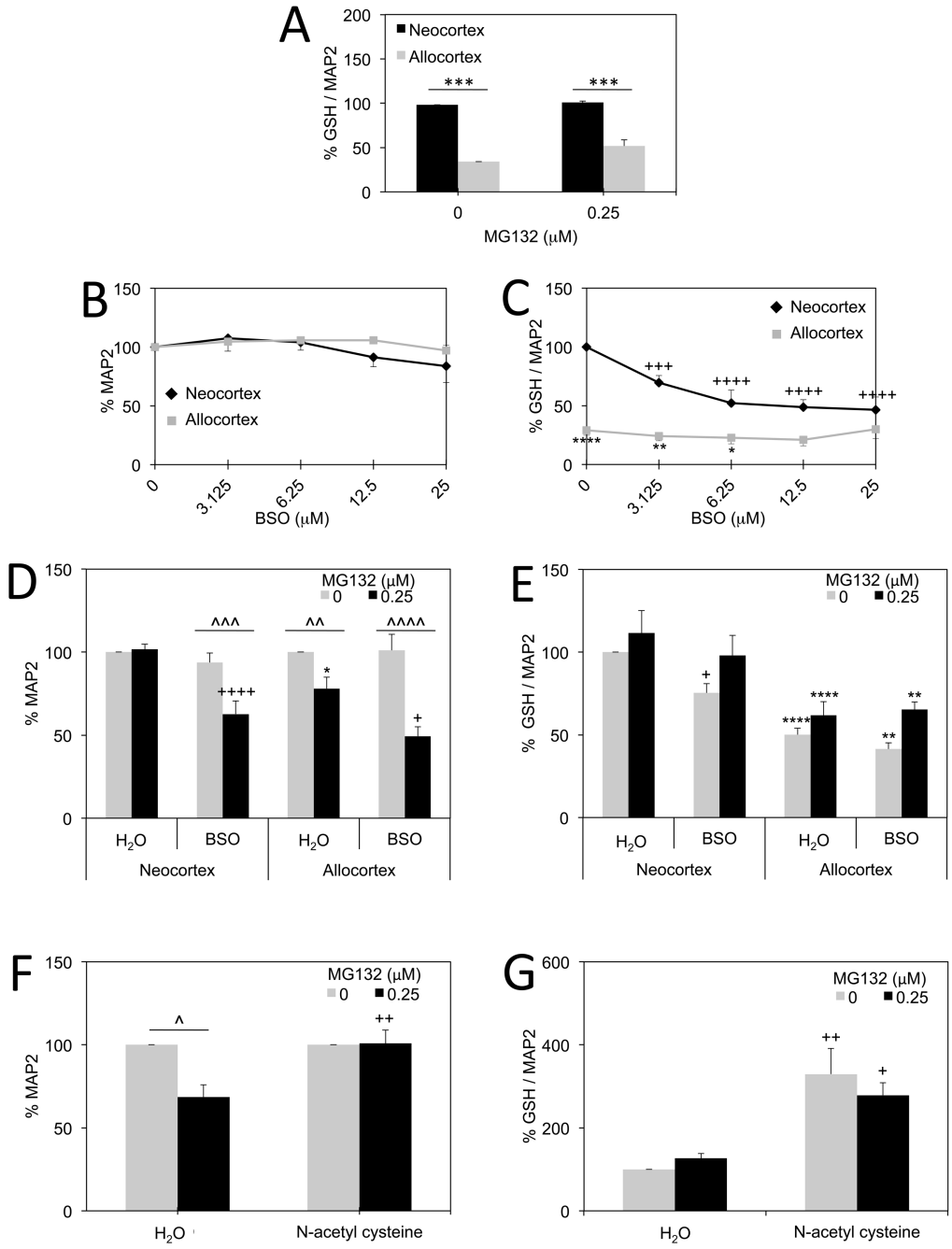

Figure 9. Role of glutathione in protection of neo- and allocortex against proteasome inhibition. **A**: Glutathione (GSH) levels as a function of total MAP2 levels in neocortex and allocortex in the presence or absence of MG132. Allocortical cells exhibited less glutathione than neocortical cells in both conditions *in vitro*. **B-C**: MAP2 levels (**B**) and glutathione levels (**C**) as a function of indicated concentrations of buthionine sulfoximine (BSO). Neocortical cells exhibited much greater glutathione loss with buthionine sulfoximine than allocortical cells. Buthionine sulfoximine was not lethal to neurons at the indicated concentrations. **D-E**: Neocortical and allocortical neurons were treated with vehicle or MG132 (0.25 μM) and vehicle or buthionine sulfoximine (12.5 μM). Both allocortical neurons and neocortical neurons were more vulnerable to combined treatment with buthionine sulfoximine and MG132 than either toxin alone (**D**). The glutathione assay revealed again that neocortical cells lost more glutathione with buthionine sulfoximine than allocortical cells, but that allocortical cells had overall less glutathione than

neocortical cells in all four groups (**E**). F-G: N-acetyl cysteine (3 mM) completely prevented the toxicity of 0.25 μM MG132 in allocortical cultures (**F**) and considerably raised glutathione levels both with and without MG132 on board (**G**). Shown are the mean and standard error of the mean of at least 3 independent experiments. For all panels, * $p \leq 0.05$, ** $p \leq 0.01$, *** $p \leq 0.001$, or **** $p \leq 0.0001$ allocortex versus neocortex; ^ $p \leq 0.05$, ^^ $p \leq 0.01$, ^^^ $p \leq 0.001$, or ^^^^ $p \leq 0.0001$ MG132 versus vehicle; + $p \leq 0.05$, ++ $p \leq 0.01$, +++ $p \leq 0.001$, ++++ $p \leq 0.0001$ buthionine sulfoximine versus water or N-acetyl cysteine versus water; Bonferroni *post hoc* correction following two-way ANOVA. Reprinted from "Neocortex and Allocortex Respond Differentially to Cellular Stress *In Vitro* and *In Vivo*," by J. Posimo, A. Titler, H. Choi, A. Unnithan, and R. Leak 2013, *PLoS ONE,* 8(3): e58596. doi:10.1371/journal.pone.0058596. Copyright 2013 by Posimo et al. Reprinted with permission.

Discussion

The present study is the first to report that the neo- and allocortex are differentially vulnerable to low levels of proteotoxicity, consistent with the staged appearance of protein aggregations in the cortical edifice in Parkinson's disease (H. Braak, Del Tredici, Rüb, et al., 2003; H. Braak, Rüb, et al., 2006; Stranahan & Mattson, 2010). Although neocortex was more resistant to proteotoxic stress, it was more vulnerable to oxidative stress than allocortex, as shown following exposure to two oxidative toxins: paraquat and H_2O_2. This unexpected finding was consistent with the higher survival rates of allocortex in BME/BCS media, as cell culture procedures are thought to elicit high basal levels of oxidative stress on their own (Halliwell, 2014). Neurobasal media with B27 supplementation may offer superior antioxidant support, leading to significant improvements in neuronal survival (C. Xie, Markesbery, & Lovell, 2000). The discrepancy between the responses to proteasome inhibitors and oxidative toxins was unexpected because 1) oxidative and proteotoxic stress typically work in synergistic manners and 2) allocortical cultures exhibited lower levels of two antioxidants, ceruloplasmin and glutathione, than neocortical cultures. On the other hand, the allocortex is known to exhibit less myelination than neocortex and therefore may be subjected to higher metabolic demands and higher levels of oxidative stress *in vivo* (H. Braak, Rüb, Gai, & Del Tredici, 2003). In response to poor myelination and higher free radical levels, allocortex may have evolved greater defenses against oxidative injuries. Alternatively, postnatal allocortex cultures from rat pups may not reflect the

selective vulnerabilities that are evident *in vivo* in humans, especially in aged human subjects. It is worth noting that Braak's staging scheme is not based on measures of oxidative stress *per se* but on immunohistochemical staining for misfolded α-synuclein, an established sign of proteotoxic stress. Furthermore, the frontal neocortex does exhibit high levels of oxidative stress in incidental Lewy body disease (Dalfó et al., 2005), suggesting that our H_2O_2 results may indeed reflect conditions in the diseased human brain. It is also possible that neocortical vulnerability to oxidative stress reflects the earlier amyloid deposition in this structure in Alzheimer's disease (H. Braak & Braak, 1991), although amyloid deposition does not correlate with cell loss or with clinical symptoms (Arriagada et al., 1992; Bierer et al., 1995; Giannakopoulos et al., 2003). In contrast to the findings with oxidative toxins, neocortex was more resilient than allocortex following exposure to the proteasome inhibitors MG132 and PSI, as shown by two independent viability assays and as confirmed by manual counts of $MAP2^+$ neuronal elements. These results indicate that proteasome inhibitors are more appropriate than oxidative toxins for modeling the topography of α-synuclein and tau inclusions in Parkinson's and Alzheimer's disease. As with any cell culture model, one important limitation is that cell death is acute *in vitro* compared to the extended neurodegenerative process that unfolds over decades in patients. MG132 and H_2O_2 are nevertheless relevant to Parkinson's disease because inhibition of the ubiquitin-proteasome system and indices of oxidative stress are evident in the disorder (Alam et al., 1997; D. Dexter et al., 1986; Floor & Wetzel, 1998; Jenner, 1998; McNaught et al., 2003; McNaught, Belizaire, Jenner, Olanow, & Isacson, 2002; McNaught & Jenner, 2001; Sian, Dexter, Lees, Daniel, Agid, et al., 1994).

The two major intracellular protein degradation systems, the ubiquitin proteasome system and autophagy, are both highly neuroprotective and prevent loss of protein homeostasis

(Nedelsky, Todd, & Taylor, 2008). Thus, both of these systems were investigated in our primary culture model to assess the role they may play in the differential vulnerability of neo- and allocortex to proteotoxic stress. The macroautophagy inhibitor, wortmannin, exerted no impact on neo- and allocortical vulnerability to MG132, suggesting that neurons from either region do not rely on macroautophagy for protection against MG132. Additionally, raising macroautophagy defenses with rapamycin failed to protect allocortex against MG132. NH_4Cl, a pan autophagy inhibitor, had no impact on MG132 toxicity in allocortex. Thus, we conclude that allocortex does not rely on autophagy to battle MG132-associated proteotoxicity *in vitro*. In contrast, when neocortex was treated with NH_4Cl, MG132 toxicity was significantly exacerbated. Therefore, neocortical cells may rely on chaperone-mediated or microautophagy for protection against proteasome inhibition. These differences in autophagic defenses in neo- and allocortex are consistent with previous observations that lipofuscin granules–evidence of autophagy failure–are more prevalent in regions with denser protein inclusions (H. Braak et al., 2000; H. Braak, Rüb, et al., 2006). Efforts to differentiate between these different types of autophagy were abandoned due to a lack of specificity of three different LAMP2a antibodies and the small effect size following NH_4Cl treatment. Thus, we focused our efforts on the role of the ubiquitin proteasome system instead.

Consistent with Braak staging schemes, allocortex was subjected to greater proteotoxic stress than neocortex according to the viability assays, proteasome activity data, and ubiquitin-conjugated protein levels. As expected, allocortical proteasome activity levels were even lower than neocortical levels following MG132 treatment. In addition, ubiquitin-conjugated protein levels rose significantly higher following MG132 treatment, especially in allocortex, suggesting that MG132 was effective in reducing misfolded protein clearance in both regions. Allocortex

also exhibited higher levels of the proteasome activators PA700 and PA28 than neocortex. This may seem unexpected because allocortex exhibited higher levels of ubiquitin-conjugated proteins than neocortex and therefore might be hypothesized to have fewer proteasome particles. However, the results are consistent with previous studies showing that proteasome subunit levels are increased in the presence of elevated ubiquitin-conjugated proteins (Bazzaro et al., 2006). Thus, we speculate that higher levels of proteotoxic stress in allocortex elicit a greater compensatory response in proteasome subunit expression than in neocortex.

Consistent with greater proteasome subunit levels in allocortex, allocortex also expressed higher levels of the heat shock chaperone Hsp70 and the antioxidant catalase than neocortex following treatment with 0.25 μM MG132. Thus, the rise in stress-sensitive proteins in allocortex may reflect higher levels of proteotoxic stress than in neocortex. Furthermore, without this defensive response, allocortex would probably have been even more vulnerable to MG132 toxicity. However, it must be conceded that our Western blotting data are only correlative. In order to determine if the upregulation of stress-sensitive proteins in allocortex confer protection against proteotoxicity, knockdown or inhibition studies must be performed. Furthermore, mRNA studies would be required to determine whether protein synthesis is enhanced or protein clearance is inhibited, as both responses would result in increases in protein levels by Western blot analyses. Nevertheless, the observed rise in stress-sensitive proteins in allocortex is consistent with the hypothesis that the levels of these proteins are in proportion to the degree of proteotoxic stress.

Glutathione is one of the most abundant and ubiquitous antioxidants, being present in millimolar concentrations in most tissues. The involvement of glutathione was investigated in the present study because proteotoxic and oxidative stress are often synergistic (Dringen, 2000;

Pompella, Visvikis, Paolicchi, De Tata, & Casini, 2003). The glutathione synthesis inhibitor BSO was more effective in neocortex than allocortex, perhaps because allocortex already had extremely low levels of glutathione synthesis under baseline conditions. Nonetheless, MG132 toxicity was exacerbated in neurons from both regions in the presence of BSO, suggesting that perhaps both types of neurons use glutathione in self-defense against proteotoxicity. As expected, N-acetyl cysteine increased glutathione levels in allocortex and protected it against MG132 toxicity. Limitations of these studies include recognition of both reduced and oxidized glutathione by the glutathione antibody. However, the vast majority of cellular glutathione is kept in the reduced state, even in injured conditions (Pastore, Federici, Bertini, & Piemonte, 2003; Shen, Dalton, Nebert, & Shertzer, 2005). A second limitation is that the difference in glutathione levels between neo- and allocortex may only be evident during postnatal development or be attributable to the harvesting and culturing procedures.

The ferroxidase ceruloplasmin did not rise with MG132 treatment *in vitro*. Thus, the higher levels of ceruloplasmin in neocortex under baseline conditions and with 0.25 μM MG132 are not likely to reflect greater stress levels. Many studies have linked ceruloplasmin to Parkinson's disease. As mentioned earlier, lower serum levels of ceruloplasmin have been correlated with a younger disease onset (Bharucha et al., 2008). In addition, loss of function mutations in ceruloplasmin lead to extrapyramidal symptoms and parkinsonism associated with iron toxicity (Hochstrasser et al., 2004; Hochstrasser et al., 2005; Jin et al., 2011; Lirong et al., 2009; H. F. Shang, Jiang, Burgunder, Chen, & Zhou, 2006). Ceruloplasmin immunostaining is higher in the remaining neurons of the SNpc in Parkinson's disease compared to healthy control subjects (Loeffler et al., 1996). Therefore, higher levels of ceruloplasmin in neocortical neurons may at least partly explain neocortical resilience against Parkinson's pathology.

Specific Aim 1c: Determine the differential susceptibility of neocortex and three allocortical subregions (entorhinal cortex, hippocampus, and olfactory bulb) to α-synuclein fibril-induced proteotoxic stress. Test the hypothesis that brain region of origin dictates the extent of Lewy-like inclusion formation and cell death *in vitro*.

Results

Inclusion formation in hippocampal and olfactory bulb primary cultures

Aggregated α-synuclein fibrils can elicit Parkinson's pathology in a number of cellular and animal models (Luk, Kehm, Carroll, et al., 2012; Luk, Kehm, Zhang, et al., 2012; Luk et al., 2009; Recasens et al., 2014; Sacino, Brooks, McKinney, et al., 2014; Sacino, Brooks, Thomas, et al., 2014; Volpicelli-Daley, Luk, & Lee, 2014a; Volpicelli-Daley et al., 2011a). As stated above, Lewy pathology forms across widespread brain regions in Parkinson's disease and is not restricted to the ventral mesencephalon as previously hypothesized (H. Braak, Del Tredici, Bratzke, Hamm-Clement, Sandmann-Keil, & Rub, 2002; H. Braak, Del Tredici, Rub, et al., 2003; H. Braak, Rub, et al., 2006). For example, cortical Lewy pathology spreads extensively throughout the allocortex following the appearance of inclusions in the entorhinal area. Thus, we sought to elicit Lewy-like inclusions and cell loss in primary cultures of the neocortex and three subregions of the allocortex–the hippocampus, the olfactory bulb, and the entorhinal area–using preformed α-synuclein fibrils kindly donated by Kelvin Luk and Virginia Lee from the University of Pennsylvania (Note: In the Figures, if not specified, the label 'allocortex' refers to the entorhinal area). First we observed that hippocampal and olfactory bulb primary neurons form inclusions positive for the aggregated form of α-synuclein (phosphorylated at serine 129 or pSer129) within 7 days of treatment with α-synuclein fibrils (Fig. 10A). The inclusions were

found within the cellular processes and the soma, where the aggregated protein appeared to be wrapped around the nucleus (Fig. 10B merged).

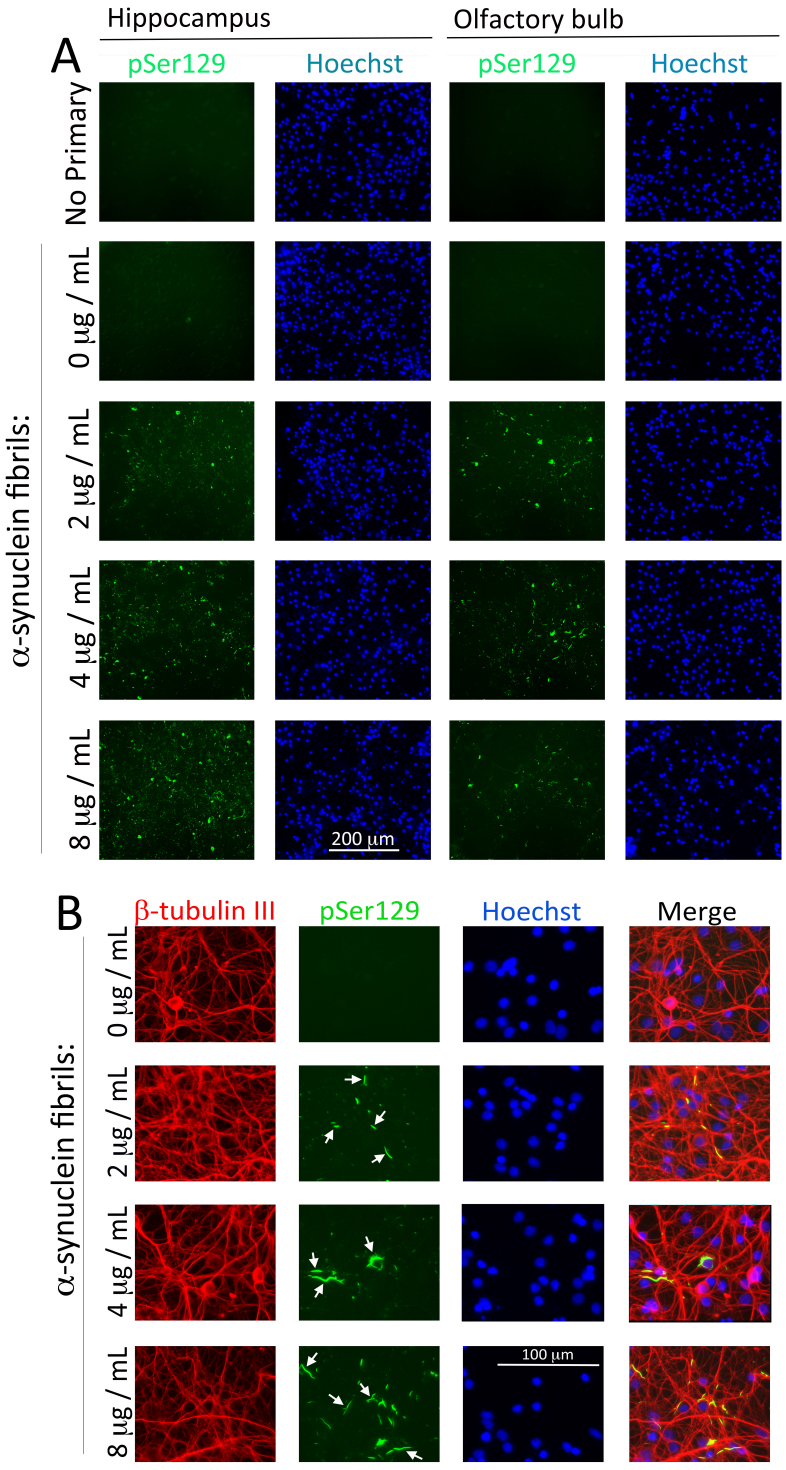

Figure 10: α-synuclein fibrils elicit the formation of neuronal inclusions. Hippocampal and olfactory bulb cultures

were treated with α-synuclein fibrils on DIV2 and fixed one week later. **(A)** Cells were immunocytochemically stained for the aggregated form of α-synuclein, which is phosphorylated at serine 129 (pSer129). Nuclei were stained with Hoechst. **(B)** Higher magnification images of olfactory bulb cultures immunostained for pSer129 and the specific neuronal marker β-tubulin III. White arrows denote some of the Lewy-like α-synuclein^{+} inclusions that colocalize with β-tubulin III.

pSer129^{+} inclusions are insoluble in Triton-X 100

In the human disease, Lewy bodies and Lewy neurites have precipitated out of solution and remain insoluble even in the presence of mild detergents in postmortem tissue (Galloway, Mulvihill, & Perry, 1992). Thus, we treated hippocampal neurons with α-synuclein fibrils and then fixed with 4% paraformaldehyde in the presence or absence of 1% Triton X-100 one week later to determine if our inclusions are indeed insoluble. In agreement Luk and colleagues, the pSer129^{+} inclusions in our hippocampal cultures were insoluble in Triton X detergent as expected (Fig. 11) (Volpicelli-Daley et al., 2011a). Thus, treatment with α-synuclein fibrils *in vitro* recapitulates the insolubility of the inclusions that develop in Parkinson's disease.

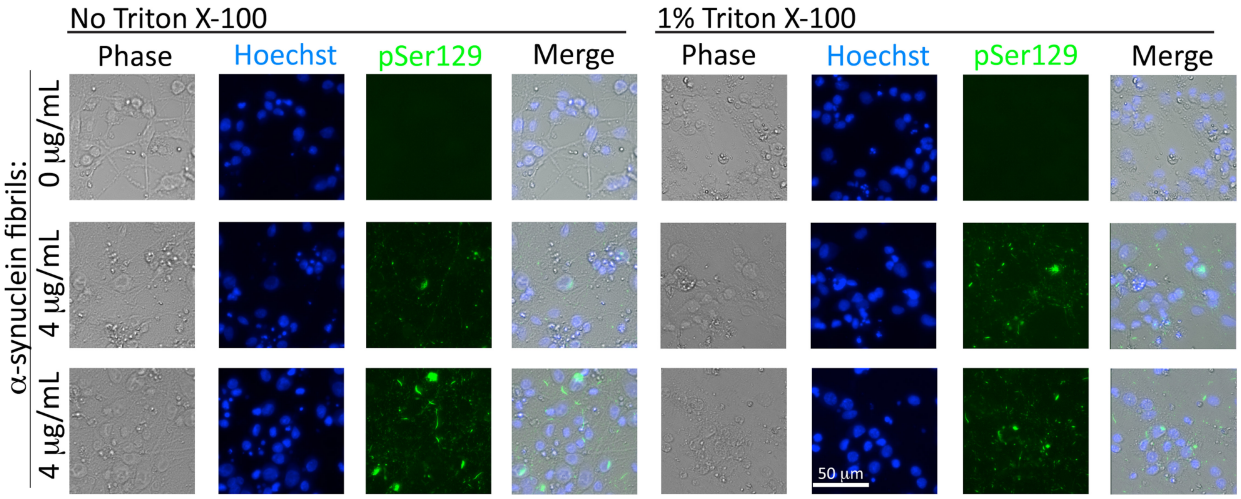

*Figure 11: α-synuclein inclusion formations are insoluble in detergent***.** Hippocampal neurons were treated on DIV2 with α-synuclein fibrils and fixed with 4% paraformaldehyde in the presence or absence of 1% Triton X-100 one week later. Cells were then immunocytochemically stained for α-synuclein phosphorylated at serine 129. Nuclei were stained with Hoechst.

α-synuclein fibrils increase the number of Thioflavin S^{+} amyloid structures

In Parkinson's and Alzheimer's disease, proteins that precipitate out of solution after acquiring beta-sheet pleated structures are commonly identified by the Thioflavin S stain as amyloid in nature (Westermark, Johnson, & Westermark, 1999). In addition to determining the insolubility of the inclusions formed by α-synuclein fibril treatment, we used Thioflavin S staining to assess the presence of amyloid structures. As hippocampal neurons formed the most inclusions when treated with α-synuclein fibrils, this hypothesis was tested in hippocampal cultures. In the absence of fibrils, Thioflavin S staining was absent (Fig. 12Aa-c). Treatment with α-synuclein fibrils dramatically enhanced staining for Thioflavin S (Fig. 12Ad-i, B). Thus, α-synuclein fibril treatment increases amyloid structures in hippocampal neurons as expected.

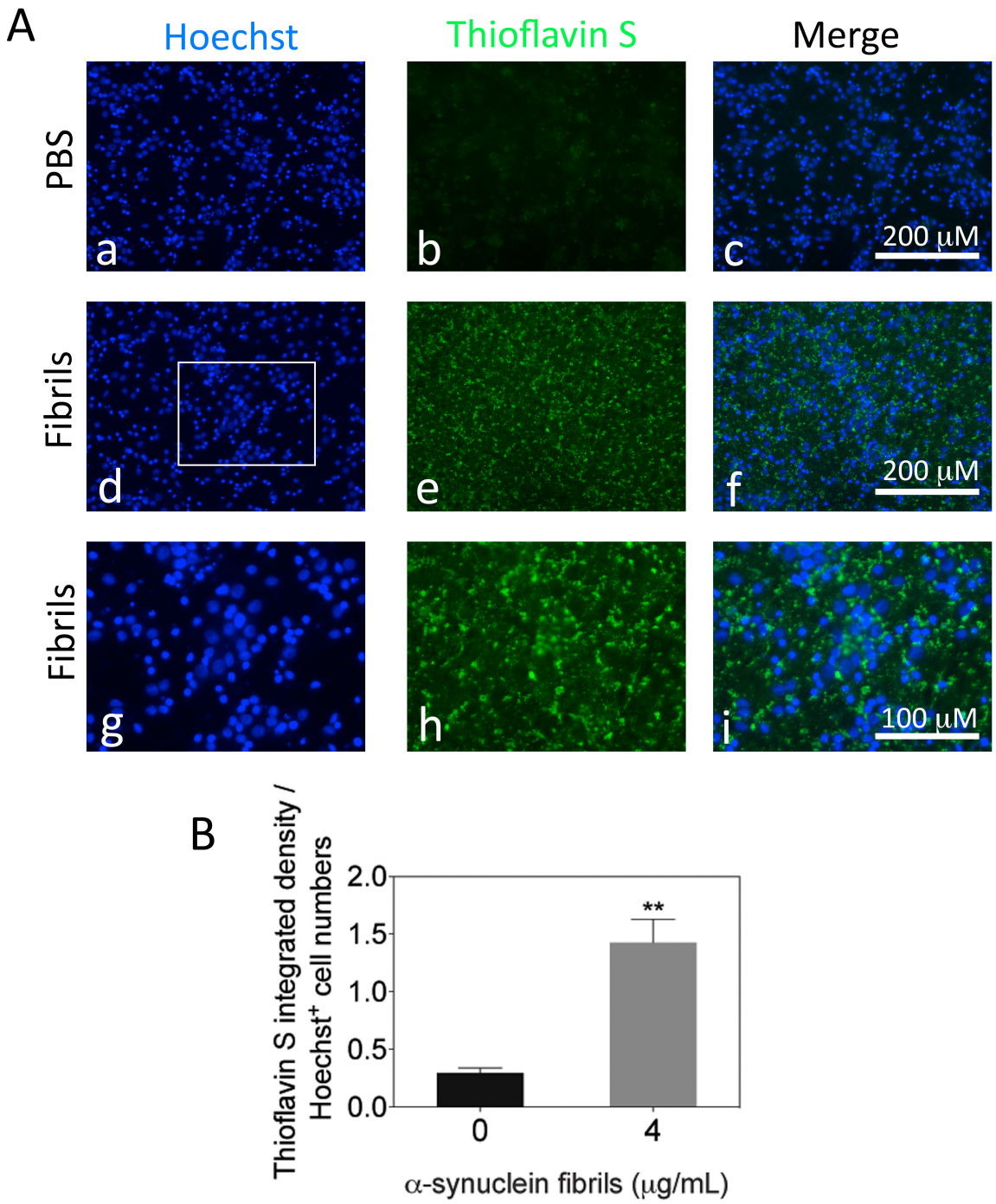

Figure 12: α-synuclein fibrils elicit Thioflavin S$^+$ amyloid formations. Hippocampal cultures were treated with α-synuclein fibrils on DIV2 and fixed one week later. (**A**) Amyloid structures with β-pleated sheets were stained with Thioflavin S (green). Nuclei were stained with Hoechst (blue). (**Ag-i**) Higher magnification images correspond to the white insets in panel d. (**B**) Thioflavin S staining was quantified in Image J by a blinded observer and expressed as a fraction of Hoechst$^+$ cell numbers. Shown are the mean and SEM of 3 independent experiments, each performed in triplicate. ** $p \leq 0.01$ versus 0 µg/mL α-synuclein fibrils.

α-synuclein fibril treatment does not elicit cell loss

Next we treated primary cultures from neocortex and three subregions of allocortex in parallel with synuclein fibrils to test the hypothesis that cellular viability would be reduced. Primary neocortical, entorhinal, hippocampal, and olfactory bulb cultures were treated with α-synuclein fibrils for one week but no significant decrease in cellular viability was observed by the DRAQ5 and MAP2 assays (Fig. 13A-D). In agreement with the infrared assays, no loss in viability was elicited with α-synuclein fibril treatment according to blinded counts of $Hoechst^{+}$ cell numbers (Fig. 13E, F). Furthermore, there were no significant changes in average nuclear size, also a sign of cellular stress (Fig. 13G, H). The size of $Hoechst^{+}$ nuclei in neocortex cultures was smaller than in the hippocampus following α-synuclein fibril treatment, although the difference was minor (Fig. 13H). Instead of eliciting cellular loss, α-synuclein fibril treatment slightly increased signal in the nuclear DRAQ5 assay in neocortical cultures. A similar pattern was observed in the numbers of $Hoechst^{+}$ cells (Fig. 13B, F), suggestive of a mild hormetic effect. Also consistent with a hormetic effect, MAP2 levels were significantly increased in hippocampal cultures treated with α-synuclein fibrils (Fig. 13D). This effect was further investigated in subsequent studies.

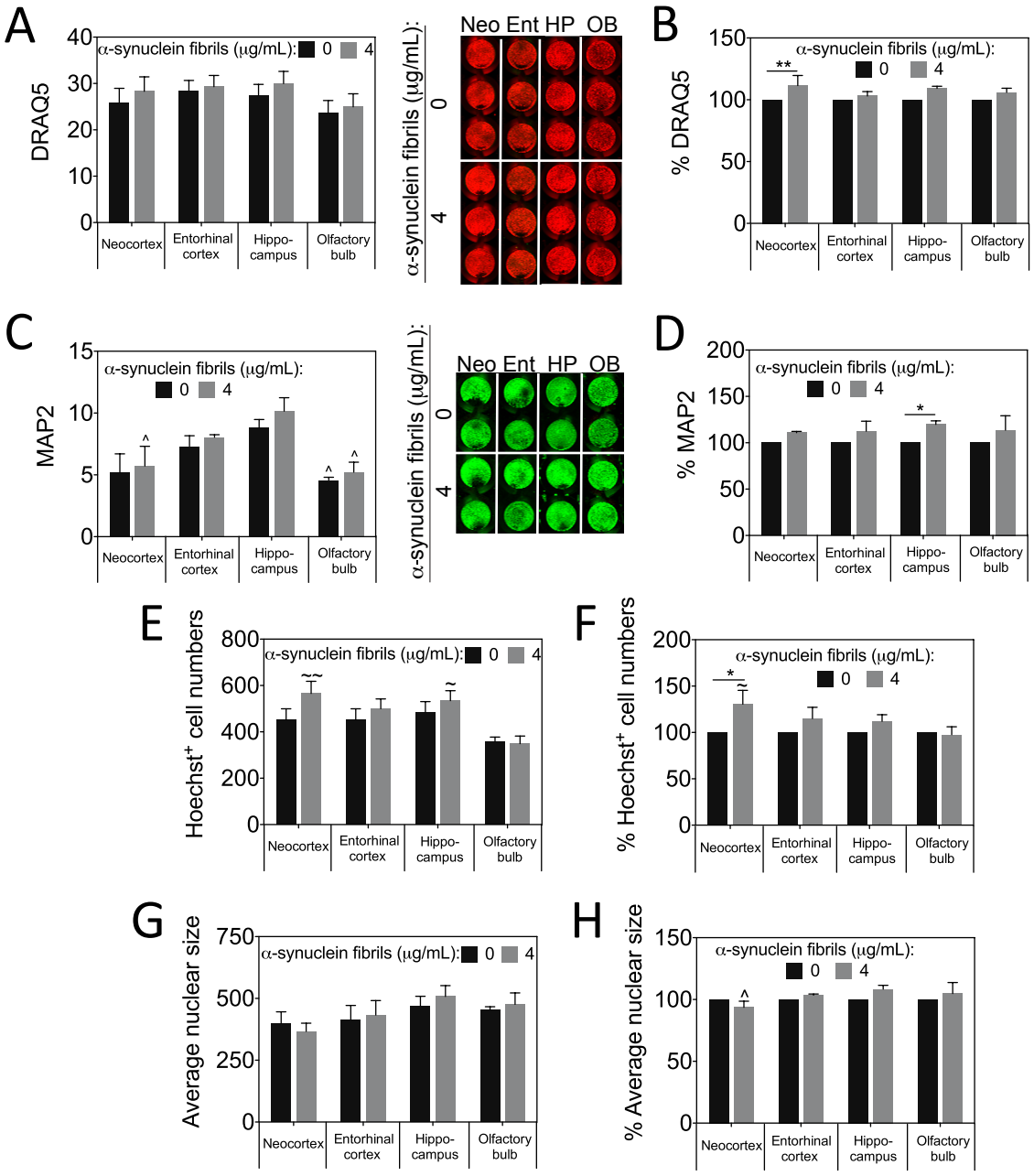

*Figure 13: Impact of α-synuclein fibril treatment in neo- and allocortical neurons***.** Neocortical neurons and neurons from three allocortical subregions−entorhinal cortex, hippocampus, and olfactory bulb-were treated with vehicle or 4 μg/mL α-synuclein fibrils on DIV2. Three viability assays were performed on DIV9. (**A-F**) Nuclei were stained with DRAQ5 or Hoechst and neurons were stained for MAP2 using the In-Cell Western technique. Raw and normalized data are both presented. The normalized data in B, D, F, and H are presented as fold change from the corresponding vehicle-treated group. **(B, F)** α-synuclein treatment increased DRAQ5 signal and Hoechst$^+$ cells in neocortical cultures. **(G, H)** There was no significant difference in average nuclear size, with the exception that α-synuclein treated neocortical cultures exhibited slightly smaller nuclei than hippocampal cultures. **(D)** MAP2 levels were significantly higher in hippocampal cultures treated with α-synuclein fibrils. Shown are the mean and SEM of 3-6 independent experiments, each performed in duplicate or triplicate. * $p \leq 0.05$, ** $p \leq 0.01$ versus 0 μg/mL α-synuclein fibrils. ^ $p \leq 0.05$ versus hippocampus. ~ $p \leq 0.05$, ~~ $p \leq 0.01$ versus olfactory bulb, two-way ANOVA followed by Bonferroni *post hoc* correction.

α-synuclein fibril treatment elicits an increase in MAP2 levels in hippocampal neurons

As previously discussed, MAP2 levels were significantly increased in α-synuclein fibril treated hippocampal neurons as assessed by an infrared In-Cell Western assay on the LICOR Odyssey Imager (Fig. 13D). However, immunocytochemical analyses revealed that α-synuclein fibril treatment did not affect the number and cell density of $MAP2^+$ neurons (Fig. 14A, B). $MAP2^+$ area fraction–the fraction of the field of view with $MAP2^+$ immunoreactivity–was also analyzed but showed no increase with α-synuclein fibril treatment (Fig. 14C). It is possible that some dendritic processes are too lightly stained to be recognized by an EVOS epifluorescence microscope, whereas the infrared Odyssey imager can visualize this difference due to much higher sensitivity.

In order to verify the increase in MAP2 in fibril-treated hippocampal neurons, Western blotting was performed. α-synuclein fibril treatment significantly increased MAP2, GAPDH, and β-actin levels as if there was on overall increase in protein content (Fig. 14F-H). When MAP2 levels were expressed as a function of GAPDH levels, there was no change in MAP2 concentration (Fig. 14D). However, when we plotted protein concentration as determined by the bicinchoninic assay, a significant decrease in protein levels with α-synuclein fibril treatment became evident (Fig. 14E). It is possible that the bicinchoninic assay does not work well under conditions of protein aggregation as in the fibril-treated groups and that the fibrils elicit a small increase in dendritic arbors without a concomitant change in cell numbers. Indeed, MAP2 is commonly used as a dendritic marker (Bernhardt & Matus, 1984). These findings raise the possibility that neurons respond to the presence of inclusions in their processes by upregulating dendritic outgrowth to compensate for the blockade of retrograde and anterograde transport systems. Future studies to investigate this possibility are warranted.

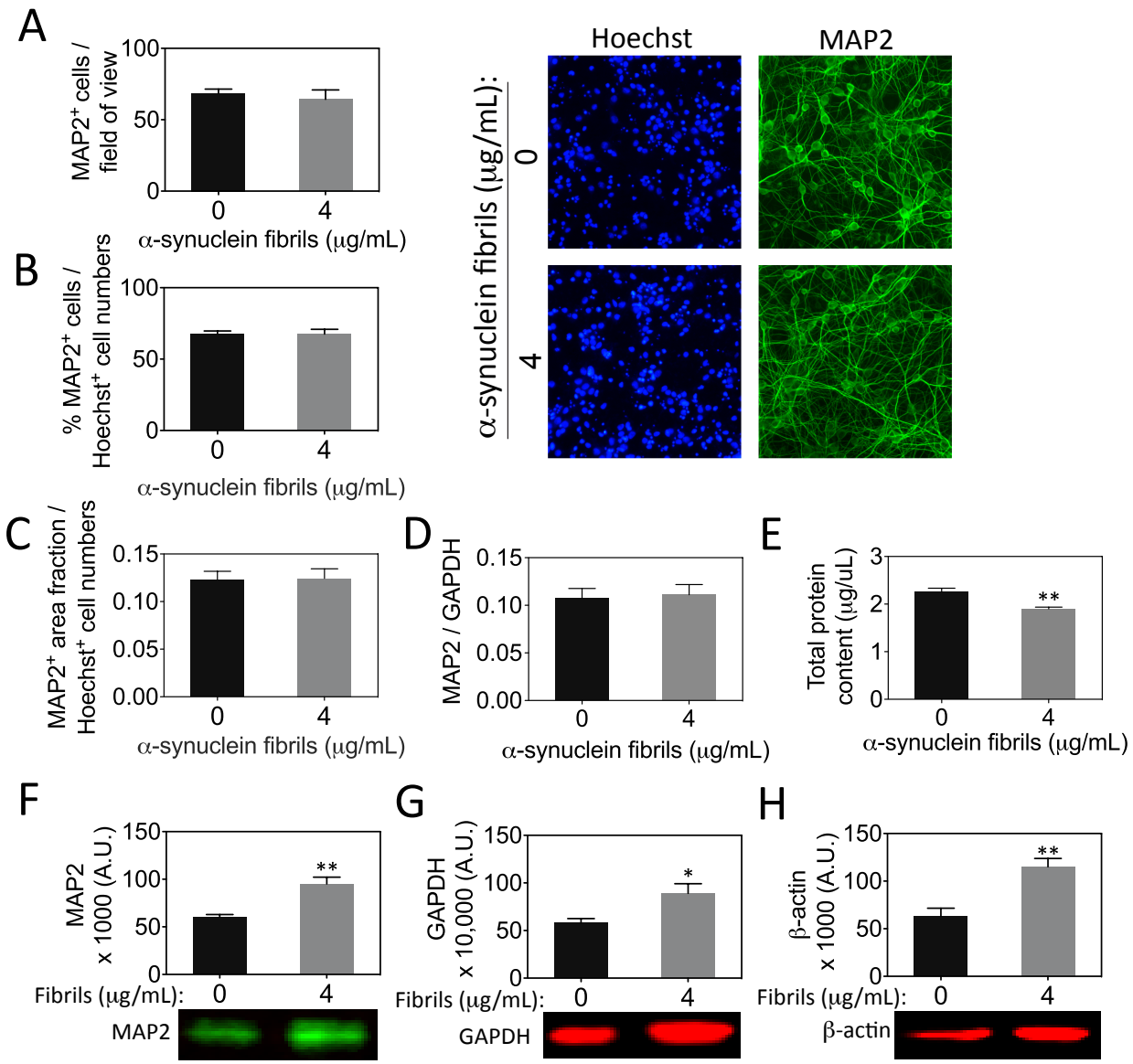

Figure 14: Effect of α-synuclein fibrils on hippocampal MAP2 levels. **(A-C)** α-synuclein fibrils had no effect on the number, density, or area fraction of $MAP2^+$ hippocampal neurons as assessed by an EVOS epifluorescence microscope. Representative images of MAP2 and Hoechst-stained cells after treatment with α-synuclein fibrils. (**D**) There was no significant change in MAP2 levels as a function of GAPDH levels in hippocampal neurons. (**E**) Total protein levels were significantly decreased in α-synuclein fibril treated hippocampal neurons as assessed by the bicinchoninic assay. (**F-H**) Levels of MAP2, GAPDH, and β-actin were increased in α-synuclein fibril-treated hippocampal neurons according to Western immunoblots. Shown are the mean and SEM of 3-5 independent experiments, each performed in triplicate. * $p \leq 0.05$, ** $p \leq 0.01$ versus 0 μg/mL α-synuclein fibrils, two-tailed Student *t* test.

Brain region of origin determines vulnerability to inclusion formation in vitro

Our next goal was to establish whether neocortical cultures developed fewer inclusions than allocortical cultures. As expected, pSer129^{+} inclusion formation occurred in all primary neuronal cultures treated with α-synuclein fibrils (Fig. 15A-E). Hippocampal neurons had the highest inclusion numbers whereas olfactory bulb and neocortical cultures had the lowest (Fig. 15A, D). Inclusion numbers were assessed as a function of both DRAQ5 and Hoechst^{+} cell numbers as each method exhibits unique strengths and weaknesses, as discussed in Specific Aim 1a. Inclusion area fraction was highest in hippocampal cultures and lowest in olfactory bulb cultures, consistent with the inclusion number results (Fig. 15C, E). Neocortical neurons had the largest average inclusion size compared to the other neuronal cultures (Fig. 15F). These patterns are highly suggestive of selective susceptibility to α-synuclein pathology, with the highest susceptibility in hippocampal neurons. One potential explanation for these results is the differential expression of endogenous α-synuclein; if α-synuclein levels are naturally low in a given brain region, there would be less available for inclusion formation. Consistent with this view, Western blotting analysis revealed that hippocampal neurons expressed the highest levels of α-synuclein of all the brain regions examined (Fig. 15G).

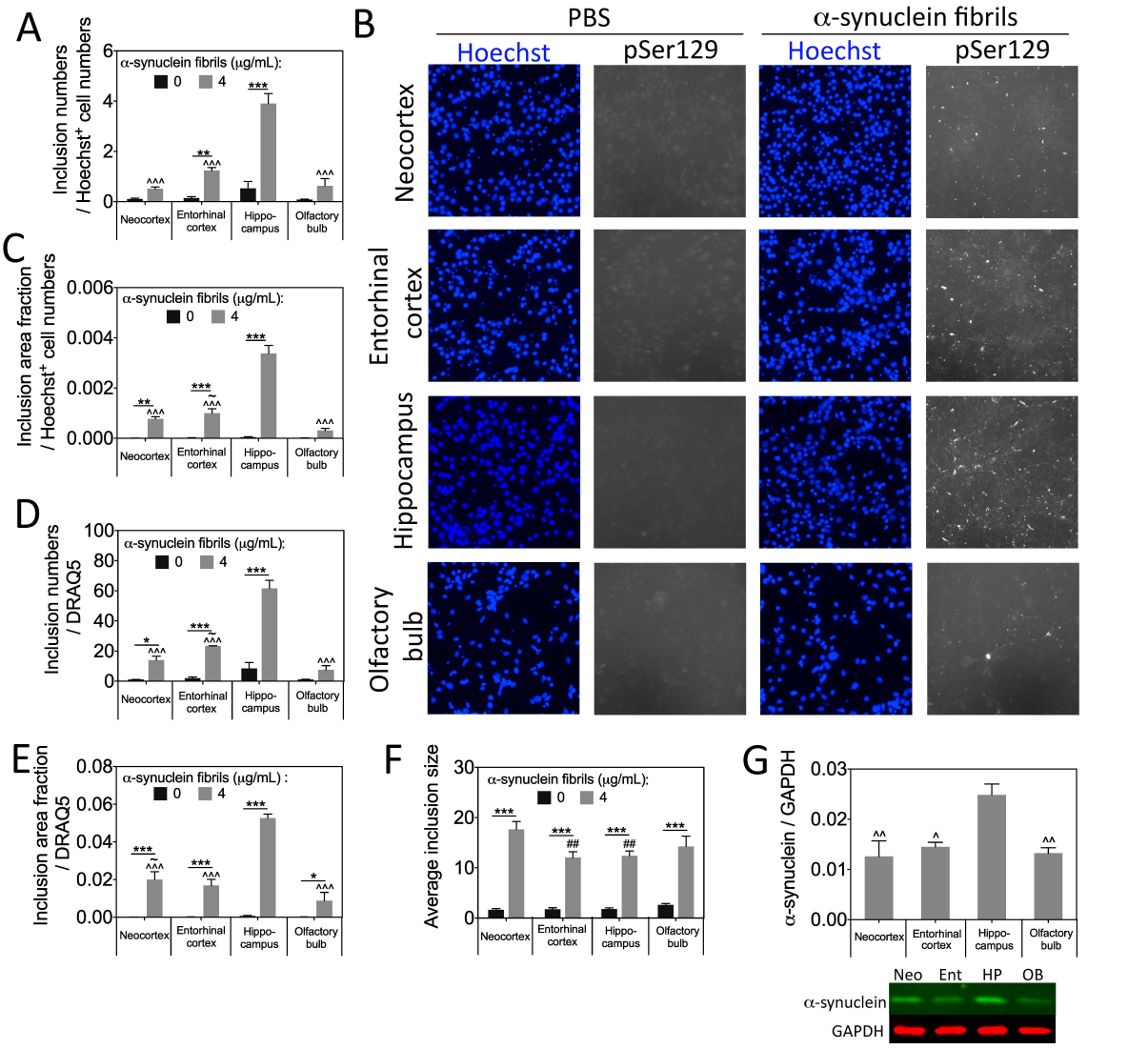

Figure 15: Impact of α-synuclein fibril treatment on neuronal and nuclear markers. **(A, C)** The number of pSer129^{+} inclusion counts and the fraction of the total surface area that was occupied by inclusions were expressed as a function of Hoechst^{+} cell numbers. Hippocampal neurons exhibited the highest levels of inclusion formation. (**B**) Representative Hoechst and pSer129 images from each brain region examined. **(D, E)** The same measurements as in A and C were expressed as a function of the nuclear stain DRAQ5. **(F)** The average size of the pSer129^{+} inclusions was significantly higher in neocortical cultures than in entorhinal cortical and hippocampal cultures. (**G**) Basal levels of α-synuclein expression in neurons from each brain region. Shown are the mean and SEM of 5-6 independent experiments, each performed in triplicate * $p \leq 0.05$, ** $p \leq 0.01$, *** $p \leq 0.001$ versus 0 μg/mL α-synuclein fibrils. ^ $p \leq 0.05$, ^^ $p \leq 0.01$, ^^^ $p \leq 0.001$ versus hippocampus. ## $p \leq 0.01$ versus neocortex. ~ $p \leq 0.05$ versus olfactory bulb, one or two-way ANOVA followed by Bonferroni *post hoc* correction.

Discussion

The goal of Specific Aim 1c was to assess the effects of α-synuclein fibril treatment in primary neuronal cultures harvested from multiple brain regions. We tested the hypothesis that neocortex would be the least susceptible to synucleinopathy and cell loss and that brain region of origin would play an important role in determining susceptibility to inclusion formation. We gathered partial support for our hypotheses, as brain region did determine the extent of inclusion formation, but the Lewy-like inclusions did not elicit cell loss *in vitro* as previously reported (Luk et al., 2009; Volpicelli-Daley et al., 2014a; Volpicelli-Daley et al., 2011b). This discrepancy may be attributed to differences in the duration of treatment; our cultures were assayed after one week whereas previous studies reported effects after two weeks. Other significant differences include the type of sonicator and probe used (Kelvin Luk, personal communication). Nevertheless, α-synuclein fibril treatment successfully elicited inclusion formation in all four primary culture types. The inclusions formed in our hands exhibited Lewy-like characteristics, as they were detergent-insoluble and found most abundantly throughout cellular processes.

As mentioned above, we observed that the degree of inclusion formation was heavily dependent on the brain region of origin. This is consistent with the view that not all brain regions are equally susceptible to synucleinopathy. However, the degree of susceptibility to α-synuclein fibril-induced inclusion formation did not correlate with the observed progression of pathology in the disease, with the exception that hippocampus was more vulnerable than neocortex (H. Braak, Del Tredici, Rüb, et al., 2003). According to Braak's staging scheme, the most susceptible regions in our studies should have been the olfactory bulb, hippocampus, entorhinal cortex, and neocortex, in descending order. In contrast, we observed that olfactory bulb and

neocortical neurons developed the least inclusions whereas hippocampal neurons developed the most. As mentioned in the Introduction, the selective susceptibility of different brain regions in Parkinson's disease is superimposed upon the efferent and afferent projection patterns. Obviously, the latter determine whether or not neurons have access to misfolded α-synuclein according to Braak's transmissibility hypothesis. Nevertheless, one of the strengths of our model is that removal of the inter-neuronal connections between brain regions by mechanical dissociation led to the discovery of inherent selective susceptibilities to synucleinopathy.

α-synuclein fibril-treated olfactory bulb and neocortical neurons developed the least number of inclusions *in vitro.* This is consistent with the observation that the neocortex is the last region affected by α-synuclein pathology (H. Braak, Del Tredici, Rüb, et al., 2003). However, olfactory structures are affected by α-synuclein pathology very early in the disease, leading us to expect that this region would have been especially vulnerable to inclusion formation (H. Braak, Del Tredici, Rüb, et al., 2003). Our results are consistent with the view that olfactory regions are not inherently vulnerable to protein misfolding stress but that they develop inclusions early in Parkinson's disease perhaps because they lie in close proximity to the route of entry of a pathogenic insult. Nasal and vagal routes of entry of a pathogen in Parkinson's disease have been proposed by several investigators in recent years (H. Braak, Rüb, et al., 2003; Rey, Petit, Bousset, Melki, & Brundin, 2013).

Consistent with Braak staging theory, entorhinal neurons developed inclusions more readily then neocortical neurons when only these two brain regions were statistically analyzed. This finding is in agreement with previous data from Specific Aim 1b, which showed that neocortex was more resistant to the proteasome inhibitors MG132 and PSI than allocortex. Together these studies suggest that entorhinal neurons are more susceptible to proteotoxicity and

consequently, inclusion formation, than neocortical neurons. Notably, hippocampal neurons developed the most extensive inclusion formation although they do not develop Lewy pathology until stage 3 of the disease, well after olfactory Lewy bodies make an appearance (Lerner & Bagic, 2008). The reason for the enhanced susceptibility of hippocampal neurons may be higher basal expression of endogenous α-synuclein compared to neurons from the entorhinal cortex, neocortex, and olfactory bulb. Higher levels of α-synuclein might provide a greater pool of potential substrates for α-synuclein fibrils to seed protein misfolding.

In conclusion, neurons exhibit selective susceptibility to synucleinopathy as expected. These findings underscore the importance of brain region both when testing potential therapies and choosing a model system to study.

Chapter 2

Specific Aim 2: Examine whether neo- and allocortical cells differ in their reliance on heat shock proteins for defense against protein misfolding stress. Test the hypothesis that neocortex is less vulnerable than allocortex to loss of protein homeostasis from simultaneous inhibition of heat shock protein and proteasome activity. If supported, this would suggest that the stressed allocortex is more vulnerable to loss of heat shock protein activity because it needs to rely on these defenses more when challenged with protein misfolding stress. Furthermore, these findings would lend insight into the mechanisms underlying selective vulnerability patterns in telencephalic subregions.

Rationale

Heat shock proteins and the ubiquitin-proteasome system are primary cellular defenses against proteotoxic stress. Heat shock proteins are chaperones that refold misfolded proteins and form part of the essential vitagene network that preserves homeostasis in the brain (Cornelius, Perrotta, Graziano, Calabrese, & Calabrese, 2013). Misfolded proteins are tagged with ubiquitin and guided to the proteasome by heat shock proteins if they are irreparably damaged and cannot be refolded. Following proteasome inhibition, misfolded proteins are no longer degraded and promote the formation of protein aggregates and cell death (Rideout, Larsen, Sulzer, & Stefanis, 2001; Rideout & Stefanis, 2002; Sun et al., 2006). However, the role of heat shock proteins in regionally selective vulnerability to proteotoxicity in the telencephalon has not been defined.

Results

Optimization of Primary Culture Model

Earlier work revealed that neocortical neurons did not survive the culturing process as well as entorhinal allocortical neurons. As a result of this baseline toxicity of the culturing

conditions, we switched to Neurobasal-A medium, which is specifically designed to promote the survival of postnatal neurons. In this new medium, neo- and allocortical neurons survived culturing conditions equally well and densely expressed the synaptic marker synaptophysin (Fig 16A, B). There was no difference in the overall number of $MAP2^+$ cells in neo- versus allocortical cultures (Fig 16C). However, allocortical cultures exhibited lower neuronal densities (fewer $MAP2^+$ cells as a fraction of $Hoechst^+$ cell numbers) than neocortical cultures, although the difference was very slight (<10%) (Fig. 16D). No differences were observed between neo- and allocortical cultures in MAP2 or ATP levels as assessed by the In-Cell Western and Cell Titer Glo assays, respectively (Fig. 16E, F). For all subsequent experiments, we therefore used Neurobasal-A media.

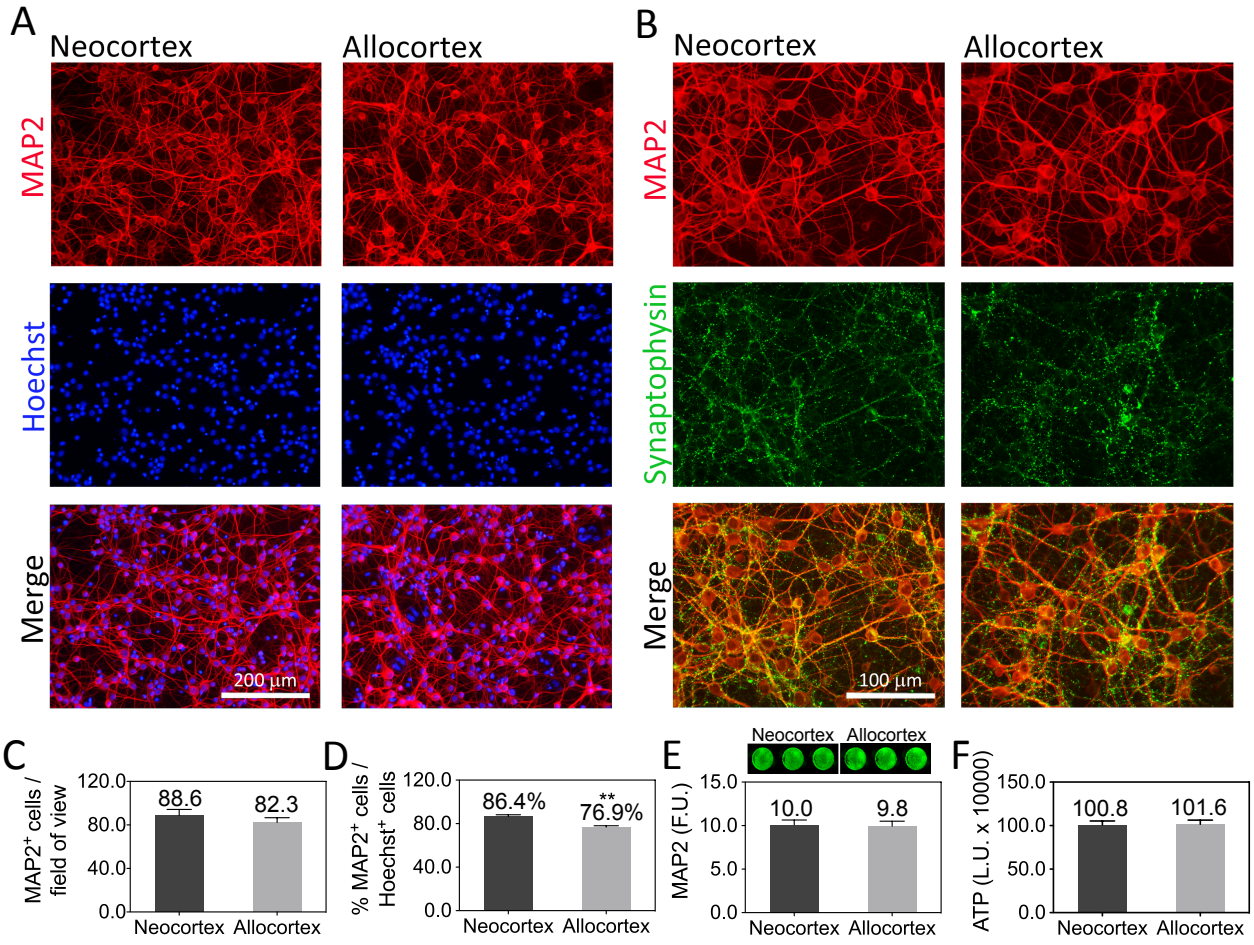

*Figure 16: Primary postnatal cultures of neo- and allocortex***.** (**A, B**) Primary sensorimotor neocortex and entorhinal allocortex cells were harvested from 1 or 2 day-old rat pups and stained for the neuronal marker MAP2, the synaptic marker synaptophysin, and the nuclear stain Hoechst on DIV4. (**C, D**) $MAP2^+$ neurons and Hoechst-stained nuclei were counted by a blinded observer to assess the neuronal density and purity of the cultures. Neocortex had slightly higher levels of $MAP2^+$ neurons as a percentage of total cell numbers. (**E, F**) No difference in overall MAP2 content or ATP levels was observed between neo- and allocortical cultures on DIV4, according to the In-Cell Western assay for MAP2 and the Cell Titer Glo assay for ATP. A representative In-Cell Western image is shown above panel E. Shown are the mean ± SEM of at least 3 independent experiments. ** $p \leq 0.01$ vs neocortex, two-tailed Student's *t*-test. Reprinted from Neurobiology of Aging, 36 (5), J. Posimo, J. Weilnau, A. Gleixner, M. Broeren, N. Weiland, J. Brodsky, P. Wipf, and R. Leak, "Heat shock protein defenses in the neocortex and allocortex of the telencephalon," p. 1924-1937. Copyright 2015 by Elsevier, reprinted with permission from Elsevier.

Regional Differences in Vulnerability to Cellular Stress

After reestablishing our culture model with improvements in neuronal density and basal survival, we examined the stress vulnerability of cells harvested from neocortex and three allocortical subregions (entorhinal allocortex, piriform cortex, and hippocampus). As observed previously, neocortex was more resistant to MG132 toxicity than entorhinal allocortex according to the MAP2 and ATP assays (Fig 17A, B). At the highest concentration of MG132, entorhinal allocortical neurons exhibited higher levels of ATP, which may be attributed to glial cells because this difference is absent in the MAP2 assay. Additionally, neocortex cultures were more resistant to MG132 compared to piriform cortex and hippocampus cultures according to the MAP2 assay (Fig. 17C, E). Neocortex and hippocampus cultures exhibited similar ATP levels, suggesting equivalent metabolic fitness (Fig. 17F). Piriform cortex exhibited higher ATP levels than neocortex at the highest concentrations of MG132 (Fig. 17D). Again, these regional differences may be attributable to the glia present in the cultures as they were not in agreement with the result of the MAP2 assay. Consistent with our previous findings with H_2O_2, entorhinal cortex cultures were more resistant to the oxidative toxin paraquat than neocortex cultures. Thus, the allocortex appears to possess antioxidant impressive defenses, although these are not sufficient to make it as resistant as neocortex to MG132. Taken together, these findings

demonstrate that neocortical neurons are more resistant to proteotoxicity than allocortical neurons, a phenomenon that is generalizable across multiple allocortical subregions.

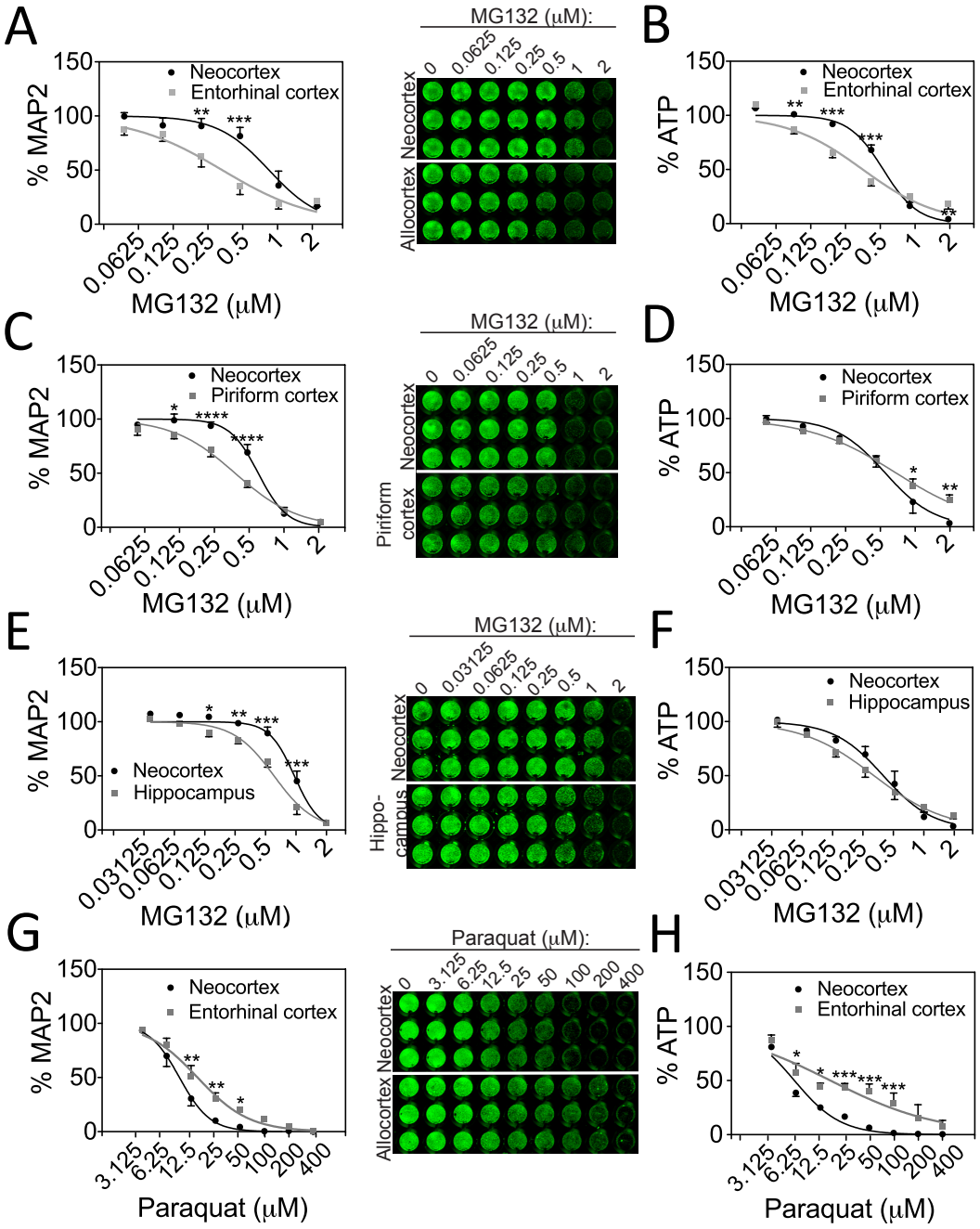

Figure 17: Regional differences in vulnerability to cellular stress. MAP2 content (**A, C, E, G**) and ATP levels (**B, D, F, H**) in neocortex cultures and cultures harvested from entorhinal, piriform, and hippocampal allocortex 48h after treatment with the proteasome inhibitor MG132 or the oxidative toxin paraquat. Fitted curves were extrapolated from non-linear regression analyses after conversion of the X-axis to a log scale. MAP2 and ATP levels at 0 μM MG132 were set to 100% (not shown in log scale graphs). For ease of presentation, concentrations of

MG132 are listed in micromolar units rather than in log units on the X-axis. Neocortical neurons were more resistant to proteotoxic stress from MG132 than neurons from three allocortical subregions according to the MAP2 assay, but less resistant to oxidative stress from paraquat. The ATP metabolic assay agreed with some, but not all of the MAP2 In-Cell Westerns. Shown are the mean ± SEM of 3-4 independent experiments. * $p \leq 0.05$, ** $p \leq 0.01$, *** $p \leq 0.001$, **** $p \leq 0.0001$ neo- vs allocortex, Bonferroni *post hoc* correction following two-way ANOVA. Reprinted from Neurobiology of Aging, 36 (5), J. Posimo, J. Weilnau, A. Gleixner, M. Broeren, N. Weiland, J. Brodsky, P. Wipf, and R. Leak, "Heat shock protein defenses in the neocortex and allocortex of the telencephalon," p. 1924-1937. Copyright 2015 by Elsevier, reprinted with permission from Elsevier.

Heat Shock Protein and Co-chaperone Expression in Neo- and Allocortex

Heat shock proteins are molecular chaperones that can prevent the aggregation of unfolded/misfolded polypeptides by refolding them or directing irreparably damaged proteins to the proteasome for catalytic removal (Feder & Hofmann, 1999). Thus, heat shock proteins are important modulators of cell survival in neurodegenerative diseases. The molecular chaperone Hsp90 interacts with a number of co-chaperones as well as Hsp70 to prevent protein aggregation. Studies have shown that Hsp90 is consistently found in α-synuclein inclusions such as Lewy bodies and Lewy neurites and in tau inclusions (Uryu et al., 2006). The co-chaperone CHIP is recruited to Hsp90 or Hsp70 complexes when protein refolding is inefficient, in order to promote client protein ubiquitylation and degradation through the proteasome (Labbadia & Morimoto, 2015). CHIP has been shown to decrease α-synuclein aggregations *in vitro* and *in vivo* (Dimant et al., 2014). We found that levels of Hsp90 and the co-chaperone CHIP were not significantly different in neo- and allocortical cultures as a function of MG132 treatment, with the exception of a significant drop in neocortical levels of CHIP when comparing the data from 0.125 μM MG132 treatment with 0.25 μM MG132 treatment, forming a U-shaped concentration-response curve (Fig. 18A, B).

The co-chaperones Hop and Hip mediate the association of Hsc70 and Hsp90, acting as folding cofactors and facilitating the maturation of client proteins (Taipale et al., 2010). There was a significant rise in the co-chaperones Hip and Hop in neocortical cultures in response to

0.125 μM MG132 (Fig. 18C, D). Additionally, neocortical cultures expressed significantly higher levels of Hip in response to 0.125 μM MG132 than allocortical cultures. Hsp70 levels rose significantly higher in allocortex than neocortex following MG132 treatment (Fig. 18E). Hsc70 is the constitutively expressed form of Hsp70 and guides misfolded proteins containing the C-terminal KFERQ motif to the lysosome for degradation (Arias & Cuervo, 2011). Hsc70 levels are known to decline in the SNpc in Parkinson's disease (Alvarez-Erviti et al., 2010; Chu, Dodiya, Aebischer, Olanow, & Kordower, 2009; Mandel et al., 2005). We found that Hsc70 levels were significantly higher in allocortex than neocortex cultures in response to the highest concentration of MG132 (Fig. 18F).

The small heat shock protein Hsp25 forms multimeric oligomers that trap misfolded proteins, preventing the formation of protein aggregations and providing a reservoir of client substrates for the Hsp70 machinery (Haslbeck et al., 2005). Hsp25 and HO1 levels were increased to greater levels in allocortical than neocortical cultures following MG132 treatment (Fig. 18G, H). Hsp40 acts as a co-chaperone of Hsp70, positively regulating its activity by stimulating ATPase activity (Kampinga & Craig, 2010). Hsp60 encapsulates proteins to prevent aggregation while refolding occurs (Kim et al., 2013). Low concentrations of MG132 elicited a rise in Hsp40 levels in neo- and allocortex cultures, whereas Hsp60 levels were unaffected (Fig. 18I, J). The increased allocortical levels of Hsp70, Hsc70, HO1, and Hsp25 in response to MG132 demonstrate that allocortex mounts more robust stress responsive changes than neocortex.

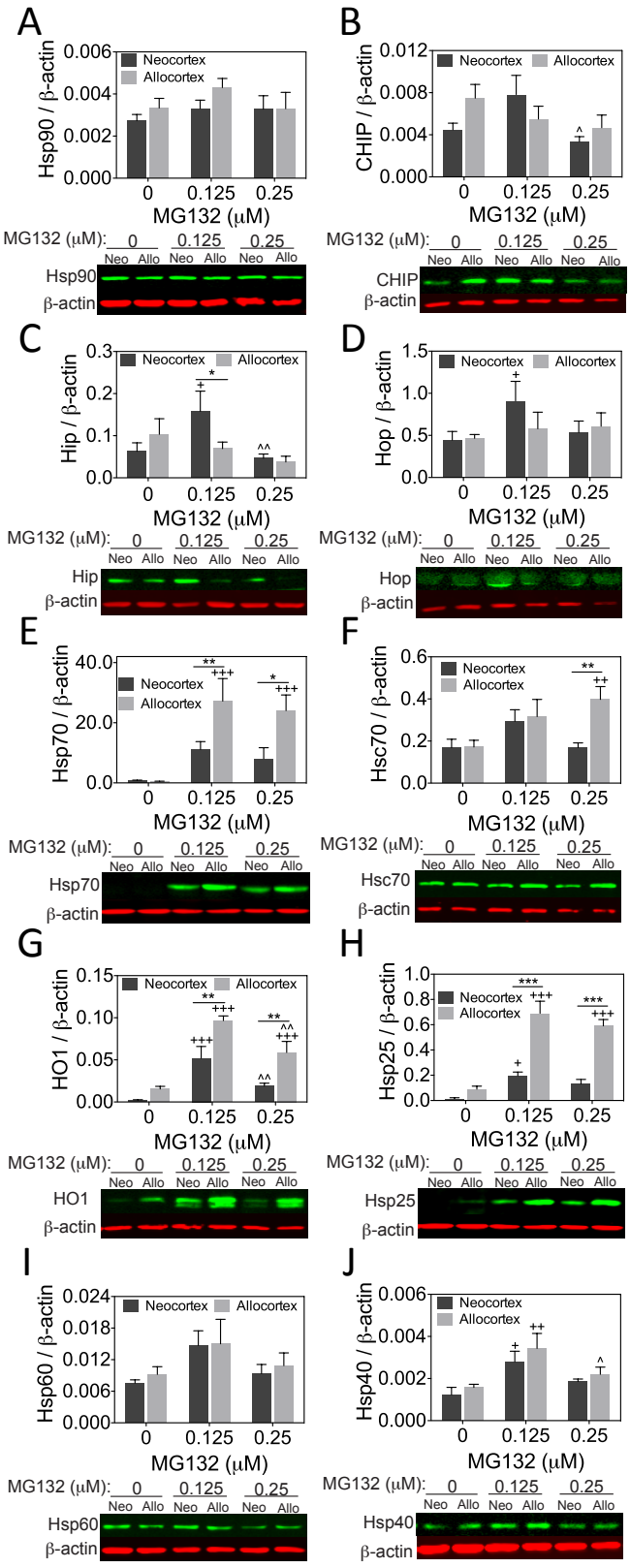
A
Hsp90 / β-actin
Neocortex
Allocortex
MG132 (μM)
Hsp90
β-actin
B
CHIP / β-actin
CHIP
C
Hip / β-actin
Hip
D
Hop / β-actin
Hop
E
Hsp70 / β-actin
Hsp70
F
Hsc70 / β-actin
Hsc70
G
HO1 / β-actin
HO1
H
Hsp25 / β-actin
Hsp25
I
Hsp60 / β-actin
Hsp60
J
Hsp40 / β-actin
Hsp40
Neo Allo

*Figure 18: Heat shock protein and co-chaperone expression in neo- and allocortical cultures***.** Levels of the heat shock proteins Hsp90, Hsp70, Hsc70, HO1, Hsp25, Hsp60, and Hsp40 (**A, E, F, G, H, I, J**) and the co-chaperones CHIP, Hip, and Hop (**B, C, D**) in neo- and allocortical (entorhinal) cultures 24h after treatment with MG132, as measured by infrared two-color Western blotting. Allocortex exhibited greater MG132-induced increases in Hsp70, Hsc70, HO1, and Hsp25, but neocortex exhibited greater stress-induced increases in Hip and Hop. Shown are the mean ± SEM of 6 independent experiments. * $p \leq 0.05$, ** $p \leq 0.01$, *** $p \leq 0.001$ vs neocortex, + $p \leq 0.05$, ++ $p \leq 0.01$, +++ $p \leq 0.001$ vs 0 μM MG132, ^ $p \leq 0.05$, ^^ $p \leq 0.01$ vs 0.125 μM MG132, LSD *post hoc* following two-way ANOVA. Reprinted from Neurobiology of Aging, 36 (5), J. Posimo, J. Weilnau, A. Gleixner, M. Broeren, N. Weiland, J. Brodsky, P. Wipf, and R. Leak, "Heat shock protein defenses in the neocortex and allocortex of the telencephalon," p. 1924-1937. Copyright 2015 by Elsevier, reprinted with permission from Elsevier.

Allocortex Relies More on Hsp70/Hsc70 than Neocortex Under Proteotoxic Conditions

Next we used the Hsp70 and Hsc70 activity inhibitors VER155008 and MAL3-101 to determine the functional consequences of the robust increases in Hsp70 and Hsc70 levels with MG132 treatment. According to both the MAP2 and ATP assays, VER155008 and MAL3-101 exacerbated MG132 toxicity in neo- and allocortex (Fig. 19A-D). Furthermore, this exacerbation of toxicity was more pronounced in allocortex than neocortex according to the MAP2 assay (Fig. 19A, C). In order to further assess the potential role of Hsp70 and Hsc70 induction, the Hsp70/Hsc70 activator 115-7c was applied. Treatment with various concentrations of 115-7c protected neocortical but not allocortical cultures from MG132 toxicity, even in experiments in which the proteasome inhibitor was especially toxic (Fig. 19E, F). We repeated the viability measurements after treatments with various concentrations of MG132 and the most protective concentration of 115-7c. In these latter experiments, only neocortical neurons were significantly protected by 115-7c against 1 and 2 μM MG132 (Fig. 19G). It is possible that 115-7c does not robustly protect allocortical cultures because Hsp70 molecules are already maximally engaged due to an overwhelming number of misfolded proteins. Thus, the effects of MG132, VER155008, and 115-7c on the K48-linked ubiquitinated protein pool were subsequently examined in order to test the hypothesis that allocortex possesses higher levels of misfolded proteins. As expected, allocortex expressed significantly higher levels of K48-linked

ubiquitinated proteins than neocortex when treated with 0.125 μM MG132 (Fig. 19H). However at 1 μM MG132, a concentration at which the MAP2 and ATP assays showed neo- and allocortex to be equally vulnerable, there was no significant difference in K48-linked ubiquitinated proteins (Fig. 19I). Further, neither VER155008 nor 115-7c had any effect on K48-linked ubiquitination levels in neo- or allocortex, indicating that Hsp70 and Hsc70 activity may not modulate this measure.

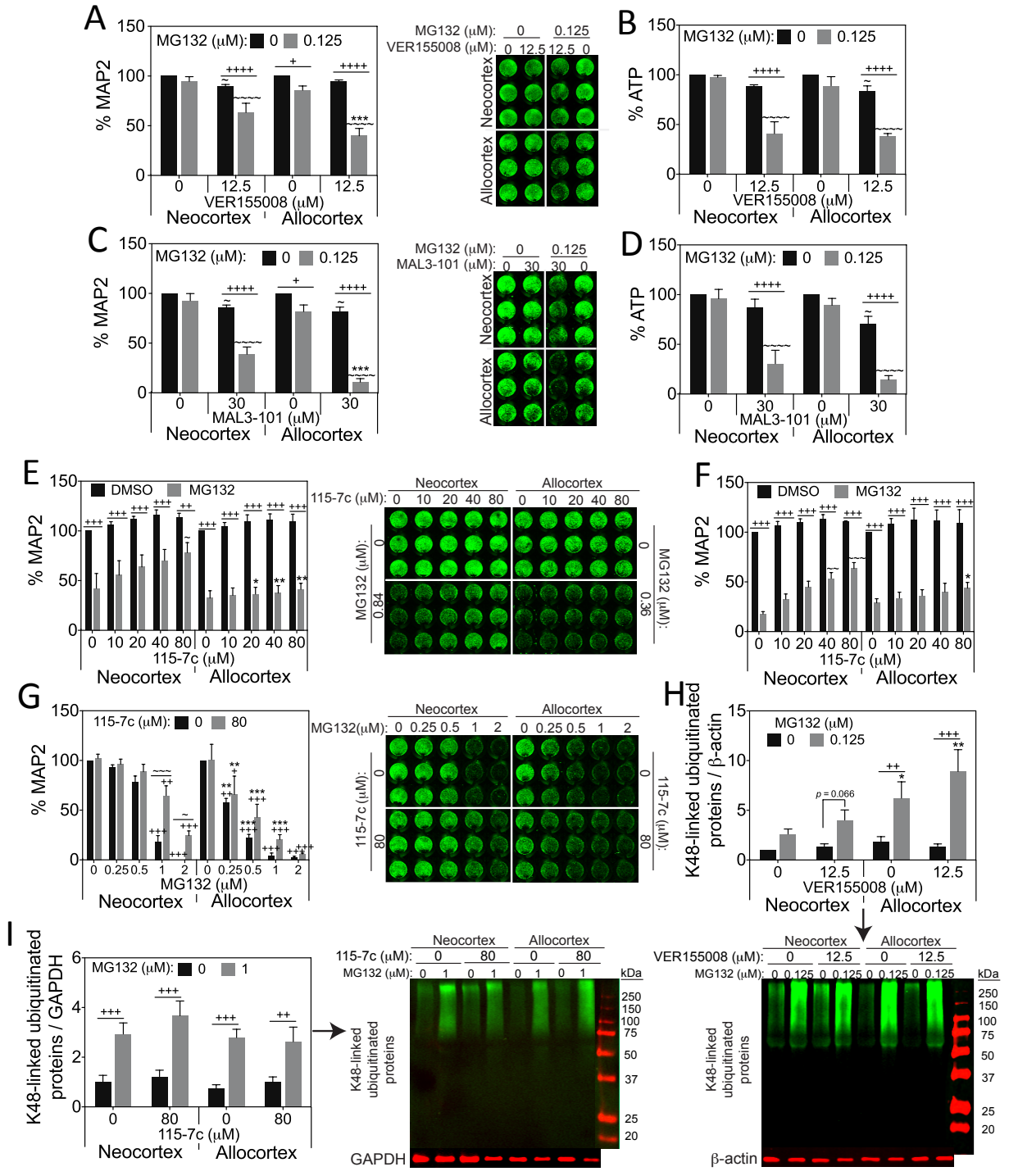

Figure 19: Allocortical neurons rely more on Hsp70/Hsc70 than neocortical neurons under proteotoxic conditions. MAP2 and ATP levels in neo- and allocortical (entorhinal) cultures treated with MG132 and the Hsp70/Hsc70 inhibitors VER155008 (**A, B**) or MAL3-101 (**C, D**), and the Hsp70 activity enhancer 115-7c for 48h (**E-G**). See text for details on MG132 concentrations in E & F. Loss of Hsp70/Hsc70 activity with VER155008 or MAL3-101 synergistically exacerbated cell loss in response to MG132 according to the MAP2 assay, especially in allocortical neurons. Enhancement of Hsp70 activity with 115-7c protected neocortical neurons against proteotoxicity better

than allocortical neurons. (**H, I**) K48-linked ubiquitinated proteins in neo- and allocortical cultures treated 24h with MG132 and VER155008 or MG132 and 115-7c. Ubiquitinated protein levels were higher in allocortical cultures than neocortical cultures after treatment with low concentrations of MG132 (0.125 μM). Hsp70 activity manipulation with VER155008 and 115-7c exerted no effects on ubiquitinated proteins. Shown are the mean ± SEM of 3-7 independent experiments. * $p \leq 0.05$, ** $p \leq 0.01$, *** $p \leq 0.001$ vs neocortex, + $p \leq 0.05$, ++ $p \leq 0.01$, +++ $p \leq 0.001$, ++++ $p \leq 0.0001$ vs 0 μM MG132, ~ $p \leq 0.05$, ~~ $p \leq 0.01$, ~~~ $p \leq 0.001$, ~~~~ $p \leq 0.0001$ vs 0 μM VER155008, MAL3-101, or 115-7c, Bonferroni *post hoc* correction following three-way ANOVA for MAP2 and ATP assays or LSD *post hoc* correction following three-way ANOVA for immunoblotting data. Reprinted from Neurobiology of Aging, 36 (5), J. Posimo, J. Weilnau, A. Gleixner, M. Broeren, N. Weiland, J. Brodsky, P. Wipf, and R. Leak, "Heat shock protein defenses in the neocortex and allocortex of the telencephalon," p. 1924-1937. Copyright 2015 by Elsevier, reprinted with permission from Elsevier.

Allocortex Relies more on HO1 to Defend against Proteotoxicity than Neocortex

In our comprehensive examination of heat shock proteins, HO1 levels were found to be higher in allocortical cultures than neocortical cultures following MG132 treatment (Fig. 8G). This suggests that allocortex may rely more on HO1 than neocortex to defend against proteotoxicity, similar to the Hsp70/Hsc70 data. The HO1 inhibitor SnPP was applied to directly test this hypothesis. As expected, MG132 toxicity was synergistically potentiated in allocortex more than neocortex (Fig. 20A). However, allocortex had higher ATP levels after MG132 treatment than neocortex in the presence of SnPP, suggesting that allocortex was either less metabolically vulnerable to HO1 activity loss or that it increased ATP output in response to greater stress (Fig. 20B).

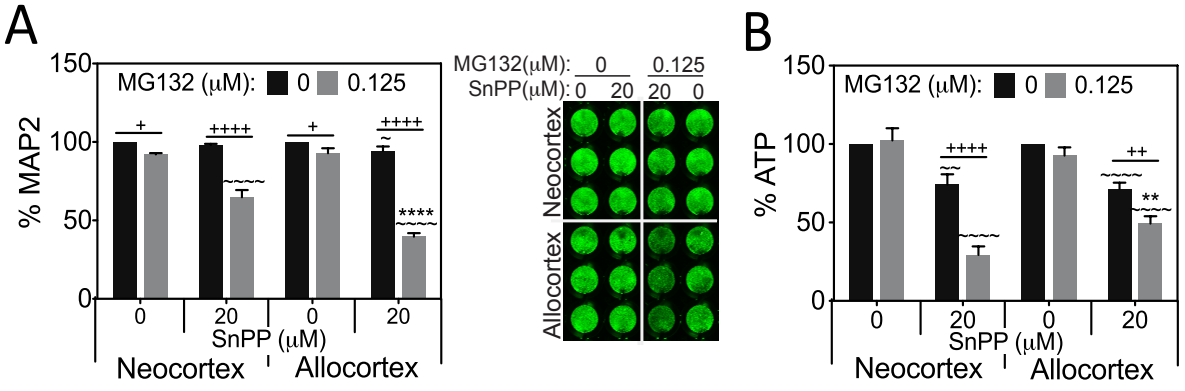

Figure 20: Allocortical neurons rely on HO1 more than neocortical neurons under proteotoxic conditions. (A, B) MAP2 and ATP levels were assessed in neo- and allocortical cultures 48h after treatment with the HO1 activity inhibitor tin protoporphyrin (SnPP) and MG132. Loss of HO1 activity synergistically exacerbated MG132 toxicity according to the MAP2 assay, especially in allocortical neurons. However, loss of ATP in response to VER155008 and MG132 co-treatment was not as severe in allocortical cultures as in neocortical cultures. Shown are the mean ±

SEM of 3-4 independent experiments. ** $p \leq 0.01$, **** $p \leq 0.0001$ vs neocortex, + $p \leq 0.05$, ++ $p \leq 0.01$, ++++ $p \leq 0.0001$ vs 0 μM MG132, ~~ $p \leq 0.01$, ~~~~ $p \leq 0.0001$ vs 0 μM SnPP, Bonferroni post hoc correction following three-way ANOVA. Reprinted from Neurobiology of Aging, 36 (5), J. Posimo, J. Weilnau, A. Gleixner, M. Broeren, N. Weiland, J. Brodsky, P. Wipf, and R. Leak, "Heat shock protein defenses in the neocortex and allocortex of the telencephalon," p. 1924-1937. Copyright 2015 by Elsevier, reprinted with permission from Elsevier.

Neo- and Allocortical Astrocytes Do Not Differ in their Reliance on Hsp/Hsc70 Defenses

As mentioned previously, our neo- and allocortical cultures contain a small percentage of glia, including $GFAP^+$ astrocytes. The number of $GFAP^+$ cells was similar in neo- and allocortex, although GFAP staining was more intense in allocortex (9.5% $GFAP^+$ cells in neocortex; 13.2% $GFAP^+$ cells in allocortex) (Fig. 21A). Consequently, there were higher levels of GFAP in allocortex than neocortex by Western blot analyses (Fig. 21B). These findings raised the possibility that distinct astrocytic responses in neocortical and allocortical cultures may contribute to the differential effects of MG132 and the Hsp70/Hsc70 modulators. To examine this question, neocortical and allocortical astrocytes were cultured in parallel and treated with VER155008 and MG132 in collaboration with Justin Weilnau. Neocortex-derived astrocyte cultures were found to be 92% $GFAP^+$ and allocortex-derived astrocyte cultures were 95% $GFAP^+$. Blinded counts of $Hoechst^+$ nuclei revealed only slight exacerbation of MG132 toxicity with VER155008 in neocortical astrocytes and no significant differences between neo- and allocortical astrocytes (Fig. 21C, H). In addition, DRAQ5 nuclear staining revealed that MG132 toxicity was only slightly exacerbated by VER155008 in both neo- and allocortical astrocyte cultures (Fig. 21D, E). There was no exacerbation of MG132 toxicity with VER155008 as assessed by the ATP assay, even when ATP levels were expressed as a function of cell numbers, a measurement of ATP output per cell (Fig. 21F, G). However, ATP output per cell rose with MG132 in allocortical astrocytes treated with VER155008, a sign of greater metabolic stress (Fig. 21G). Nevertheless, neo- and allocortical astrocytes exhibited no significant differences by

any of the three assays (Hoechst^{+} cell numbers, DRAQ5 levels, and ATP levels). In sum, these findings support the view that the differences in reliance on Hsp70 defenses in neo- and allocortex is neuronal and not astrocytic in origin.

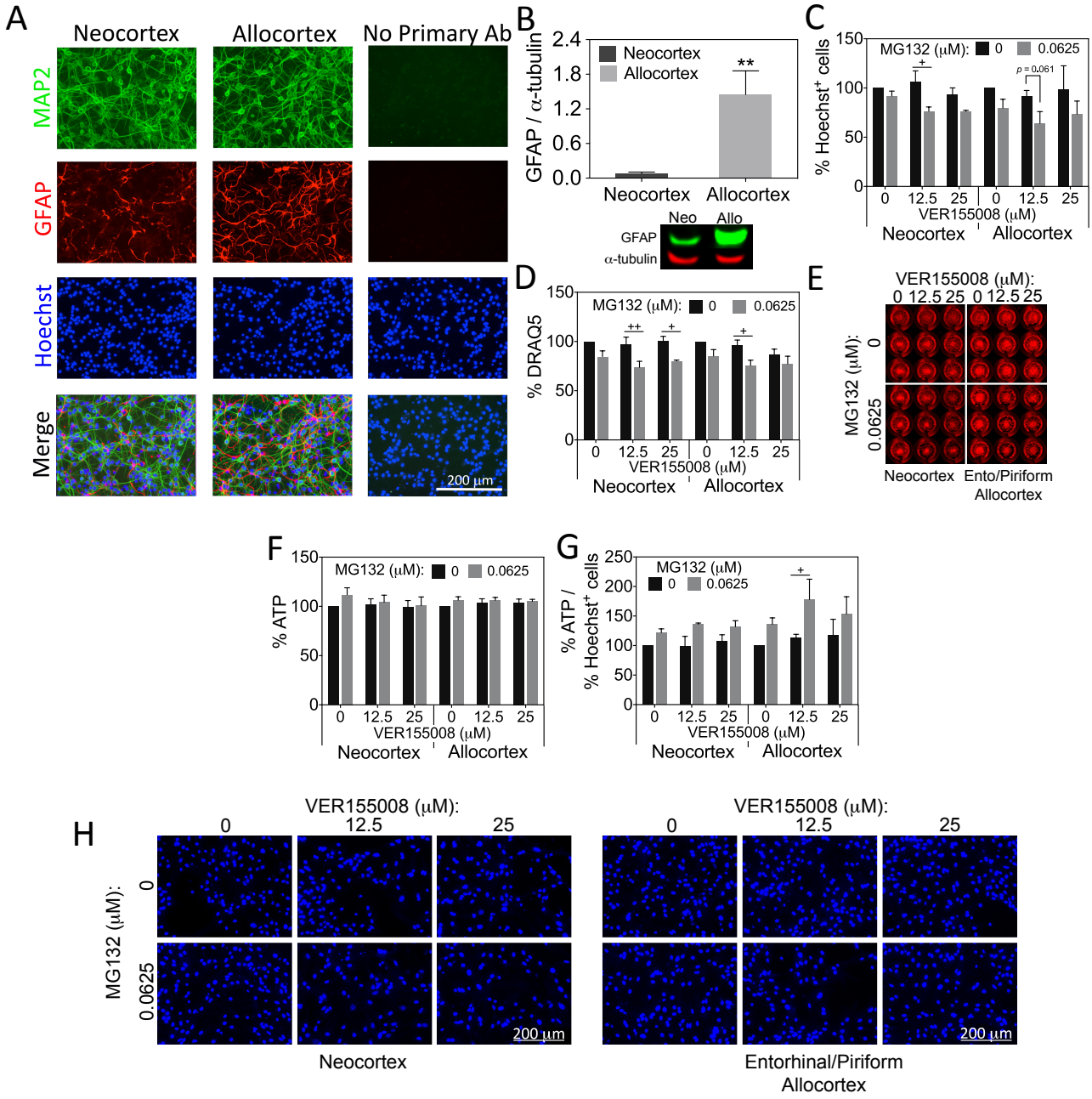

Figure 21: Neo- and allocortical astrocytes do not differ in their reliance on Hsp70/Hsc70 defenses. (**A**) Neo- and allocortical (entorhinal) neuronal cultures were stained for MAP2, GFAP, and Hoechst. Some GFAP^{+} astrocytes were visible in both cultures. Omission of primary antibodies led to loss of fluorescent signal. (**B**) Western blots for GFAP verify the presence of this protein in cultures from both brain regions and reveal that GFAP protein levels are

higher in allocortex cultures. Shown are the mean ± SEM of 6 independent experiments. ** $p \leq 0.01$ vs neocortex, two-tailed Student's *t*-test. (**C-H**) Astrocyte cultures harvested from neo- and allocortex were treated with MG132 and the Hsp70/Hsc70 inhibitor VER155008 for 48h and the number of Hoechst$^+$ cells, DRAQ5 nuclear staining, and ATP levels were assessed. ATP levels were also expressed as a function of Hoechst$^+$ cells in panel **G**. Representative DRAQ5 and Hoechst images from the data in panels C and D are shown (**E, H**). Unlike in neurons, there was no robust exacerbation of MG132 toxicity in neo- or allocortical astrocytes after loss of Hsp70/Hsc70 activity, even at higher concentrations of VER155008. Shown are the mean ± SEM of 3 independent experiments. + $p \leq 0.05$, ++ $p \leq 0.01$ vs 0 μM MG132, Bonferroni *post hoc* correction following three-way ANOVA. Reprinted from Neurobiology of Aging, 36 (5), J. Posimo, J. Weilnau, A. Gleixner, M. Broeren, N. Weiland, J. Brodsky, P. Wipf, and R. Leak, "Heat shock protein defenses in the neocortex and allocortex of the telencephalon," p. 1924-1937. Copyright 2015 by Elsevier, reprinted with permission from Elsevier.

Hsp70 Inhibition Does Not Exacerbate Paraquat Toxicity in Neo- and Allocortex

Hsp70 defenses are essential to combat toxicity associated with protein misfolding stress. Our previous work has shown that Hsp70 is less effective against oxidative toxicity (Crum et al., 2015). In order to verify this in the current model, we treated neo- and allocortical cultures with the oxidative toxin paraquat and the Hsp70/Hsc70 activity inhibitors VER155008 and MAL3-101. No robust effect was observed when these inhibitors were applied in conjunction with paraquat in either neo- or allocortical cultures, supporting our previous work that Hsp70 defenses are not essential for protection against oxidative toxins (Fig. 22A-D). Finally, heat shock protein levels were examined in neo- and allocortex cultures after treatment with paraquat. Paraquat treatment did not elicit any significant changes in Hsp90, Hsp60, Hsp40, or Hsc70 levels in neo- and allocortex cultures (Fig. 22E-H). Furthermore, Hsp70 levels were undetectable in neo- and allocortical cultures treated with paraquat, suggesting that Hsp70 is not even upregulated in response to oxidative stress. On the other hand, HO1 levels rose significantly higher in allocortical cultures than neocortical cultures after paraquat treatment (Fig. 22I). Furthermore, allocortex expressed significantly higher levels of Hsp25 than neocortex with and without paraquat treatment (Fig. 22J). These results support the view that allocortex responds to oxidative stress with a greater increase in Hsp25 and HO1 than neocortex but that Hsp70 is not engaged in response to paraquat exposure. These finding are consistent with previous studies in

which HO1 and Hsp25 are induced by free-radical injury (Maines & Panahian, 2001; Merendino et al., 2002).

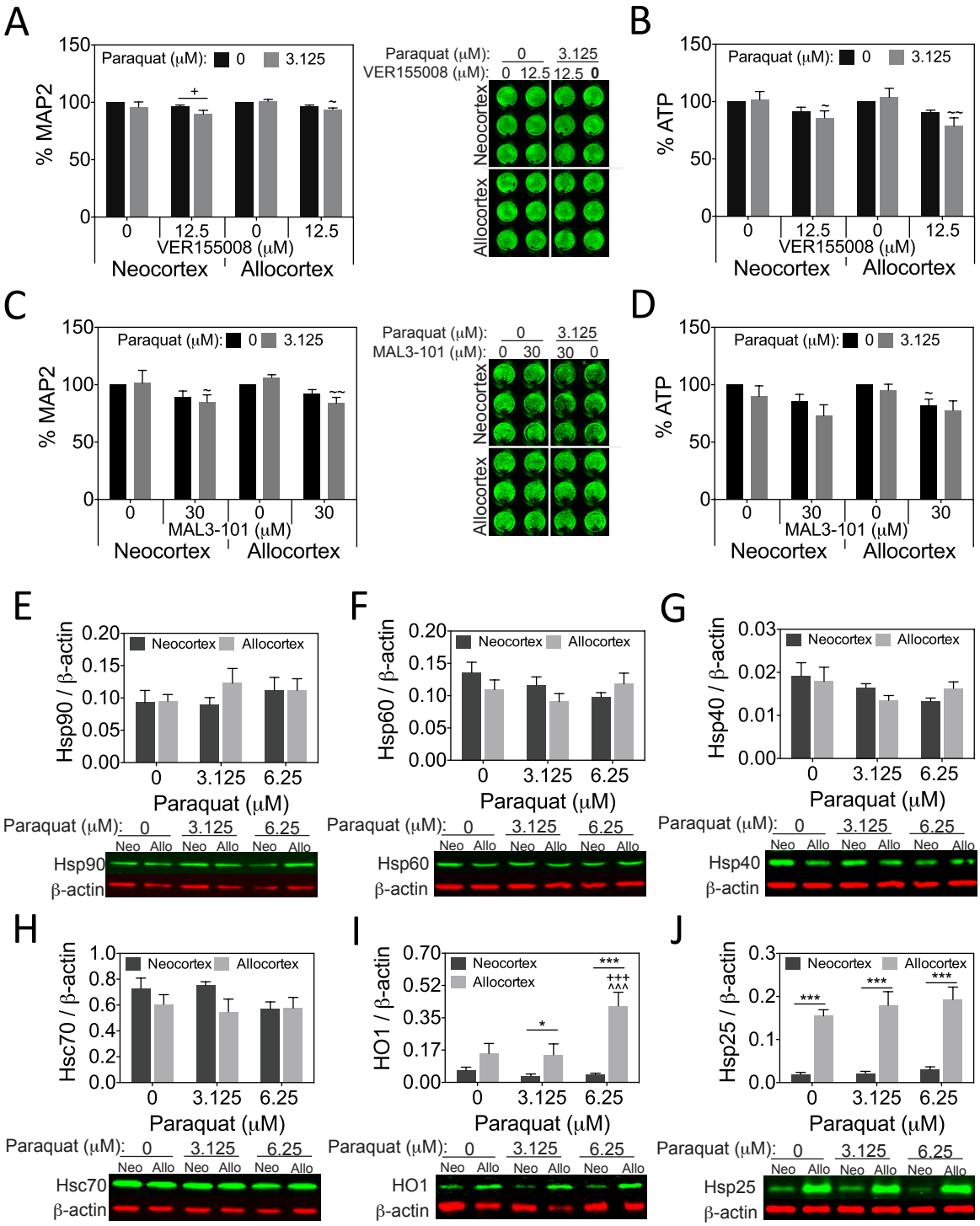

Figure 22: Paraquat toxicity in neo- and allocortical neurons is not exacerbated by Hsp70/Hsc70 inhibition. MAP2 and ATP levels in neo- and allocortical (entorhinal) cultures 48h after treatment with paraquat or vehicle in the absence or presence of the Hsp70/Hsc70 inhibitors VER155008 (**A, B**) or MAL3-101 (**C, D**). Paraquat-induced cell loss was not robustly exacerbated by inhibition of Hsp70/Hsc70 activity in either neo- or allocortical neurons according to the MAP2 and ATP assays. Expression of heat shock proteins Hsp90, Hsp60, Hsp40, Hsc70, HO1, and Hsp25 in neo- and allocortical cultures treated with paraquat (**E-J**). Of all the proteins shown, paraquat only increased levels of the antioxidant defense protein HO1 in allocortical cultures. Allocortical cultures had higher levels of HO1 and Hsp25 than neocortical cultures. Shown are the mean ± SEM of 3-6 independent experiments. * $p \leq 0.05$, *** $p \leq 0.001$ vs neocortex, + $p \leq 0.05$, +++ $p \leq 0.001$ vs 0 μM paraquat, ~ $p \leq 0.05$, ~~ $p \leq 0.01$ vs 0 μM VER155008 or MAL3-101, ^^^ $p \leq 0.001$ vs 3.125 μM paraquat, Bonferroni *post hoc* correction following three-way ANOVA for MAP2 and ATP data or LSD *post hoc* correction following two-way ANOVA for immunoblotting data. Reprinted from Neurobiology of Aging, 36 (5), J. Posimo, J. Weilnau, A. Gleixner, M. Broeren, N. Weiland, J. Brodsky, P. Wipf, and R. Leak, "Heat shock protein defenses in the neocortex and allocortex of the telencephalon," p. 1924-1937. Copyright 2015 by Elsevier, reprinted with permission from Elsevier.

Discussion

The goal of Specific Aim 2 was to assess the role of heat shock proteins in neocortical and entorhinal allocortical neurons as a defense against proteotoxic stress. In support of our hypothesis, we found that neocortex is more resistant to loss of protein homeostasis. Given the stress-inducible nature of heat shock proteins, the results of this Specific Aim suggest that allocortex cultures are under greater levels of proteotoxic stress, because Hsp70 and Hsc70 levels were higher in allocortical cultures after treatment with low concentrations of MG132. This view is strongly supported by the viability measurements, because allocortical neurons exhibited a greater propensity to die following toxic proteasome inhibition, especially when Hsp70/Hsc70 activity was simultaneously inhibited. Proteotoxic stress is defined as an increased burden of misfolded proteins and subsequent loss of protein homeostasis, and is reflected in the K-48 ubiquitinated protein pool (Sadowski & Sarcevic, 2010). As expected, allocortical cultures expressed higher levels of K-48 ubiquitinated proteins than neocortical cultures after treatment with MG132. Furthermore, the Hsp70 activator 115-7c protected neocortical but not allocortical cultures against MG132-induced proteotoxicity. This lack of significant protection is also likely to reflect greater proteotoxicity in allocortical than neocortical cultures. For example, allocortical Hsp70 molecules may already be maximally engaged due to the higher burden of misfolded

proteins in neurons from allocortex. Perhaps as a result, Hsp70 activity cannot be further stimulated to elicit neuroprotection and more protein would need to be expressed to have a significant effect upon protein misfolding. Thus, we hypothesize that allocortical cultures mount a greater heat shock protein response due to greater levels of proteotoxic stress, but that this response seems insufficient to render it as resistant as neocortex. In conclusion, our studies support the view that brain region specific Hsp70- and Hsc70-based therapies or heat shock gene induction will slow or prevent neuronal cell death in proteinopathic conditions such as Parkinson's or Alzheimer's disease.

As many studies have reported highly protective effects of HO1, the effect of HO-1 inhibition was also assessed in our *in vitro* model in order to reveal potential neo/allocortical differences (Calabrese et al., 2009). The HO1 inhibition and Western blotting experiments reveal that allocortex cells rely more on HO1 for protection against proteotoxicity than neocortex cells, similar to the Hsp70 data. In addition, Hsp25 levels were also elevated to higher levels in allocortex than neocortex with MG132 treatment. Taking both our Hsp70/Hsc70 and HO1 findings into consideration, we speculate that allocortex also relies more heavily on Hsp25 for protection than neocortex. Further studies with Hsp25 inhibitors are needed to test this hypothesis directly.

The reason underlying the greater vulnerability of allocortex to proteasomal stress is still unclear, as allocortical cells did not exhibit overall lower levels of defensive proteins. However, allocortical neurons are known to exhibit less myelination and greater accumulation of lipofuscin, a byproduct of failed lysosomal degradation, and may therefore be subject to greater levels of oxidative and proteotoxic stress in humans (H. Braak, Rüb, et al., 2003). It is possible that allocortex evolved to express higher levels of antioxidant and chaperone proteins due to a

greater risk of proteotoxicity with aging. Despite these attempts, the additional defenses are insufficient to make allocortex quite as resilient to loss of protein homeostasis as neocortex. It is possible that the relative resilience of the neocortex observed in the present study is related to higher expression of the co-chaperones Hip and Hop after proteotoxic stress exposure. We previously showed that neocortex also expresses higher levels of the ferroxidase ceruloplasmin and the antioxidant glutathione, both of which were not stress-responsive in our model. Further, neocortex appeared to rely on autophagy to combat proteotoxicity whereas allocortex did not (Posimo, Titler, Choi, Unnithan, & Leak, 2013). In addition to these explanations, the differential vulnerability of the neocortex and allocortex to human diseases may reflect their vastly different efferent and afferent connectomes.

Astrocytes are known to develop inclusions in a similar staging pattern as the intraneuronal pathology (H. Braak, Sastre, & Del Tredici, 2007). Furthermore, evidence suggests that astrocytes are subjected to proteotoxic stress in neurodegenerative conditions. For example, astrocytes can remove α-synuclein from the extracellular space and upregulate heat shock proteins (H. Braak et al., 2007; Dabir, Trojanowski, Richter-Landsberg, Lee, & Forman, 2004; Durrenberger et al., 2009; Lee et al., 2010; Renkawek, Stege, & Bosman, 1999; Seidel et al., 2012). In the present study, no significant differences between neo- and allocortical astrocytes were observed. These findings support the view that the differences observed in our mixed cultures are largely neuronal in origin.

The results of our MAP2 and ATP assays are not always in agreement. Both assays have been validated in multiple publications and shown to measure distinct aspects of cellular fitness (Posimo et al., 2013; Posimo et al., 2014; Unnithan, Choi, Titler, Posimo, & Leak, 2012). As mentioned above, ATP levels are often upregulated in stressed cells, suggesting that this assay

cannot be used as an approximation of cell numbers as claimed by the manufacturer. Furthermore, the ATP measurements do not distinguish between neurons and glia. Thus, higher ATP levels may not represent higher cell numbers but may suggest greater metabolic stress, in either neurons or glia or both. Further studies to determine ATP output as a function of cell numbers in purely neuronal models would help to address this limitation.

As discussed previously, limitations of this study include the possible selection of cells predisposed to survive the culturing process. On the other hand, if resistant neo- and allocortical cells were indeed selected differently during the culturing protocol, such a difference would not explain why both survived equally well under basal conditions in Neurobasal-A media. Differential survival of the culturing protocol would also not explain why neocortical cells were more resistant to proteasome inhibitors but less resistant to oxidative toxins. Another limitation of this study may be that neo- and allocortex are at different developmental stages when harvested on postnatal day 1 or 2. For example, allocortex may develop more rapidly than neocortex during embryonic life and thus may experience more mechanical stress due to greater shearing of axonal projections and dendritic processes upon trituration and dissociation (Kostovic, 1990; Kostovic, Petanjek, & Judas, 1993; Prayer, 2011). However, this would also not explain why vulnerabilities to proteasome inhibitors and oxidative toxins are reversed. Finally, although varying amounts of non-neuronal elements such as glia may contribute to differential responses to cellular stress, our astrocyte culture data do not suggest that this is a serious confound.

Chapter 3

Specific Aim 3: Characterize the age-related changes in antioxidant and heat shock protein profiles of the neo- and allocortex *in vivo.* Based on our *in vitro* findings, we hypothesize that levels of stress sensitive proteins will increase more in allocortex than neocortex with age.

Rationale

Aging is a natural model of proteotoxicity and the major risk factor for neurodegenerative diseases (Dasuri et al., 2009; Keller, Gee, & Ding, 2002; Keller, Hanni, & Markesbery, 2000). Additionally, aging has been associated with increased oxidative damage since the 1950s (Harman, 1956). Thus, we examined the impact of aging on defensive proteins such as glutathione, heat shock proteins, and proteins related to the proteasome in neo- and allocortex *in vivo.*

Results

Neocortex and Allocortex Respond Differently to Aging In Vivo

As discussed in Specific Aim 1b, glutathione levels were found to be significantly higher in neocortex than allocortex *in vitro* (Fig. 23A). Therefore, we wanted to establish whether glutathione levels exhibited similar patterns *in vivo.* Glutathione levels were measured in rat brain tissue as a function of age (Fig. 23A). Surprisingly, no significant differences were found between neo- and allocortical levels of glutathione at any age. However, allocortical glutathione levels were significantly higher at 19-22 months than at 2-4 months of age (Fig. 23A). Moreover, a linear regression analysis revealed a significant correlation between age and glutathione levels in allocortex but not in neocortex ($p = 0.0136$, $R^2 = 0.9014$). This age-related rise in allocortical glutathione levels may be a compensatory mechanism against a parallel

increase in age-related cellular stress. Alternatively, aged allocortex may survive oxidative insults better than aged neocortex, as shown for postnatal cultures *in vitro.*

Next we measured levels of ubiquitin-conjugated proteins and PA28 to assess age-related proteasomal stress. Ubiquitin-conjugated protein levels were not significantly different between neo- and allocortex and did not rise with aging (data not shown). Neocortical PA28 levels were significantly higher in 19-22 month than 2-4 month old animals. However, allocortical PA28 levels were significantly higher at 16-19 months than 2-4 months of age. Furthermore, PA28 levels were higher in allocortex than neocortex at every age (Fig. 23B, C). At 19-22 months, neo- and allocortical PA28 levels were no longer significantly different, supporting the view that neocortex and allocortex may display equivalent levels of proteasomal stress toward the end of life.

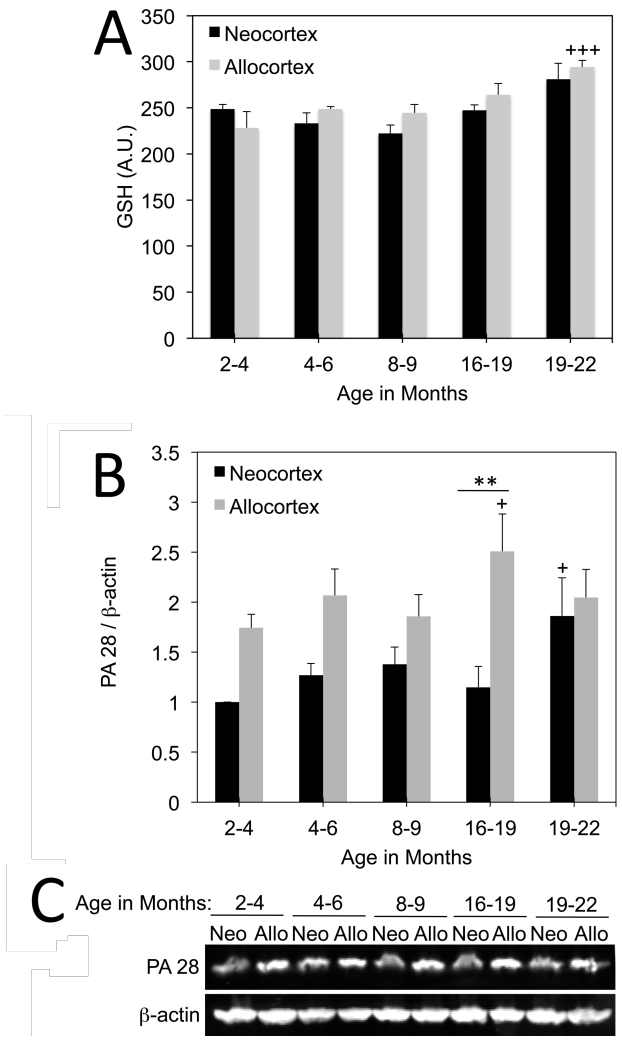

Figure 23. Impact of natural aging on neocortex and allocortex in vivo. **A**: Glutathione levels in whole tissue lysates of rat neo- and allocortex as a function of age. Allocortical glutathione levels were similar to those in neocortex but rose in an age-dependent manner and were significantly higher at 19-22 months of age relative to the youngest group (2-4 months). Neocortical glutathione did not change significantly as a function of age. **B-C**: Western immunoblotting for PA28 levels as a function of age and brain region. PA28 levels rose in neocortex at 19-22 months and in allocortex at 16-19 months relative to the youngest age group. Allocortical PA28 levels were significantly higher than in neocortex at 16-19 months of age. Data are expressed as mean and standard error of the mean from 4-5 rats per group. For all panels, ** $p \leq 0.01$, allocortex versus neocortex; + $p \leq 0.05$, +++ $p \leq 0.001$ versus levels in the 2-4 month old group; Bonferroni *post hoc* correction following two-way ANOVA. Reprinted from "Neocortex and Allocortex Respond Differentially to Cellular Stress *In Vitro* and *In Vivo*," by J. Posimo, A. Titler, H. Choi, A. Unnithan, and R. Leak 2013, *PLoS ONE,* 8(3): e58596. doi:10.1371/journal.pone.0058596. Copyright 2013 by Posimo et al. Reprinted with permission.

Heat Shock Protein Expression in Neo- and Allocortex as a Function of Age In Vivo

In addition to glutathione measurements, we examined the impact of aging on heat shock protein expression in neocortical and allocortical tissue from female rats. Hsp90 and CHIP levels were significantly higher in neo- than allocortex in the 19-22 month old group (Fig. 24A, B). However, CHIP levels were significantly higher in allocortex than neocortex in the youngest animals. In addition, CHIP levels were significantly higher at all ages in neocortex and at 16-19 months in allocortex compared to levels in the 2-4 month old animals. CHIP levels in allocortex were decreased at 19-22 months compared to the youngest animals. Neocortical Hsp90 levels were raised in the 16-19 and 19-22 month old animals compared to the 2-4 month old group. The lower levels of Hsp90 and CHIP in aged allocortex compared to aged neocortex may indicate a collapse of chaperone defenses in this brain region.

Hip levels are significantly higher in allocortex than neocortex at 2-4 months (Fig. 24C). Furthermore, Hip levels were significantly increased in neocortex in the 4-6 month group compared to the youngest animals. Hsp70 levels peaked in neo- and allocortex at 8-9 months but returned to lower levels thereafter (Fig. 24F). HO1 levels were higher in allocortex than neocortex at 2-4 and 8-9 months of age (Fig. 24G). Hsp25 levels in allocortex were higher in the 19-22 month old group compared to the youngest animals (Fig. 24H). No significant changes as a function of age or brain region of origin were observed for Hop, Hsc70, Hsp60, or Hsp40 (Fig. 24D-E, I-J). It is noteworthy that HO1 and Hsp25 levels were higher in allocortex than neocortex at some ages, consistent with the *in vitro* data showing higher stress-induced changes in the these proteins following MG132 treatment.

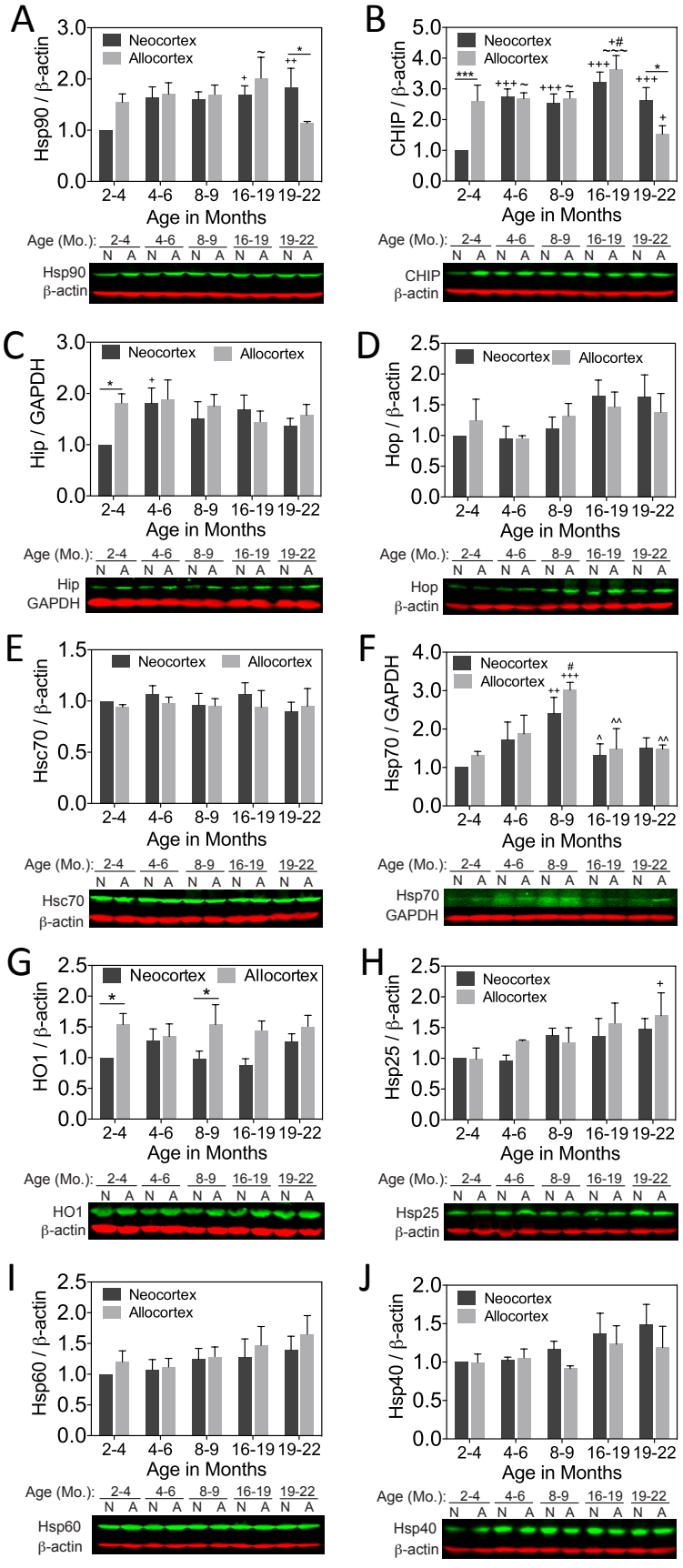
A
Hsp90 / β-actin
Neocortex
Allocortex
Age in Months
Age (Mo.): 2-4 4-6 8-9 16-19 19-22
N A N A N A N A N A
Hsp90
β-actin
B
CHIP / β-actin
CHIP
β-actin
C
Hip / GAPDH
Hip
GAPDH
D
Hop / β-actin
Hop
β-actin
E
Hsc70 / β-actin
Hsc70
β-actin
F
Hsp70 / GAPDH
Hsp70
GAPDH
G
HO1 / β-actin
HO1
β-actin
H
Hsp25 / β-actin
Hsp25
β-actin
I
Hsp60 / β-actin
Hsp60
β-actin
J
Hsp40 / β-actin
Hsp40
β-actin

Figure 24: Heat shock proteins and co-chaperones in neo- and allocortex as a function of age in vivo. Female rats were sacrificed at 2-3.9, 4-6, 8-9, 16-18.9, and 19-22 months of age. Heat shock proteins Hsp90, Hsc70, Hsp70, HO1, Hsp25, Hsp60, and Hsp40 (A, E, F, G, H, I, J) and co-chaperones CHIP, Hip, and Hop (B, C, D) were measured in sensorimotor neocortex and entorhinal allocortex by infrared immunoblotting. Allocortical tissue exhibited higher levels of HO1 at multiple ages and higher levels of Hip at the youngest age. Age-related changes (usually increases) in Hsp90, CHIP, Hip, Hsp25 and Hsp70 were also apparent. Allocortical tissue exhibited lower levels of Hsp90 and CHIP than neocortical tissue in the oldest group, but allocortex and neocortex expressed equivalent levels of Hsp70 at all ages. n= 3-6 animals per group. * $p \leq 0.05$, *** $p \leq 0.001$ vs neocortex, + $p \leq 0.05$, ++ $p \leq 0.01$, +++ $p \leq 0.001$ vs 2-4 mo., # $p \leq 0.05$ vs 4-6 mo., ^ $p \leq 0.05$, ^^ $p \leq 0.01$ vs 8-9 mo., ~ $p \leq 0.05$, ~~~ $p \leq 0.001$ vs 19-22 mo., LSD post hoc correction following two-way ANOVA. Reprinted from Neurobiology of Aging, 36 (5), J. Posimo, J. Weilnau, A. Gleixner, M. Broeren, N. Weiland, J. Brodsky, P. Wipf, and R. Leak, "Heat shock protein defenses in the neocortex and allocortex of the telencephalon," p. 1924-1937. Copyright 2015 by Elsevier, reprinted with permission from Elsevier.

Discussion

This study compares regional variations in antioxidant, proteasomal, and heat shock protein defenses in the sensorimotor neocortex and entorhinal allocortex *in vivo*, and determines the impact of aging on these topographical patterns. Our hypothesis that levels of stress sensitive molecules would be raised to greater levels in allocortex than neocortex with aging was supported by some (eg. Hsp25, HO1), but not all molecules.

Glutathione levels were significantly different between neo- and allocortex in our *in vitro* model in either the absence or presence of MG132. Thus, we sought to assess glutathione levels in these regions as a function of age *in vivo*. However, we found that glutathione levels were similar between neo- and allocortex across all ages. This discrepancy between our *in vitro* and *in vivo* results may have arisen because our primary cultures are mainly neuronal, whereas the cortical tissue lysates contain large numbers of glia, particularly astrocytes. Astrocytes are the major source of glutathione in the brain and differences between neo- and allocortical neurons may have been masked by their abundant presence in the lysates. Furthermore, the postnatal time of harvest of neo- and allocortex may also help explain the discrepancy between the two sets of data. For example, neocortical cells might have higher levels of glutathione than allocortical cells neonatally but this difference might be lost upon further brain development into adulthood.

Future flow cytometry studies that distinguish neurons from astrocytes would be valuable to test the hypothesis that neocortical neurons have higher levels of glutathione than allocortical neurons *in vivo*. The rise in allocortical glutathione levels with age may be attributed to increasing levels of cellular stress as levels were highest in the oldest group and correlated robustly with advancing age.

Ubiquitin-conjugated protein levels were similar in neo- and allocortex *in vivo* and did not rise with aging. Nonetheless, other studies have shown that proteasome activity is decreased in the cortex with aging (Dasuri et al., 2009; Keller et al., 2002; Keller et al., 2000). Age-related proteasomal stress in neo- and allocortex was supported by increases in PA28 expression. Allocortex expressed higher levels of PA28 than neocortex in 16-19 month old animals, suggesting that allocortex may be under greater levels of proteasome-related stress *in vivo*, consistent with the *in vitro* findings. However, PA28 levels in the oldest group were similar in neo- and allocortex, suggesting that neocortex experiences some proteasome-related stress later in life.

When examining heat shock protein levels *in vivo*, many differences from our *in vitro* data (Chapter 2, Figure 18) were observed. Once again, the discrepancies may have arisen because of greater number of astrocytes *in vivo* or the postnatal time of harvest for the *in vitro* cultures. Additionally, the insults applied to these samples are quite distinct, as proteasome inhibition is certainly not the same as natural aging. Levels of Hsp70 were similar between neo- and allocortex *in vivo* whereas MG132-stressed allocortical neurons exhibited higher expression of this heat shock protein *in vitro*. In addition, allocortex expressed higher levels of the co-chaperone Hip in the youngest animals, whereas MG132-treated neocortex expressed higher levels *in vitro*. In contrast, the pattern of HO1 expression in neo/allocortical cultures was in

agreement with the pattern of expression in tissue. Thus, HO1 levels were higher in allocortex at several ages *in vivo* and following paraquat and MG132 treatment *in vitro*. Hsp90 and CHIP levels were higher in neocortex than allocortex in the oldest aged animals, a finding that may warrant further examination in age-related diseases. Finally, Hsp25 levels were increased in allocortex both with age *in vivo* and with MG132 treatment *in vitro*. This finding is in agreement with previous work showing higher expression of this protein in the cortex, striatum, substantia nigra, and the olfactory bulb of aged animals relative to younger controls (Crum et al., 2015; Dickey et al., 2009; Gleixner et al., 2014; Gupte et al., 2010; Schultz et al., 2001).

Conclusion

In conclusion, we have discovered a number of differences in neo- and allocortical cells, strongly supporting the view that brain region and selective vulnerabilities must be taken into account when modeling diseases and designing new therapies. Previous studies are in general agreement that topographic differences in vulnerability are common in the central nervous system. For example, Mattson and colleagues demonstrated that the CA1 and CA3 subregions of the hippocampus are less resistant than other hippocampal areas (Mattson, Guthrie, & Kater, 1989). In the substantia nigra, caudal and ventrolateral dopaminergic neurons are more vulnerable than more rostral, dorsomedial dopaminergic neurons and neurons in the adjacent ventral tegmental area (H. Braak, Del Tredici, Rüb, et al., 2003; Damier et al., 1999). Furthermore, dopaminergic neurons in the retina do not degenerate in Parkinson's disease and are more resistant to parkinsonian neurotoxins than dopaminergic neurons in the ventral mesencephalon (Nagel, Bahr, & Dietz, 2009). Our study now adds to this body of literature, as we are the first to demonstrate that allocortical neurons are more vulnerable to proteotoxic but not oxidative stress than neocortical neurons. These vulnerability differences are likely to be superimposed upon neuroanatomical connectivity differences to determine whether or not a given neuron develops protein inclusions in Parkinson's disease.

Multiple independent and unbiased viability assays helped us reach the abovementioned conclusions. An ATP assay and two infrared viability assays, nuclear staining with DRAQ5 and the In-Cell Western assay for the neuronal marker MAP2, were used in parallel to assess the functional and structural integrity of the cells in culture. Our ATP and infrared assays were linear and correlated with plating density, though not all assays were equally sensitive. Nevertheless, each assay was well in proportion to cell number at or below our chosen plating density of

100,000 cells per well. These viability assays were used as an alternative to the more laborious manual nuclear cell counts, which suffer from a number of disadvantages. On the other hand, all assays suffer from caveats and rely on assumptions that are not always met, as discussed previously in Specific Aim 1a. Our reliance on multiple assays helps mitigate the impact of the caveats of each individual assay. Furthermore, a more comprehensive view of cellular fitness can be achieved by using multiple assays.

Using these assays in our *in vitro* model, allocortical neurons were found to be more resistant to H_2O_2 toxicity than neocortical neurons. This striking difference warrants further investigation as it suggests that allocortex has evolved impressive defenses against oxidative stress. However, neocortex was more resistant to proteasome inhibition than allocortex despite expressing lower levels of heat shock proteins, proteasomal subunits, and catalase. Consistent with the proteasome inhibitor data, neocortex did not form inclusions as readily as entorhinal cortex after treatment with α-synuclein fibrils. This suggests that entorhinal cortex is more vulnerable to proteotoxicity than neocortex, in agreement with postmortem studies of inclusion topography. Thus we have gathered support for the view that brain region of origin is a major determinant of inclusion formation, even in structures that are typically treated as a single unit in *in vitro* studies, such as the cerebral cortex.

In our hands, α-synuclein fibrils were not able to elicit cell loss *in vitro* as previously reported. This may be due to differences in treatment protocol and sonicators, as discussed in Specific Aim 1c. The hippocampus was the most susceptible to inclusion formation while olfactory bulb and neocortex were the least susceptible. These findings may be explained by our Western blotting data showing that basal levels of endogenous α-synuclein were highest in hippocampus. A recent study revealed that hippocampus has higher levels of α-synuclein

immunoreactivity compared to entorhinal cortex, neocortex, and specific regions of the olfactory bulb in the mouse brain, entirely consistent with our findings (Taguchi, Watanabe, Tsujimura, & Tanaka, 2015). These results suggest that abundant levels of α-synuclein may increase susceptibility to inclusion formation, as this protein is the major component of Lewy bodies. Our findings are also in agreement with work on α-synuclein knockout mice showing that endogenous α-synuclein expression is essential for the formation and spread of inclusions after injection of α-synuclein fibrils into the brain (Luk, Kehm, Carroll, et al., 2012).

Allocortical neurons were significantly more vulnerable to loss of Hsp70/Hsc70 activity and less able to recover from MG132 toxicity upon enhancement of Hsp70 activity. Thus, allocortex may have been all the more vulnerable to proteotoxicity had it not raised heat shock protein defenses so robustly. Our findings indicate that pharmacotherapies or gene therapies boosting Hsp70 activity would be more protective in neocortex than allocortex. The chaperone system in allocortex may already be maximally engaged in response to protein misfolding stress, suggesting that therapies targeted to this region may need to involve other molecules besides Hsp70, such as glutathione, or induce the expression of greater numbers of Hsp70 molecules.

Glutathione and ceruloplasmin were not found to be robustly stress-sensitive in our model and were basally higher in neocortex than allocortex *in vitro*. Moreover, inhibition of glutathione synthesis rendered neo- and allocortex all the more vulnerable to proteasome inhibition. Consistent with these observations, enhancing glutathione synthesis with N-acetyl cysteine protected allocortex from MG132 toxicity. These findings support the view that high glutathione expression may be partially responsible for neocortical resistance to proteotoxic stress. In addition, inhibition of autophagy heightened neocortical vulnerability to proteotoxicity

but had no effect on MG132 toxicity in allocortex. Thus, neocortex (but not allocortex) may be relying on autophagic defenses to battle MG132-induced proteotoxicity.

Limitations of our studies have been discussed throughout this document and will only be briefly mentioned here. For example, very young, postnatal day 1-2 rat neurons were used to model an age-related neurodegenerative disorder. It is possible that older neurons would respond differently, perhaps even showing greater intrinsic vulnerability differences than young neocortex and allocortex. For this reason, we also examined neo- and allocortical tissue as a function of age and found that CHIP and Hsp90 expression is lower in allocortex than neocortex in the oldest animals. We also recognize that neurons *in vitro* often respond differently than neurons *in vivo*. Many neuroanatomical circuits are disrupted in *in vitro* studies and the process of dissociation and adherence to plastic dishes may change protein expression and impact vulnerability patterns. Nevertheless, numerous investigators have used embryonic or postnatal cells as *in vitro* models of Parkinson's and Alzheimer's disease (Volpicelli-Daley et al., 2014a; Volpicelli-Daley et al., 2011a; Yao et al., 2009; Zhang et al., 2011).

Another limitation of our studies is the reliance on pharmacological inhibitors, all of which surely exert off-target effects. For example, MG132 is also known to inhibit cathepsins and calpains, lysosomal and non-lysosomal proteases, in addition to the proteasome (Kisselev & Goldberg, 2001). These off-target effects would nevertheless all lead to further proteotoxicity, suggesting that the responses that we observe after treatment with MG132 can indeed be attributed to loss of protein homeostasis. Furthermore, there are decreases in both proteasomal and lysosomal functions in Parkinson's disease (Cook, Stetler, & Petrucelli, 2012). Wherever possible, we attempted to use multiple inhibitors to decrease the impact of off-target effects on our interpretations. For example, neocortical neurons were more resistant to proteotoxicity than

allocortical neurons following exposure to three separate proteasome inhibitors (MG132, PSI, ALLN), a finding that was confirmed with α-synuclein fibril treatments. Furthermore, two Hsp70/Hsc70 activity inhibitors, VER155008 and MAL3-101, with unique mechanisms of action were applied to our *in vitro* model.

In conclusion, neocortex and allocortex respond differently when treated with toxins *in vitro* and to aging *in vivo*. The differential response of these regions to proteasome inhibition and α-synuclein fibril treatment parallels the clinical findings that human allocortex is more vulnerable to intracellular inclusions than neocortex in Alzheimer's and Parkinson's disease. This enhanced vulnerability to proteotoxicity may result in greater accrual of aggregated proteins in allocortical regions as a function of age and disease stage. Nevertheless, our findings indicate that allocortical neurons have impressive defenses against oxidative toxicity and exhibit multiple compensatory responses to proteotoxicity. Such allocortical defenses may help explain the slow and delayed nature of degeneration in Parkinson's and Alzheimer's disease. Enhancing such natural defenses in more vulnerable regions, including, but not limited to the allocortex, may further slow or perhaps even halt the progression of these disorders.

References

Adair, J. C., Knoefel, J. E., & Morgan, N. (2001). Controlled trial of N-acetylcysteine for patients with probable Alzheimer's disease. *Neurology, 57*(8), 1515-1517.

Adam, C., Baeurle, A., Brodsky, J. L., Wipf, P., Schrama, D., Becker, J. C., & Houben, R. (2014). The HSP70 Modulator MAL3-101 Inhibits Merkel Cell Carcinoma. *PLoS One, 9*(4), e92041. doi:10.1371/journal.pone.0092041

Agarwal, S., & Sohal, R. S. (1994). DNA oxidative damage and life expectancy in houseflies. *Proc Natl Acad Sci U S A, 91*(25), 12332-12335.

Alam, Z. I., Daniel, S. E., Lees, A. J., Marsden, D. C., Jenner, P., & Halliwell, B. (1997). A generalised increase in protein carbonyls in the brain in Parkinson's but not incidental Lewy body disease. *J Neurochem, 69*(3), 1326-1329.

Albert, M. S. (1996). Cognitive and neurobiologic markers of early Alzheimer disease. *Proc Natl Acad Sci U S A, 93*(24), 13547-13551.

Alladi, P. A., Mahadevan, A., Yasha, T. C., Raju, T. R., Shankar, S. K., & Muthane, U. (2009). Absence of age-related changes in nigral dopaminergic neurons of Asian Indians: relevance to lower incidence of Parkinson's disease. *Neuroscience, 159*(1), 236-245. doi:10.1016/j.neuroscience.2008.11.051

Alvarez-Erviti, L., Rodriguez-Oroz, M. C., Cooper, J. M., Caballero, C., Ferrer, I., Obeso, J. A., & Schapira, A. H. (2010). Chaperone-mediated autophagy markers in Parkinson disease brains. *Arch Neurol, 67*(12), 1464-1472. doi:10.1001/archneurol.2010.198

Anderson, J. P., Walker, D. E., Goldstein, J. M., de Laat, R., Banducci, K., Caccavello, R. J., . . . Chilcote, T. J. (2006). Phosphorylation of Ser-129 is the dominant pathological modification of alpha-synuclein in familial and sporadic Lewy body disease. *J Biol Chem, 281*(40), 29739-29752. doi:10.1074/jbc.M600933200

Appel-Cresswell, S., Vilarino-Guell, C., Encarnacion, M., Sherman, H., Yu, I., Shah, B., . . . Farrer, M. J. (2013). Alpha-synuclein p.H50Q, a novel pathogenic mutation for Parkinson's disease. *Mov Disord, 28*(6), 811-813. doi:10.1002/mds.25421

Arias, E., & Cuervo, A. M. (2011). Chaperone-mediated autophagy in protein quality control. *Curr Opin Cell Biol, 23*(2), 184-189. doi:10.1016/j.ceb.2010.10.009

Aridon, P., Geraci, F., Turturici, G., D'Amelio, M., Savettieri, G., & Sconzo, G. (2011). Protective role of heat shock proteins in Parkinson's disease. *Neurodegener Dis, 8*(4), 155-168. doi:10.1159/000321548

Arriagada, P. V., Growdon, J. H., Hedley-Whyte, E. T., & Hyman, B. T. (1992). Neurofibrillary tangles but not senile plaques parallel duration and severity of Alzheimer's disease. *Neurology, 42*(3 Pt 1), 631-639.

Athanassiadou, A., Voutsinas, G., Psiouri, L., Leroy, E., Polymeropoulos, M. H., Ilias, A., . . . Papapetropoulos, T. (1999). Genetic analysis of families with Parkinson disease that carry the Ala53Thr mutation in the gene encoding alpha-synuclein. *Am J Hum Genet, 65*(2), 555-558. doi:10.1086/302486

Auluck, P. K., Chan, H. Y., Trojanowski, J. Q., Lee, V. M., & Bonini, N. M. (2002). Chaperone suppression of alpha-synuclein toxicity in a Drosophila model for Parkinson's disease. *Science, 295*(5556), 865-868. doi:10.1126/science.1067389

Ayton, S., Lei, P., Adlard, P. A., Volitakis, I., Cherny, R. A., Bush, A. I., & Finkelstein, D. I. (2014). Iron accumulation confers neurotoxicity to a vulnerable population of nigral

neurons: implications for Parkinson's disease. *Mol Neurodegener, 9*, 27. doi:10.1186/1750-1326-9-27

Ayton, S., Lei, P., Duce, J. A., Wong, B. X., Sedjahtera, A., Adlard, P. A., . . . Finkelstein, D. I. (2013). Ceruloplasmin dysfunction and therapeutic potential for Parkinson disease. *Ann Neurol, 73*(4), 554-559. doi:10.1002/ana.23817

Aztatzi-Santillán, E., Nares-López, F. E., Márquez-Valadez, B., Aguilera, P., & Chánez-Cárdenas, M. E. (2010). The protective role of heme oxygenase-1 in cerebral ischemia. *Cent Nerv Syst Agents Med Chem, 10*(4), 310-316.

Baba, M., Nakajo, S., Tu, P. H., Tomita, T., Nakaya, K., Lee, V. M., . . . Iwatsubo, T. (1998). Aggregation of alpha-synuclein in Lewy bodies of sporadic Parkinson's disease and dementia with Lewy bodies. *Am J Pathol, 152*(4), 879-884.

Bancher, C., Braak, H., Fischer, P., & Jellinger, K. A. (1993). Neuropathological staging of Alzheimer lesions and intellectual status in Alzheimer's and Parkinson's disease patients. *Neurosci Lett, 162*(1-2), 179-182.

Bazzaro, M., Lee, M. K., Zoso, A., Stirling, W. L., Santillan, A., Shih, I. M., & Roden, R. B. (2006). Ubiquitin-proteasome system stress sensitizes ovarian cancer to proteasome inhibitor-induced apoptosis. *Cancer Res, 66*(7), 3754-3763. doi:10.1158/0008-5472.CAN-05-2321

Bennett, D. A., Beckett, L. A., Murray, A. M., Shannon, K. M., Goetz, C. G., Pilgrim, D. M., & Evans, D. A. (1996). Prevalence of parkinsonian signs and associated mortality in a community population of older people. *N Engl J Med, 334*(2), 71-76. doi:10.1056/NEJM199601113340202

Bernhardt, R., & Matus, A. (1984). Light and electron microscopic studies of the distribution of microtubule-associated protein 2 in rat brain: a difference between dendritic and axonal cytoskeletons. *J Comp Neurol, 226*(2), 203-221. doi:10.1002/cne.902260205

Besche, H. C., Peth, A., & Goldberg, A. L. (2009). Getting to first base in proteasome assembly. *Cell, 138*(1), 25-28. doi:10.1016/j.cell.2009.06.035

Bharucha, K. J., Friedman, J. K., Vincent, A. S., & Ross, E. D. (2008). Lower serum ceruloplasmin levels correlate with younger age of onset in Parkinson's disease. *J Neurol, 255*(12), 1957-1962. doi:10.1007/s00415-009-0063-7

Bierer, L. M., Hof, P. R., Purohit, D. P., Carlin, L., Schmeidler, J., Davis, K. L., & Perl, D. P. (1995). Neocortical neurofibrillary tangles correlate with dementia severity in Alzheimer's disease. *Arch Neurol, 52*(1), 81-88.

Boll, M. C., Alcaraz-Zubeldia, M., Montes, S., & Rios, C. (2008). Free copper, ferroxidase and SOD1 activities, lipid peroxidation and NO(x) content in the CSF. A different marker profile in four neurodegenerative diseases. *Neurochem Res, 33*(9), 1717-1723. doi:10.1007/s11064-008-9610-3

Boll, M. C., Sotelo, J., Otero, E., Alcaraz-Zubeldia, M., & Rios, C. (1999). Reduced ferroxidase activity in the cerebrospinal fluid from patients with Parkinson's disease. *Neurosci Lett, 265*(3), 155-158.

Braak, E., Braak, H., & Mandelkow, E. M. (1994). A sequence of cytoskeleton changes related to the formation of neurofibrillary tangles and neuropil threads. *Acta Neuropathol, 87*(6), 554-567.

Braak, H., & Braak, E. (1991). Neuropathological stageing of Alzheimer-related changes. *Acta Neuropathol, 82*(4), 239-259.

Braak, H., Del Tredici, K., Bratzke, H., Hamm-Clement, J., Sandmann-Keil, D., & Rub, U. (2002). Staging of the intracerebral inclusion body pathology associated with idiopathic Parkinson's disease (preclinical and clinical stages). *J Neurol, 249 Suppl 3*, III/1-5.

Braak, H., Del Tredici, K., Bratzke, H., Hamm-Clement, J., Sandmann-Keil, D., & Rüb, U. (2002). Staging of the intracerebral inclusion body pathology associated with idiopathic Parkinson's disease (preclinical and clinical stages). *J Neurol, 249 Suppl 3*, III/1-5.

Braak, H., Del Tredici, K., Rub, U., de Vos, R. A., Jansen Steur, E. N., & Braak, E. (2003). Staging of brain pathology related to sporadic Parkinson's disease. *Neurobiol Aging, 24*(2), 197-211.

Braak, H., Del Tredici, K., Rüb, U., de Vos, R. A., Jansen Steur, E. N., & Braak, E. (2003). Staging of brain pathology related to sporadic Parkinson's disease. *Neurobiol Aging, 24*(2), 197-211.

Braak, H., Del Tredici, K., Schultz, C., & Braak, E. (2000). Vulnerability of select neuronal types to Alzheimer's disease. *Ann N Y Acad Sci, 924*, 53-61.

Braak, H., Rub, U., Jansen Steur, E. N., Del Tredici, K., & de Vos, R. A. (2005). Cognitive status correlates with neuropathologic stage in Parkinson disease. *Neurology, 64*(8), 1404-1410. doi:10.1212/01.WNL.0000158422.41380.82

Braak, H., Rub, U., Schultz, C., & Del Tredici, K. (2006). Vulnerability of cortical neurons to Alzheimer's and Parkinson's diseases. *J Alzheimers Dis, 9*(3 Suppl), 35-44.

Braak, H., Rüb, U., Gai, W. P., & Del Tredici, K. (2003). Idiopathic Parkinson's disease: possible routes by which vulnerable neuronal types may be subject to neuroinvasion by an unknown pathogen. *J Neural Transm, 110*(5), 517-536. doi:10.1007/s00702-002-0808-2

Braak, H., Rüb, U., Schultz, C., & Del Tredici, K. (2006). Vulnerability of cortical neurons to Alzheimer's and Parkinson's diseases. *J Alzheimers Dis, 9*(3 Suppl), 35-44.

Braak, H., Sastre, M., & Del Tredici, K. (2007). Development of alpha-synuclein immunoreactive astrocytes in the forebrain parallels stages of intraneuronal pathology in sporadic Parkinson's disease. *Acta Neuropathol, 114*(3), 231-241. doi:10.1007/s00401-007-0244-3

Braunstein, M. J., Scott, S. S., Scott, C. M., Behrman, S., Walter, P., Wipf, P., . . . Batuman, O. (2011). Antimyeloma Effects of the Heat Shock Protein 70 Molecular Chaperone Inhibitor MAL3-101. *Journal of oncology, 2011*, 232037. doi:10.1155/2011/232037

Brewer, G. J., Kanzer, S. H., Zimmerman, E. A., Celmins, D. F., Heckman, S. M., & Dick, R. (2010). Copper and ceruloplasmin abnormalities in Alzheimer's disease. *Am J Alzheimers Dis Other Demen, 25*(6), 490-497. doi:10.1177/1533317510375083

Brundin, P., Li, J. Y., Holton, J. L., Lindvall, O., & Revesz, T. (2008). Research in motion: the enigma of Parkinson's disease pathology spread. *Nat Rev Neurosci, 9*(10), 741-745. doi:10.1038/nrn2477

Brunk, U. T., & Terman, A. (2002a). Lipofuscin: mechanisms of age-related accumulation and influence on cell function. *Free Radic Biol Med, 33*(5), 611-619.

Brunk, U. T., & Terman, A. (2002b). The mitochondrial-lysosomal axis theory of aging: accumulation of damaged mitochondria as a result of imperfect autophagocytosis. *Eur J Biochem, 269*(8), 1996-2002.

Calabrese, V., Cornelius, C., Mancuso, C., Barone, E., Calafato, S., Bates, T., . . . Kostova, A. T. (2009). Vitagenes, dietary antioxidants and neuroprotection in neurodegenerative diseases. *Front Biosci (Landmark Ed), 14*, 376-397.

Capo, C. R., Arciello, M., Squitti, R., Cassetta, E., Rossini, P. M., Calabrese, L., & Rossi, L. (2008). Features of ceruloplasmin in the cerebrospinal fluid of Alzheimer's disease patients. *Biometals, 21*(3), 367-372. doi:10.1007/s10534-007-9125-4

Castello, P. R., Drechsel, D. A., & Patel, M. (2007). Mitochondria are a major source of paraquat-induced reactive oxygen species production in the brain. *J Biol Chem, 282*(19), 14186-14193. doi:10.1074/jbc.M700827200

Chatterjee, M., Andrulis, M., Stuhmer, T., Muller, E., Hofmann, C., Steinbrunn, T., . . . Bargou, R. C. (2013). The PI3K/Akt signaling pathway regulates the expression of Hsp70, which critically contributes to Hsp90-chaperone function and tumor cell survival in multiple myeloma. *Haematologica, 98*(7), 1132-1141. doi:10.3324/haematol.2012.066175

Chaudhuri, K. R., Healy, D. G., Schapira, A. H., & Excellence, N. I. f. C. (2006). Non-motor symptoms of Parkinson's disease: diagnosis and management. *Lancet Neurol, 5*(3), 235-245. doi:10.1016/S1474-4422(06)70373-8

Chu, Y., Dodiya, H., Aebischer, P., Olanow, C. W., & Kordower, J. H. (2009). Alterations in lysosomal and proteasomal markers in Parkinson's disease: relationship to alpha-synuclein inclusions. *Neurobiol Dis, 35*(3), 385-398. doi:10.1016/j.nbd.2009.05.023

Connell, P., Ballinger, C. A., Jiang, J., Wu, Y., Thompson, L. J., Hohfeld, J., & Patterson, C. (2001). The co-chaperone CHIP regulates protein triage decisions mediated by heat-shock proteins. *Nat Cell Biol, 3*(1), 93-96. doi:10.1038/35050618

Cook, C., Stetler, C., & Petrucelli, L. (2012). Disruption of protein quality control in Parkinson's disease. *Cold Spring Harb Perspect Med, 2*(5), a009423. doi:10.1101/cshperspect.a009423

Cornelius, C., Perrotta, R., Graziano, A., Calabrese, E. J., & Calabrese, V. (2013). Stress responses, vitagenes and hormesis as critical determinants in aging and longevity: Mitochondria as a "chi". *Immun Ageing, 10*(1), 15. doi:10.1186/1742-4933-10-15

Coux, O., Tanaka, K., & Goldberg, A. L. (1996). Structure and functions of the 20S and 26S proteasomes. *Annu Rev Biochem, 65*, 801-847. doi:10.1146/annurev.bi.65.070196.004101

Crichton, R. R., Dexter, D. T., & Ward, R. J. (2011). Brain iron metabolism and its perturbation in neurological diseases. *J Neural Transm, 118*(3), 301-314. doi:10.1007/s00702-010-0470-z

Crum, T. S., Gleixner, A. M., Posimo, J. M., Mason, D. M., Broeren, M. T., Heinemann, S. D., . . . Leak, R. K. (2015). Heat shock protein responses to aging and proteotoxicity in the olfactory bulb. *J Neurochem*. doi:10.1111/jnc.13041

Cuervo, A. M., Bergamini, E., Brunk, U. T., Droge, W., Ffrench, M., & Terman, A. (2005). Autophagy and aging: the importance of maintaining "clean" cells. *Autophagy, 1*(3), 131-140.

Cuervo, A. M., Stefanis, L., Fredenburg, R., Lansbury, P. T., & Sulzer, D. (2004). Impaired degradation of mutant alpha-synuclein by chaperone-mediated autophagy. *Science, 305*(5688), 1292-1295. doi:10.1126/science.1101738

Dabir, D. V., Trojanowski, J. Q., Richter-Landsberg, C., Lee, V. M., & Forman, M. S. (2004). Expression of the small heat-shock protein alphaB-crystallin in tauopathies with glial pathology. *Am J Pathol, 164*(1), 155-166.

Dalfó, E., Portero-Otín, M., Ayala, V., Martínez, A., Pamplona, R., & Ferrer, I. (2005). Evidence of oxidative stress in the neocortex in incidental Lewy body disease. *J Neuropathol Exp Neurol, 64*(9), 816-830.

Damier, P., Hirsch, E. C., Agid, Y., & Graybiel, A. M. (1999). The substantia nigra of the human brain. II. Patterns of loss of dopamine-containing neurons in Parkinson's disease. *Brain, 122 (Pt 8)*, 1437-1448.

Daniel, S. E., & Hawkes, C. H. (1992). Preliminary diagnosis of Parkinson's disease by olfactory bulb pathology. *Lancet, 340*(8812), 186.

Dasuri, K., Zhang, L., Ebenezer, P., Liu, Y., Fernandez-Kim, S. O., & Keller, J. N. (2009). Aging and dietary restriction alter proteasome biogenesis and composition in the brain and liver. *Mech Ageing Dev, 130*(11-12), 777-783. doi:10.1016/j.mad.2009.10.003

De Domenico, I., Ward, D. M., di Patti, M. C., Jeong, S. Y., David, S., Musci, G., & Kaplan, J. (2007). Ferroxidase activity is required for the stability of cell surface ferroportin in cells expressing GPI-ceruloplasmin. *EMBO J, 26*(12), 2823-2831. doi:10.1038/sj.emboj.7601735

Demand, J., Alberti, S., Patterson, C., & Hohfeld, J. (2001). Cooperation of a ubiquitin domain protein and an E3 ubiquitin ligase during chaperone/proteasome coupling. *Curr Biol, 11*(20), 1569-1577.

Dexter, D., Carter, C., Agid, F., Agid, Y., Lees, A. J., Jenner, P., & Marsden, C. D. (1986). Lipid peroxidation as cause of nigral cell death in Parkinson's disease. *Lancet, 2*(8507), 639-640.

Dexter, D. T., Carayon, A., Javoy-Agid, F., Agid, Y., Wells, F. R., Daniel, S. E., . . . Marsden, C. D. (1991). Alterations in the levels of iron, ferritin and other trace metals in Parkinson's disease and other neurodegenerative diseases affecting the basal ganglia. *Brain, 114 (Pt 4)*, 1953-1975.

Dexter, D. T., Carter, C. J., Wells, F. R., Javoy-Agid, F., Agid, Y., Lees, A., . . . Marsden, C. D. (1989). Basal lipid peroxidation in substantia nigra is increased in Parkinson's disease. *J Neurochem, 52*(2), 381-389.

Dexter, D. T., Holley, A. E., Flitter, W. D., Slater, T. F., Wells, F. R., Daniel, S. E., . . . Marsden, C. D. (1994). Increased levels of lipid hydroperoxides in the parkinsonian substantia nigra: an HPLC and ESR study. *Mov Disord, 9*(1), 92-97. doi:10.1002/mds.870090115

Dexter, D. T., & Jenner, P. (2013). Parkinson disease: from pathology to molecular disease mechanisms. *Free Radic Biol Med, 62*, 132-144. doi:10.1016/j.freeradbiomed.2013.01.018

Dickey, C., Kraft, C., Jinwal, U., Koren, J., Johnson, A., Anderson, L., . . . Lewis, J. (2009). Aging analysis reveals slowed tau turnover and enhanced stress response in a mouse model of tauopathy. *Am J Pathol, 174*(1), 228-238. doi:10.2353/ajpath.2009.080764

Dickinson, D. A., & Forman, H. J. (2002). Cellular glutathione and thiols metabolism. *Biochem Pharmacol, 64*(5-6), 1019-1026.

Dickson, D. W., Uchikado, H., Fujishiro, H., & Tsuboi, Y. (2010). Evidence in favor of Braak staging of Parkinson's disease. *Mov Disord, 25 Suppl 1*, S78-82. doi:10.1002/mds.22637

Dimant, H., Zhu, L., Kibuuka, L. N., Fan, Z., Hyman, B. T., & McLean, P. J. (2014). Direct visualization of CHIP-mediated degradation of alpha-synuclein in vivo: implications for PD therapeutics. *PLoS One, 9*(3), e92098. doi:10.1371/journal.pone.0092098

Dong, Z., Wolfer, D. P., Lipp, H. P., & Büeler, H. (2005). Hsp70 gene transfer by adeno-associated virus inhibits MPTP-induced nigrostriatal degeneration in the mouse model of Parkinson disease. *Mol Ther, 11*(1), 80-88. doi:10.1016/j.ymthe.2004.09.007

Double, K. L., Dedov, V. N., Fedorow, H., Kettle, E., Halliday, G. M., Garner, B., & Brunk, U. T. (2008). The comparative biology of neuromelanin and lipofuscin in the human brain. *Cell Mol Life Sci, 65*(11), 1669-1682. doi:10.1007/s00018-008-7581-9

Double, K. L., Reyes, S., Werry, E. L., & Halliday, G. M. (2010). Selective cell death in neurodegeneration: why are some neurons spared in vulnerable regions? *Prog Neurobiol, 92*(3), 316-329. doi:10.1016/j.pneurobio.2010.06.001

Dringen, R. (2000). Metabolism and functions of glutathione in brain. *Prog Neurobiol, 62*(6), 649-671.

Drummond, G. S., & Kappas, A. (1981). Prevention of neonatal hyperbilirubinemia by tin protoporphyrin IX, a potent competitive inhibitor of heme oxidation. *Proc Natl Acad Sci U S A, 78*(10), 6466-6470.

Dubois, B., & Pillon, B. (1997). Cognitive deficits in Parkinson's disease. *J Neurol, 244*(1), 2-8.

Duda, J. E., Lee, V. M., & Trojanowski, J. Q. (2000). Neuropathology of synuclein aggregates. *J Neurosci Res, 61*(2), 121-127.

Duke, D. C., Moran, L. B., Pearce, R. K., & Graeber, M. B. (2007). The medial and lateral substantia nigra in Parkinson's disease: mRNA profiles associated with higher brain tissue vulnerability. *Neurogenetics, 8*(2), 83-94. doi:10.1007/s10048-006-0077-6

Durrenberger, P. F., Filiou, M. D., Moran, L. B., Michael, G. J., Novoselov, S., Cheetham, M. E., . . . Graeber, M. B. (2009). DnaJB6 is present in the core of Lewy bodies and is highly up-regulated in parkinsonian astrocytes. *J Neurosci Res, 87*(1), 238-245. doi:10.1002/jnr.21819

Fahn, S., & Cohen, G. (1992). The oxidant stress hypothesis in Parkinson's disease: evidence supporting it. *Ann Neurol, 32*(6), 804-812. doi:10.1002/ana.410320616

Fargnoli, J., Kunisada, T., Fornace, A. J., Schneider, E. L., & Holbrook, N. J. (1990). Decreased expression of heat shock protein 70 mRNA and protein after heat treatment in cells of aged rats. *Proc Natl Acad Sci U S A, 87*(2), 846-850.

Farrer, M., Chan, P., Chen, R., Tan, L., Lincoln, S., Hernandez, D., . . . Langston, J. W. (2001). Lewy bodies and parkinsonism in families with parkin mutations. *Ann Neurol, 50*(3), 293-300.

Faucheux, B. A., Nillesse, N., Damier, P., Spik, G., Mouatt-Prigent, A., Pierce, A., . . . Agid, Y. (1995). Expression of lactoferrin receptors is increased in the mesencephalon of patients with Parkinson disease. *Proc Natl Acad Sci U S A, 92*(21), 9603-9607.

Fearnley, J. M., & Lees, A. J. (1991). Ageing and Parkinson's disease: substantia nigra regional selectivity. *Brain, 114 (Pt 5)*, 2283-2301.

Feder, M. E., & Hofmann, G. E. (1999). Heat-shock proteins, molecular chaperones, and the stress response: evolutionary and ecological physiology. *Annu Rev Physiol, 61*, 243-282. doi:10.1146/annurev.physiol.61.1.243

Finley, D. (2009). Recognition and processing of ubiquitin-protein conjugates by the proteasome. *Annu Rev Biochem, 78*, 477-513. doi:10.1146/annurev.biochem.78.081507.101607

Floor, E., & Wetzel, M. G. (1998). Increased protein oxidation in human substantia nigra pars compacta in comparison with basal ganglia and prefrontal cortex measured with an improved dinitrophenylhydrazine assay. *J Neurochem, 70*(1), 268-275.

Fornai, F., Lenzi, P., Gesi, M., Ferrucci, M., Lazzeri, G., Busceti, C. L., . . . Paparelli, A. (2003). Fine structure and biochemical mechanisms underlying nigrostriatal inclusions and cell death after proteasome inhibition. *J Neurosci, 23*(26), 8955-8966.

Fuertes, G., Martin De Llano, J. J., Villarroya, A., Rivett, A. J., & Knecht, E. (2003). Changes in the proteolytic activities of proteasomes and lysosomes in human fibroblasts produced by serum withdrawal, amino-acid deprivation and confluent conditions. *Biochem J, 375*(Pt 1), 75-86. doi:10.1042/BJ20030282

Fujiwara, H., Hasegawa, M., Dohmae, N., Kawashima, A., Masliah, E., Goldberg, M. S., . . . Iwatsubo, T. (2002). alpha-Synuclein is phosphorylated in synucleinopathy lesions. *Nat Cell Biol, 4*(2), 160-164. doi:10.1038/ncb748

Galloway, P. G., Mulvihill, P., & Perry, G. (1992). Filaments of Lewy bodies contain insoluble cytoskeletal elements. *Am J Pathol, 140*(4), 809-822.

Genestra, M. (2007). Oxyl radicals, redox-sensitive signalling cascades and antioxidants. *Cell Signal, 19*(9), 1807-1819. doi:10.1016/j.cellsig.2007.04.009

Giannakopoulos, P., Herrmann, F. R., Bussière, T., Bouras, C., Kövari, E., Perl, D. P., . . . Hof, P. R. (2003). Tangle and neuron numbers, but not amyloid load, predict cognitive status in Alzheimer's disease. *Neurology, 60*(9), 1495-1500.

Gibb, W. R., & Lees, A. J. (1991). Anatomy, pigmentation, ventral and dorsal subpopulations of the substantia nigra, and differential cell death in Parkinson's disease. *J Neurol Neurosurg Psychiatry, 54*(5), 388-396.

Gilbert, D. F., Erdmann, G., Zhang, X., Fritzsche, A., Demir, K., Jaedicke, A., . . . Boutros, M. (2011). A novel multiplex cell viability assay for high-throughput RNAi screening. *PLoS One, 6*(12), e28338. doi:10.1371/journal.pone.0028338

Gleixner, A. M., Pulugulla, S. H., Pant, D. B., Posimo, J. M., Crum, T. S., & Leak, R. K. (2014). Impact of aging on heat shock protein expression in the substantia nigra and striatum of the female rat. *Cell Tissue Res, 357*(1), 43-54. doi:10.1007/s00441-014-1852-6

Goedert, M., Spillantini, M. G., Del Tredici, K., & Braak, H. (2013). 100 years of Lewy pathology. *Nat Rev Neurol, 9*(1), 13-24. doi:10.1038/nrneurol.2012.242

González-Hernández, T., Barroso-Chinea, P., De La Cruz Muros, I., Del Mar Pérez-Delgado, M., & Rodríguez, M. (2004). Expression of dopamine and vesicular monoamine transporters and differential vulnerability of mesostriatal dopaminergic neurons. *J Comp Neurol, 479*(2), 198-215. doi:10.1002/cne.20323

Gorell, J. M., Johnson, C. C., Rybicki, B. A., Peterson, E. L., & Richardson, R. J. (1998). The risk of Parkinson's disease with exposure to pesticides, farming, well water, and rural living. *Neurology, 50*(5), 1346-1350.

Graham, J. M., Paley, M. N., Grünewald, R. A., Hoggard, N., & Griffiths, P. D. (2000). Brain iron deposition in Parkinson's disease imaged using the PRIME magnetic resonance sequence. *Brain, 123 Pt 12*, 2423-2431.

Griffith, O. W. (1999). Biologic and pharmacologic regulation of mammalian glutathione synthesis. *Free Radic Biol Med, 27*(9-10), 922-935.

Grochot-Przeczek, A., Dulak, J., & Jozkowicz, A. (2012). Haem oxygenase-1: non-canonical roles in physiology and pathology. *Clin Sci (Lond), 122*(3), 93-103. doi:10.1042/CS20110147

Gupte, A. A., Morris, J. K., Zhang, H., Bomhoff, G. L., Geiger, P. C., & Stanford, J. A. (2010). Age-related changes in HSP25 expression in basal ganglia and cortex of F344/BN rats. *Neurosci Lett, 472*(2), 90-93. doi:10.1016/j.neulet.2010.01.049

Gómez-Isla, T., Hollister, R., West, H., Mui, S., Growdon, J. H., Petersen, R. C., . . . Hyman, B. T. (1997). Neuronal loss correlates with but exceeds neurofibrillary tangles in Alzheimer's disease. *Ann Neurol, 41*(1), 17-24. doi:10.1002/ana.410410106

Haber, S. N., Fudge, J. L., & McFarland, N. R. (2000). Striatonigrostriatal pathways in primates form an ascending spiral from the shell to the dorsolateral striatum. *J Neurosci, 20*(6), 2369-2382.

Halliday, G. M., & Stevens, C. H. (2011). Glia: initiators and progressors of pathology in Parkinson's disease. *Mov Disord, 26*(1), 6-17. doi:10.1002/mds.23455

Halliwell, B. (2014). Cell culture, oxidative stress, and antioxidants: avoiding pitfalls. *Biomed J, 37*(3), 99-105. doi:10.4103/2319-4170.128725

Hansen, C., Angot, E., Bergstrom, A. L., Steiner, J. A., Pieri, L., Paul, G., . . . Brundin, P. (2011). alpha-Synuclein propagates from mouse brain to grafted dopaminergic neurons and seeds aggregation in cultured human cells. *J Clin Invest, 121*(2), 715-725. doi:10.1172/JCI43366

Hara, T., Nakamura, K., Matsui, M., Yamamoto, A., Nakahara, Y., Suzuki-Migishima, R., . . . Mizushima, N. (2006). Suppression of basal autophagy in neural cells causes neurodegenerative disease in mice. *Nature, 441*(7095), 885-889. doi:10.1038/nature04724

Harding, A. J., & Halliday, G. M. (2001). Cortical Lewy body pathology in the diagnosis of dementia. *Acta Neuropathol, 102*(4), 355-363.

Harman, D. (1956). Aging: a theory based on free radical and radiation chemistry. *J Gerontol, 11*(3), 298-300.

Harris, Z. L., Durley, A. P., Man, T. K., & Gitlin, J. D. (1999). Targeted gene disruption reveals an essential role for ceruloplasmin in cellular iron efflux. *Proc Natl Acad Sci U S A, 96*(19), 10812-10817.

Hasegawa, M., Fujiwara, H., Nonaka, T., Wakabayashi, K., Takahashi, H., Lee, V. M., . . . Iwatsubo, T. (2002). Phosphorylated alpha-synuclein is ubiquitinated in alpha-synucleinopathy lesions. *J Biol Chem, 277*(50), 49071-49076. doi:10.1074/jbc.M208046200

Haslbeck, M., Franzmann, T., Weinfurtner, D., & Buchner, J. (2005). Some like it hot: the structure and function of small heat-shock proteins. *Nat Struct Mol Biol, 12*(10), 842-846. doi:10.1038/nsmb993

Hatic, H., Kane, M. J., Saykally, J. N., & Citron, B. A. (2012). Modulation of transcription factor Nrf2 in an in vitro model of traumatic brain injury. *Journal of neurotrauma, 29*(6), 1188-1196. doi:10.1089/neu.2011.1806

Hawkes, C. H., Shephard, B. C., & Daniel, S. E. (1997). Olfactory dysfunction in Parkinson's disease. *J Neurol Neurosurg Psychiatry, 62*(5), 436-446.

Hellman, N. E., & Gitlin, J. D. (2002). Ceruloplasmin metabolism and function. *Annu Rev Nutr, 22*, 439-458. doi:10.1146/annurev.nutr.22.012502.114457

Hertzman, C., Wiens, M., Bowering, D., Snow, B., & Calne, D. (1990). Parkinson's disease: a case-control study of occupational and environmental risk factors. *Am J Ind Med, 17*(3), 349-355.

Hineno, A., Kaneko, K., Yoshida, K., & Ikeda, S. (2011). Ceruloplasmin protects against rotenone-induced oxidative stress and neurotoxicity. *Neurochem Res, 36*(11), 2127-2135. doi:10.1007/s11064-011-0537-8

Hochstrasser, H., Bauer, P., Walter, U., Behnke, S., Spiegel, J., Csoti, I., . . . Berg, D. (2004). Ceruloplasmin gene variations and substantia nigra hyperechogenicity in Parkinson disease. *Neurology, 63*(10), 1912-1917.

Hochstrasser, H., Tomiuk, J., Walter, U., Behnke, S., Spiegel, J., Krüger, R., . . . Berg, D. (2005). Functional relevance of ceruloplasmin mutations in Parkinson's disease. *FASEB J, 19*(13), 1851-1853. doi:10.1096/fj.04-3486fje

Hohfeld, J., Minami, Y., & Hartl, F. U. (1995). Hip, a novel cochaperone involved in the eukaryotic Hsc70/Hsp40 reaction cycle. *Cell, 83*(4), 589-598.

Holmay, M. J., Terpstra, M., Coles, L. D., Mishra, U., Ahlskog, M., Öz, G., . . . Tuite, P. J. (2013). N-Acetylcysteine boosts brain and blood glutathione in Gaucher and Parkinson diseases. *Clin Neuropharmacol, 36*(4), 103-106. doi:10.1097/WNF.0b013e31829ae713

Hurd, Y. L., Pristupa, Z. B., Herman, M. M., Niznik, H. B., & Kleinman, J. E. (1994). The dopamine transporter and dopamine D2 receptor messenger RNAs are differentially expressed in limbic- and motor-related subpopulations of human mesencephalic neurons. *Neuroscience, 63*(2), 357-362.

Hurd, Y. L., Suzuki, M., & Sedvall, G. C. (2001). D1 and D2 dopamine receptor mRNA expression in whole hemisphere sections of the human brain. *J Chem Neuroanat, 22*(1-2), 127-137.

Hurtig, H. I., Trojanowski, J. Q., Galvin, J., Ewbank, D., Schmidt, M. L., Lee, V. M., . . . Arnold, S. E. (2000). Alpha-synuclein cortical Lewy bodies correlate with dementia in Parkinson's disease. *Neurology, 54*(10), 1916-1921.

Huryn, D. M., Brodsky, J. L., Brummond, K. M., Chambers, P. G., Eyer, B., Ireland, A. W., . . . Wipf, P. (2011). Chemical methodology as a source of small-molecule checkpoint inhibitors and heat shock protein 70 (Hsp70) modulators. *Proc Natl Acad Sci U S A, 108*(17), 6757-6762. doi:10.1073/pnas.1015251108

Huse, D. M., Schulman, K., Orsini, L., Castelli-Haley, J., Kennedy, S., & Lenhart, G. (2005). Burden of illness in Parkinson's disease. *Mov Disord, 20*(11), 1449-1454. doi:10.1002/mds.20609

Ii, K., Ito, H., Tanaka, K., & Hirano, A. (1997). Immunocytochemical co-localization of the proteasome in ubiquitinated structures in neurodegenerative diseases and the elderly. *J Neuropathol Exp Neurol, 56*(2), 125-131.

Imai, Y., Soda, M., & Takahashi, R. (2000). Parkin suppresses unfolded protein stress-induced cell death through its E3 ubiquitin-protein ligase activity. *J Biol Chem, 275*(46), 35661-35664. doi:10.1074/jbc.C000447200

Ingelsson, M., Fukumoto, H., Newell, K. L., Growdon, J. H., Hedley-Whyte, E. T., Frosch, M. P., . . . Irizarry, M. C. (2004). Early Abeta accumulation and progressive synaptic loss, gliosis, and tangle formation in AD brain. *Neurology, 62*(6), 925-931.

Jellinger, K. A. (2006). The morphological basis of mental dysfunction in Parkinson's disease. *J Neurol Sci, 248*(1-2), 167-172. doi:10.1016/j.jns.2006.05.002

Jellinger, K. A. (2011). Synuclein deposition and non-motor symptoms in Parkinson disease. *J Neurol Sci, 310*(1-2), 107-111. doi:10.1016/j.jns.2011.04.012

Jenner, P. (1998). Oxidative mechanisms in nigral cell death in Parkinson's disease. *Mov Disord, 13 Suppl 1*, 24-34.

Jenner, P. (2003). Oxidative stress in Parkinson's disease. *Ann Neurol, 53 Suppl 3*, S26-36; discussion S36-28. doi:10.1002/ana.10483

Jeong, S. Y., & David, S. (2003). Glycosylphosphatidylinositol-anchored ceruloplasmin is required for iron efflux from cells in the central nervous system. *J Biol Chem, 278*(29), 27144-27148. doi:10.1074/jbc.M301988200

Jin, L., Wang, J., Zhao, L., Jin, H., Fei, G., Zhang, Y., . . . Zhong, C. (2011). Decreased serum ceruloplasmin levels characteristically aggravate nigral iron deposition in Parkinson's disease. *Brain, 134*(Pt 1), 50-58. doi:10.1093/brain/awq319

Josephs, K. A., Whitwell, J. L., Ahmed, Z., Shiung, M. M., Weigand, S. D., Knopman, D. S., . . . Jack, C. R. (2008). Beta-amyloid burden is not associated with rates of brain atrophy. *Ann Neurol, 63*(2), 204-212. doi:10.1002/ana.21223

Kalia, S. K., Kalia, L. V., & McLean, P. J. (2010). Molecular chaperones as rational drug targets for Parkinson's disease therapeutics. *CNS Neurol Disord Drug Targets, 9*(6), 741-753.

Kampinga, H. H., & Craig, E. A. (2010). The HSP70 chaperone machinery: J proteins as drivers of functional specificity. *Nat Rev Mol Cell Biol, 11*(8), 579-592. doi:10.1038/nrm2941

Kaneko, K., Hineno, A., Yoshida, K., & Ikeda, S. (2008). Increased vulnerability to rotenone-induced neurotoxicity in ceruloplasmin-deficient mice. *Neurosci Lett, 446*(1), 56-58. doi:10.1016/j.neulet.2008.08.089

Kaushik, S., & Cuervo, A. M. (2009). Methods to monitor chaperone-mediated autophagy. *Methods Enzymol, 452*, 297-324. doi:10.1016/S0076-6879(08)03619-7

Kaushik, S., & Cuervo, A. M. (2012). Chaperone-mediated autophagy: a unique way to enter the lysosome world. *Trends Cell Biol, 22*(8), 407-417. doi:10.1016/j.tcb.2012.05.006

Keller, J. N., Gee, J., & Ding, Q. (2002). The proteasome in brain aging. *Ageing Res Rev, 1*(2), 279-293.

Keller, J. N., Hanni, K. B., & Markesbery, W. R. (2000). Possible involvement of proteasome inhibition in aging: implications for oxidative stress. *Mech Ageing Dev, 113*(1), 61-70.

Kessler, H., Pajonk, F. G., Meisser, P., Schneider-Axmann, T., Hoffmann, K. H., Supprian, T., . . . Bayer, T. A. (2006). Cerebrospinal fluid diagnostic markers correlate with lower plasma copper and ceruloplasmin in patients with Alzheimer's disease. *J Neural Transm, 113*(11), 1763-1769. doi:10.1007/s00702-006-0485-7

Kiffin, R., Bandyopadhyay, U., & Cuervo, A. M. (2006). Oxidative stress and autophagy. *Antioxid Redox Signal, 8*(1-2), 152-162. doi:10.1089/ars.2006.8.152

Kilpatrick, K., Novoa, J. A., Hancock, T., Guerriero, C. J., Wipf, P., Brodsky, J. L., & Segatori, L. (2013). Chemical induction of Hsp70 reduces alpha-synuclein aggregation in neuroglioma cells. *ACS chemical biology, 8*(7), 1460-1468. doi:10.1021/cb400017h

Kim, Y. E., Hipp, M. S., Bracher, A., Hayer-Hartl, M., & Hartl, F. U. (2013). Molecular chaperone functions in protein folding and proteostasis. *Annu Rev Biochem, 82*, 323-355. doi:10.1146/annurev-biochem-060208-092442

Kish, S. J., Shannak, K., Rajput, A., Deck, J. H., & Hornykiewicz, O. (1992). Aging produces a specific pattern of striatal dopamine loss: implications for the etiology of idiopathic Parkinson's disease. *J Neurochem, 58*(2), 642-648.

Kisselev, A. F., & Goldberg, A. L. (2001). Proteasome inhibitors: from research tools to drug candidates. *Chem Biol, 8*(8), 739-758.

Klionsky, D. J., Cuervo, A. M., & Seglen, P. O. (2007). Methods for monitoring autophagy from yeast to human. *Autophagy, 3*(3), 181-206.

Klucken, J., Shin, Y., Masliah, E., Hyman, B. T., & McLean, P. J. (2004). Hsp70 Reduces alpha-Synuclein Aggregation and Toxicity. *J Biol Chem, 279*(24), 25497-25502. doi:10.1074/jbc.M400255200

Koller, W. C. (1992). When does Parkinson's disease begin? *Neurology, 42*(4 Suppl 4), 27-31; discussion 41-28.

Komatsu, M., Waguri, S., Chiba, T., Murata, S., Iwata, J., Tanida, I., . . . Tanaka, K. (2006). Loss of autophagy in the central nervous system causes neurodegeneration in mice. *Nature, 441*(7095), 880-884. doi:10.1038/nature04723

Kordower, J. H., Chu, Y., Hauser, R. A., Freeman, T. B., & Olanow, C. W. (2008). Lewy body-like pathology in long-term embryonic nigral transplants in Parkinson's disease. *Nat Med, 14*(5), 504-506. doi:10.1038/nm1747

Kordower, J. H., Chu, Y., Stebbins, G. T., DeKosky, S. T., Cochran, E. J., Bennett, D., & Mufson, E. J. (2001). Loss and atrophy of layer II entorhinal cortex neurons in elderly people with mild cognitive impairment. *Ann Neurol, 49*(2), 202-213.

Kostovic, I. (1990). Structural and histochemical reorganization of the human prefrontal cortex during perinatal and postnatal life. *Prog Brain Res, 85*, 223-239; discussion 239-240.

Kostovic, I., Petanjek, Z., & Judas, M. (1993). Early areal differentiation of the human cerebral cortex: entorhinal area. *Hippocampus, 3*(4), 447-458. doi:10.1002/hipo.450030406

Krüger, R., Kuhn, W., Müller, T., Woitalla, D., Graeber, M., Kösel, S., . . . Riess, O. (1998). Ala30Pro mutation in the gene encoding alpha-synuclein in Parkinson's disease. *Nat Genet, 18*(2), 106-108. doi:10.1038/ng0298-106

Krüger, R., Vieira-Saecker, A. M., Kuhn, W., Berg, D., Müller, T., Kühnl, N., . . . Riess, O. (1999). Increased susceptibility to sporadic Parkinson's disease by a certain combined alpha-synuclein/apolipoprotein E genotype. *Ann Neurol, 45*(5), 611-617.

Kubis, N., Faucheux, B. A., Ransmayr, G., Damier, P., Duyckaerts, C., Henin, D., . . . Hirsch, E. C. (2000). Preservation of midbrain catecholaminergic neurons in very old human subjects. *Brain, 123 (Pt 2)*, 366-373.

Labbadia, J., & Morimoto, R. I. (2015). The biology of proteostasis in aging and disease. *Annu Rev Biochem, 84*, 435-464. doi:10.1146/annurev-biochem-060614-033955

Langston, J. W. (2006). The Parkinson's complex: parkinsonism is just the tip of the iceberg. *Ann Neurol, 59*(4), 591-596. doi:10.1002/ana.20834

Langston, J. W., Ballard, P., Tetrud, J. W., & Irwin, I. (1983). Chronic Parkinsonism in humans due to a product of meperidine-analog synthesis. *Science, 219*(4587), 979-980.

Lanneau, D., Wettstein, G., Bonniaud, P., & Garrido, C. (2010). Heat shock proteins: cell protection through protein triage. *ScientificWorldJournal, 10*, 1543-1552. doi:10.1100/tsw.2010.152

Leak, R. K., Castro, S. L., Jaumotte, J. D., Smith, A. D., & Zigmond, M. J. (2010). Assaying multiple biochemical variables from the same tissue sample. *J Neurosci Methods, 191*(2), 234-238. doi:10.1016/j.jneumeth.2010.06.023

Lee, H. J., Suk, J. E., Patrick, C., Bae, E. J., Cho, J. H., Rho, S., . . . Lee, S. J. (2010). Direct transfer of alpha-synuclein from neuron to astroglia causes inflammatory responses in synucleinopathies. *J Biol Chem, 285*(12), 9262-9272. doi:10.1074/jbc.M109.081125

Lennox, G., Lowe, J., Morrell, K., Landon, M., & Mayer, R. J. (1989). Anti-ubiquitin immunocytochemistry is more sensitive than conventional techniques in the detection of diffuse Lewy body disease. *J Neurol Neurosurg Psychiatry, 52*(1), 67-71.

Lerner, A., & Bagic, A. (2008). Olfactory pathogenesis of idiopathic Parkinson disease revisited. *Mov Disord, 23*(8), 1076-1084. doi:10.1002/mds.22066

Leroy, E., Boyer, R., Auburger, G., Leube, B., Ulm, G., Mezey, E., . . . Polymeropoulos, M. H. (1998). The ubiquitin pathway in Parkinson's disease. *Nature, 395*(6701), 451-452. doi:10.1038/26652

Lesage, S., Anheim, M., Letournel, F., Bousset, L., Honoré, A., Rozas, N., . . . Group, F. P. s. D. G. S. (2013). G51D α-synuclein mutation causes a novel parkinsonian-pyramidal syndrome. *Ann Neurol, 73*(4), 459-471. doi:10.1002/ana.23894

Li, J. Y., Englund, E., Holton, J. L., Soulet, D., Hagell, P., Lees, A. J., . . . Brundin, P. (2008). Lewy bodies in grafted neurons in subjects with Parkinson's disease suggest host-to-graft disease propagation. *Nat Med, 14*(5), 501-503. doi:10.1038/nm1746

Lindersson, E., Beedholm, R., Hojrup, P., Moos, T., Gai, W., Hendil, K. B., & Jensen, P. H. (2004). Proteasomal inhibition by alpha-synuclein filaments and oligomers. *J Biol Chem, 279*(13), 12924-12934. doi:10.1074/jbc.M306390200

Liou, H. H., Chen, R. C., Tsai, Y. F., Chen, W. P., Chang, Y. C., & Tsai, M. C. (1996). Effects of paraquat on the substantia nigra of the wistar rats: neurochemical, histological, and behavioral studies. *Toxicol Appl Pharmacol, 137*(1), 34-41. doi:10.1006/taap.1996.0054

Lirong, J., Jianjun, J., Hua, Z., Guoqiang, F., Yuhao, Z., Xiaoli, P., . . . Chunjiu, Z. (2009). Hypoceruloplasminemia-related movement disorder without Kayser-Fleischer rings is different from Wilson disease and not involved in ATP7B mutation. *Eur J Neurol, 16*(10), 1130-1137. doi:10.1111/j.1468-1331.2009.02733.x

Liu, H., Wang, H., Shenvi, S., Hagen, T. M., & Liu, R. M. (2004). Glutathione metabolism during aging and in Alzheimer disease. *Ann N Y Acad Sci, 1019*, 346-349. doi:10.1196/annals.1297.059

Loeffler, D. A., LeWitt, P. A., Juneau, P. L., Sima, A. A., Nguyen, H. U., DeMaggio, A. J., . . . Kanaley, L. (1996). Increased regional brain concentrations of ceruloplasmin in neurodegenerative disorders. *Brain Res, 738*(2), 265-274.

Luján, R., Maylie, J., & Adelman, J. P. (2009). New sites of action for GIRK and SK channels. *Nat Rev Neurosci, 10*(7), 475-480. doi:10.1038/nrn2668

Luk, K. C., Kehm, V., Carroll, J., Zhang, B., O'Brien, P., Trojanowski, J. Q., & Lee, V. M. (2012). Pathological alpha-synuclein transmission initiates Parkinson-like neurodegeneration in nontransgenic mice. *Science, 338*(6109), 949-953. doi:10.1126/science.1227157

Luk, K. C., Kehm, V. M., Zhang, B., O'Brien, P., Trojanowski, J. Q., & Lee, V. M. (2012). Intracerebral inoculation of pathological alpha-synuclein initiates a rapidly progressive neurodegenerative alpha-synucleinopathy in mice. *J Exp Med, 209*(5), 975-986. doi:10.1084/jem.20112457

Luk, K. C., & Lee, V. M. (2014). Modeling Lewy pathology propagation in Parkinson's disease. *Parkinsonism Relat Disord, 20 Suppl 1*, S85-87. doi:10.1016/S1353-8020(13)70022-1

Luk, K. C., Song, C., O'Brien, P., Stieber, A., Branch, J. R., Brunden, K. R., . . . Lee, V. M. (2009). Exogenous alpha-synuclein fibrils seed the formation of Lewy body-like intracellular inclusions in cultured cells. *Proc Natl Acad Sci U S A, 106*(47), 20051-20056. doi:10.1073/pnas.0908005106

Magrané, J., Smith, R. C., Walsh, K., & Querfurth, H. W. (2004). Heat shock protein 70 participates in the neuroprotective response to intracellularly expressed beta-amyloid in neurons. *J Neurosci, 24*(7), 1700-1706. doi:10.1523/JNEUROSCI.4330-03.2004

Maines, M. D., & Panahian, N. (2001). The heme oxygenase system and cellular defense mechanisms. Do HO-1 and HO-2 have different functions? *Adv Exp Med Biol, 502*, 249-272.

Mandel, S., Grunblatt, E., Riederer, P., Amariglio, N., Jacob-Hirsch, J., Rechavi, G., & Youdim, M. B. (2005). Gene expression profiling of sporadic Parkinson's disease substantia nigra

pars compacta reveals impairment of ubiquitin-proteasome subunits, SKP1A, aldehyde dehydrogenase, and chaperone HSC-70. *Ann N Y Acad Sci, 1053*, 356-375. doi:10.1196/annals.1344.031

Martin, H. L., & Teismann, P. (2009). Glutathione--a review on its role and significance in Parkinson's disease. *FASEB J, 23*(10), 3263-3272. doi:10.1096/fj.08-125443

Martinez-Hernandez, R., Montes, S., Higuera-Calleja, J., Yescas, P., Boll, M. C., Diaz-Ruiz, A., & Rios, C. (2011). Plasma ceruloplasmin ferroxidase activity correlates with the nigral sonographic area in Parkinson's disease patients: a pilot study. *Neurochem Res, 36*(11), 2111-2115. doi:10.1007/s11064-011-0535-x

Martinez-Vicente, M., Talloczy, Z., Kaushik, S., Massey, A. C., Mazzulli, J., Mosharov, E. V., . . . Cuervo, A. M. (2008). Dopamine-modified alpha-synuclein blocks chaperone-mediated autophagy. *J Clin Invest, 118*(2), 777-788. doi:10.1172/JCI32806

Massey, A. J., Williamson, D. S., Browne, H., Murray, J. B., Dokurno, P., Shaw, T., . . . Wood, M. (2010). A novel, small molecule inhibitor of Hsc70/Hsp70 potentiates Hsp90 inhibitor induced apoptosis in HCT116 colon carcinoma cells. *Cancer chemotherapy and pharmacology, 66*(3), 535-545. doi:10.1007/s00280-009-1194-3

Mattila, P. M., Rinne, J. O., Helenius, H., Dickson, D. W., & Röyttä, M. (2000). Alpha-synuclein-immunoreactive cortical Lewy bodies are associated with cognitive impairment in Parkinson's disease. *Acta Neuropathol, 100*(3), 285-290.

Mattson, M. P., Guthrie, P. B., & Kater, S. B. (1989). Intrinsic factors in the selective vulnerability of hippocampal pyramidal neurons. *Prog Clin Biol Res, 317*, 333-351.

McCormack, A. L., Di Monte, D. A., Delfani, K., Irwin, I., DeLanney, L. E., Langston, W. J., & Janson, A. M. (2004). Aging of the nigrostriatal system in the squirrel monkey. *J Comp Neurol, 471*(4), 387-395. doi:10.1002/cne.20036

McCormack, A. L., Thiruchelvam, M., Manning-Bog, A. B., Thiffault, C., Langston, J. W., Cory-Slechta, D. A., & Di Monte, D. A. (2002). Environmental risk factors and Parkinson's disease: selective degeneration of nigral dopaminergic neurons caused by the herbicide paraquat. *Neurobiol Dis, 10*(2), 119-127.

McNaught, K. S., Belizaire, R., Isacson, O., Jenner, P., & Olanow, C. W. (2003). Altered proteasomal function in sporadic Parkinson's disease. *Exp Neurol, 179*(1), 38-46.

McNaught, K. S., Belizaire, R., Jenner, P., Olanow, C. W., & Isacson, O. (2002). Selective loss of 20S proteasome alpha-subunits in the substantia nigra pars compacta in Parkinson's disease. *Neurosci Lett, 326*(3), 155-158.

McNaught, K. S., & Jenner, P. (2001). Proteasomal function is impaired in substantia nigra in Parkinson's disease. *Neurosci Lett, 297*(3), 191-194.

McNaught, K. S., Mytilineou, C., Jnobaptiste, R., Yabut, J., Shashidharan, P., Jennert, P., & Olanow, C. W. (2002). Impairment of the ubiquitin-proteasome system causes dopaminergic cell death and inclusion body formation in ventral mesencephalic cultures. *J Neurochem, 81*(2), 301-306.

McNaught, K. S., Perl, D. P., Brownell, A. L., & Olanow, C. W. (2004). Systemic exposure to proteasome inhibitors causes a progressive model of Parkinson's disease. *Ann Neurol, 56*(1), 149-162. doi:10.1002/ana.20186

McNaught, K. S., Shashidharan, P., Perl, D. P., Jenner, P., & Olanow, C. W. (2002). Aggresome-related biogenesis of Lewy bodies. *Eur J Neurosci, 16*(11), 2136-2148.

McNeill, A., Pandolfo, M., Kuhn, J., Shang, H., & Miyajima, H. (2008). The neurological presentation of ceruloplasmin gene mutations. *Eur Neurol, 60*(4), 200-205. doi:10.1159/000148691

McRitchie, D. A., Hardman, C. D., & Halliday, G. M. (1996). Cytoarchitectural distribution of calcium binding proteins in midbrain dopaminergic regions of rats and humans. *J Comp Neurol, 364*(1), 121-150. doi:10.1002/(SICI)1096-9861(19960101)364:1<121::AID-CNE11>3.0.CO;2-1

Merendino, A. M., Paul, C., Vignola, A. M., Costa, M. A., Melis, M., Chiappara, G., . . . Arrigo, A. P. (2002). Heat shock protein-27 protects human bronchial epithelial cells against oxidative stress-mediated apoptosis: possible implication in asthma. *Cell Stress Chaperones, 7*(3), 269-280.

Miller, F. D., & Gauthier, A. S. (2007). Timing is everything: making neurons versus glia in the developing cortex. *Neuron, 54*(3), 357-369. doi:10.1016/j.neuron.2007.04.019

Molina-Holgado, F., Gaeta, A., Francis, P. T., Williams, R. J., & Hider, R. C. (2008). Neuroprotective actions of deferiprone in cultured cortical neurones and SHSY-5Y cells. *J Neurochem, 105*(6), 2466-2476. doi:10.1111/j.1471-4159.2008.05332.x

Moloney, T. C., Hyland, R., O'Toole, D., Paucard, A., Kirik, D., O'Doherty, A., . . . Dowd, E. (2014). Heat shock protein 70 reduces α-synuclein-induced predegenerative neuronal dystrophy in the α-synuclein viral gene transfer rat model of Parkinson's disease. *CNS Neurosci Ther, 20*(1), 50-58. doi:10.1111/cns.12200

Morens, D. M., Davis, J. W., Grandinetti, A., Ross, G. W., Popper, J. S., & White, L. R. (1996). Epidemiologic observations on Parkinson's disease: incidence and mortality in a prospective study of middle-aged men. *Neurology, 46*(4), 1044-1050.

Mori, H., Kondo, T., Yokochi, M., Matsumine, H., Nakagawa-Hattori, Y., Miyake, T., . . . Mizuno, Y. (1998). Pathologic and biochemical studies of juvenile parkinsonism linked to chromosome 6q. *Neurology, 51*(3), 890-892.

Mougenot, A. L., Nicot, S., Bencsik, A., Morignat, E., Verchere, J., Lakhdar, L., . . . Baron, T. (2012). Prion-like acceleration of a synucleinopathy in a transgenic mouse model. *Neurobiol Aging, 33*(9), 2225-2228. doi:10.1016/j.neurobiolaging.2011.06.022

Musci, G., Bonaccorsi di Patti, M. C., Fagiolo, U., & Calabrese, L. (1993). Age-related changes in human ceruloplasmin. Evidence for oxidative modifications. *J Biol Chem, 268*(18), 13388-13395.

Nagel, F., Bahr, M., & Dietz, G. P. (2009). Tyrosine hydroxylase-positive amacrine interneurons in the mouse retina are resistant against the application of various parkinsonian toxins. *Brain Res Bull, 79*(5), 303-309. doi:10.1016/j.brainresbull.2009.04.010

Nagel, F., Falkenburger, B. H., Tönges, L., Kowsky, S., Pöppelmeyer, C., Schulz, J. B., . . . Dietz, G. P. (2008). Tat-Hsp70 protects dopaminergic neurons in midbrain cultures and in the substantia nigra in models of Parkinson's disease. *J Neurochem, 105*(3), 853-864. doi:10.1111/j.1471-4159.2007.05204.x

Nedelsky, N. B., Todd, P. K., & Taylor, J. P. (2008). Autophagy and the ubiquitin-proteasome system: collaborators in neuroprotection. *Biochim Biophys Acta, 1782*(12), 691-699. doi:10.1016/j.bbadis.2008.10.002

Nedergaard, S., Flatman, J. A., & Engberg, I. (1993). Nifedipine- and omega-conotoxin-sensitive Ca2+ conductances in guinea-pig substantia nigra pars compacta neurones. *J Physiol, 466*, 727-747.

Olivieri, S., Conti, A., Iannaccone, S., Cannistraci, C. V., Campanella, A., Barbariga, M., . . . Alessio, M. (2011). Ceruloplasmin oxidation, a feature of Parkinson's disease CSF, inhibits ferroxidase activity and promotes cellular iron retention. *J Neurosci, 31*(50), 18568-18577. doi:10.1523/JNEUROSCI.3768-11.2011

Pastore, A., Federici, G., Bertini, E., & Piemonte, F. (2003). Analysis of glutathione: implication in redox and detoxification. *Clin Chim Acta, 333*(1), 19-39.

Paxinos, G., & Watson, C. (1998). *The Rat Brain in Stereotaxic Coordinates* (4th Edition ed.). San Diego, CA: Academic Press, Elsevier Science.

Perry, T. L., Godin, D. V., & Hansen, S. (1982). Parkinson's disease: a disorder due to nigral glutathione deficiency? *Neurosci Lett, 33*(3), 305-310.

Petrucelli, L., O'Farrell, C., Lockhart, P. J., Baptista, M., Kehoe, K., Vink, L., . . . Cookson, M. R. (2002). Parkin protects against the toxicity associated with mutant alpha-synuclein: proteasome dysfunction selectively affects catecholaminergic neurons. *Neuron, 36*(6), 1007-1019.

Petty, R. D., Sutherland, L. A., Hunter, E. M., & Cree, I. A. (1995). Comparison of MTT and ATP-based assays for the measurement of viable cell number. *J Biolumin Chemilumin, 10*(1), 29-34. doi:10.1002/bio.1170100105

Pickering, A. M., Koop, A. L., Teoh, C. Y., Ermak, G., Grune, T., & Davies, K. J. (2010). The immunoproteasome, the 20S proteasome and the PA28αβ proteasome regulator are oxidative-stress-adaptive proteolytic complexes. *Biochem J, 432*(3), 585-594. doi:10.1042/BJ20100878

Pollanen, M. S., Dickson, D. W., & Bergeron, C. (1993). Pathology and biology of the Lewy body. *J Neuropathol Exp Neurol, 52*(3), 183-191.

Polymeropoulos, M. H., Lavedan, C., Leroy, E., Ide, S. E., Dehejia, A., Dutra, A., . . . Nussbaum, R. L. (1997). Mutation in the alpha-synuclein gene identified in families with Parkinson's disease. *Science, 276*(5321), 2045-2047.

Pompella, A., Visvikis, A., Paolicchi, A., De Tata, V., & Casini, A. F. (2003). The changing faces of glutathione, a cellular protagonist. *Biochem Pharmacol, 66*(8), 1499-1503.

Posimo, J. M., Titler, A. M., Choi, H. J., Unnithan, A. S., & Leak, R. K. (2013). Neocortex and allocortex respond differentially to cellular stress in vitro and aging in vivo. *PLoS One, 8*(3), e58596. doi:10.1371/journal.pone.0058596

Posimo, J. M., Unnithan, A. S., Gleixner, A. M., Choi, H. J., Jiang, Y., Pulugulla, S. H., & Leak, R. K. (2014). Viability assays for cells in culture. *J Vis Exp*(83), e50645. doi:10.3791/50645

Poulopoulos, M., Levy, O. A., & Alcalay, R. N. (2012). The neuropathology of genetic Parkinson's disease. *Mov Disord, 27*(7), 831-842. doi:10.1002/mds.24962

Prayer, D. (2011). Fetal MRI. *Top Magn Reson Imaging, 22*(3), 89. doi:10.1097/RMR.0b013e318267609f

Puopolo, M., Raviola, E., & Bean, B. P. (2007). Roles of subthreshold calcium current and sodium current in spontaneous firing of mouse midbrain dopamine neurons. *J Neurosci, 27*(3), 645-656. doi:10.1523/JNEUROSCI.4341-06.2007

Recasens, A., & Dehay, B. (2014). Alpha-synuclein spreading in Parkinson's disease. *Front Neuroanat, 8*, 159. doi:10.3389/fnana.2014.00159

Recasens, A., Dehay, B., Bove, J., Carballo-Carbajal, I., Dovero, S., Perez-Villalba, A., . . . Vila, M. (2014). Lewy body extracts from Parkinson disease brains trigger alpha-synuclein

pathology and neurodegeneration in mice and monkeys. *Ann Neurol, 75*(3), 351-362. doi:10.1002/ana.24066

Renkawek, K., Stege, G. J., & Bosman, G. J. (1999). Dementia, gliosis and expression of the small heat shock proteins hsp27 and alpha B-crystallin in Parkinson's disease. *Neuroreport, 10*(11), 2273-2276.

Rey, N. L., Petit, G. H., Bousset, L., Melki, R., & Brundin, P. (2013). Transfer of human α-synuclein from the olfactory bulb to interconnected brain regions in mice. *Acta Neuropathol, 126*(4), 555-573. doi:10.1007/s00401-013-1160-3

Rhodes, S. L., & Ritz, B. (2008). Genetics of iron regulation and the possible role of iron in Parkinson's disease. *Neurobiol Dis, 32*(2), 183-195. doi:10.1016/j.nbd.2008.07.001

Richly, H., Rape, M., Braun, S., Rumpf, S., Hoege, C., & Jentsch, S. (2005). A series of ubiquitin binding factors connects CDC48/p97 to substrate multiubiquitylation and proteasomal targeting. *Cell, 120*(1), 73-84. doi:10.1016/j.cell.2004.11.013

Rideout, H. J., Lang-Rollin, I. C., Savalle, M., & Stefanis, L. (2005). Dopaminergic neurons in rat ventral midbrain cultures undergo selective apoptosis and form inclusions, but do not up-regulate iHSP70, following proteasomal inhibition. *J Neurochem, 93*(5), 1304-1313. doi:10.1111/j.1471-4159.2005.03124.x

Rideout, H. J., Larsen, K. E., Sulzer, D., & Stefanis, L. (2001). Proteasomal inhibition leads to formation of ubiquitin/alpha-synuclein-immunoreactive inclusions in PC12 cells. *J Neurochem, 78*(4), 899-908.

Rideout, H. J., & Stefanis, L. (2002). Proteasomal inhibition-induced inclusion formation and death in cortical neurons require transcription and ubiquitination. *Mol Cell Neurosci, 21*(2), 223-238.

Riederer, P., Sofic, E., Rausch, W. D., Schmidt, B., Reynolds, G. P., Jellinger, K., & Youdim, M. B. (1989). Transition metals, ferritin, glutathione, and ascorbic acid in parkinsonian brains. *J Neurochem, 52*(2), 515-520.

Riss, T. L., & Moravec, R. A. (2004). Use of multiple assay endpoints to investigate the effects of incubation time, dose of toxin, and plating density in cell-based cytotoxicity assays. *Assay Drug Dev Technol, 2*(1), 51-62. doi:10.1089/154065804322966315

Roeser, H. P., Lee, G. R., Nacht, S., & Cartwright, G. E. (1970). The role of ceruloplasmin in iron metabolism. *J Clin Invest, 49*(12), 2408-2417. doi:10.1172/JCI106460

Sacino, A. N., Brooks, M., McKinney, A. B., Thomas, M. A., Shaw, G., Golde, T. E., & Giasson, B. I. (2014). Brain injection of alpha-synuclein induces multiple proteinopathies, gliosis, and a neuronal injury marker. *J Neurosci, 34*(37), 12368-12378. doi:10.1523/JNEUROSCI.2102-14.2014

Sacino, A. N., Brooks, M., Thomas, M. A., McKinney, A. B., Lee, S., Regenhardt, R. W., . . . Giasson, B. I. (2014). Intramuscular injection of alpha-synuclein induces CNS alpha-synuclein pathology and a rapid-onset motor phenotype in transgenic mice. *Proc Natl Acad Sci U S A, 111*(29), 10732-10737. doi:10.1073/pnas.1321785111

Sadowski, M., & Sarcevic, B. (2010). Mechanisms of mono- and poly-ubiquitination: Ubiquitination specificity depends on compatibility between the E2 catalytic core and amino acid residues proximal to the lysine. *Cell Div, 5*, 19. doi:10.1186/1747-1028-5-19

Saito, Y., Kawashima, A., Ruberu, N. N., Fujiwara, H., Koyama, S., Sawabe, M., . . . Murayama, S. (2003). Accumulation of phosphorylated alpha-synuclein in aging human brain. *J Neuropathol Exp Neurol, 62*(6), 644-654.

Saxena, S., & Caroni, P. (2011). Selective neuronal vulnerability in neurodegenerative diseases: from stressor thresholds to degeneration. *Neuron, 71*(1), 35-48. doi:10.1016/j.neuron.2011.06.031

Saykally, J. N., Rachmany, L., Hatic, H., Shaer, A., Rubovitch, V., Pick, C. G., & Citron, B. A. (2012). The nuclear factor erythroid 2-like 2 activator, tert-butylhydroquinone, improves cognitive performance in mice after mild traumatic brain injury. *Neuroscience, 223*, 305-314. doi:10.1016/j.neuroscience.2012.07.070

Schenkman, M., Wei Zhu, C., Cutson, T. M., & Whetten-Goldstein, K. (2001). Longitudinal evaluation of economic and physical impact of Parkinson's disease. *Parkinsonism Relat Disord, 8*(1), 41-50.

Schipper, H. M., Liberman, A., & Stopa, E. G. (1998). Neural heme oxygenase-1 expression in idiopathic Parkinson's disease. *Exp Neurol, 150*(1), 60-68. doi:10.1006/exnr.1997.6752

Schipper, H. M., Song, W., Zukor, H., Hascalovici, J. R., & Zeligman, D. (2009). Heme oxygenase-1 and neurodegeneration: expanding frontiers of engagement. *J Neurochem, 110*(2), 469-485. doi:10.1111/j.1471-4159.2009.06160.x

Schlecht, R., Scholz, S. R., Dahmen, H., Wegener, A., Sirrenberg, C., Musil, D., . . . Bukau, B. (2013). Functional analysis of Hsp70 inhibitors. *PLoS One, 8*(11), e78443. doi:10.1371/journal.pone.0078443

Schlossmacher, M. G., Frosch, M. P., Gai, W. P., Medina, M., Sharma, N., Forno, L., . . . Kosik, K. S. (2002). Parkin localizes to the Lewy bodies of Parkinson disease and dementia with Lewy bodies. *Am J Pathol, 160*(5), 1655-1667. doi:10.1016/S0002-9440(10)61113-3

Schrag, A., Ben-Shlomo, Y., & Quinn, N. P. (2000). Cross sectional prevalence survey of idiopathic Parkinson's disease and Parkinsonism in London. *BMJ, 321*(7252), 21-22.

Schultz, C., Dick, E. J., Cox, A. B., Hubbard, G. B., Braak, E., & Braak, H. (2001). Expression of stress proteins alpha B-crystallin, ubiquitin, and hsp27 in pallido-nigral spheroids of aged rhesus monkeys. *Neurobiol Aging, 22*(4), 677-682.

Seidel, K., Vinet, J., Dunnen, W. F., Brunt, E. R., Meister, M., Boncoraglio, A., . . . Carra, S. (2012). The HSPB8-BAG3 chaperone complex is upregulated in astrocytes in the human brain affected by protein aggregation diseases. *Neuropathol Appl Neurobiol, 38*(1), 39-53. doi:10.1111/j.1365-2990.2011.01198.x

Semchuk, K. M., Love, E. J., & Lee, R. G. (1993). Parkinson's disease: a test of the multifactorial etiologic hypothesis. *Neurology, 43*(6), 1173-1180.

Shang, F., & Taylor, A. (2011). Ubiquitin-proteasome pathway and cellular responses to oxidative stress. *Free Radic Biol Med, 51*(1), 5-16. doi:10.1016/j.freeradbiomed.2011.03.031

Shang, H. F., Jiang, X. F., Burgunder, J. M., Chen, Q., & Zhou, D. (2006). Novel mutation in the ceruloplasmin gene causing a cognitive and movement disorder with diabetes mellitus. *Mov Disord, 21*(12), 2217-2220. doi:10.1002/mds.21121

Shehadeh, L. A., Yu, K., Wang, L., Guevara, A., Singer, C., Vance, J., & Papapetropoulos, S. (2010). SRRM2, a potential blood biomarker revealing high alternative splicing in Parkinson's disease. *PLoS One, 5*(2), e9104. doi:10.1371/journal.pone.0009104

Shen, D., Dalton, T. P., Nebert, D. W., & Shertzer, H. G. (2005). Glutathione redox state regulates mitochondrial reactive oxygen production. *J Biol Chem, 280*(27), 25305-25312. doi:10.1074/jbc.M500095200

Sherman, M. Y., & Goldberg, A. L. (2001). Cellular defenses against unfolded proteins: a cell biologist thinks about neurodegenerative diseases. *Neuron, 29*(1), 15-32.

Shimizu, K., Matsubara, K., Ohtaki, K., Fujimaru, S., Saito, O., & Shiono, H. (2003). Paraquat induces long-lasting dopamine overflow through the excitotoxic pathway in the striatum of freely moving rats. *Brain Res, 976*(2), 243-252.

Shimura, H., Hattori, N., Kubo, S., Mizuno, Y., Asakawa, S., Minoshima, S., . . . Suzuki, T. (2000). Familial Parkinson disease gene product, parkin, is a ubiquitin-protein ligase. *Nat Genet, 25*(3), 302-305. doi:10.1038/77060

Sian, J., Dexter, D. T., Lees, A. J., Daniel, S., Agid, Y., Javoy-Agid, F., . . . Marsden, C. D. (1994). Alterations in glutathione levels in Parkinson's disease and other neurodegenerative disorders affecting basal ganglia. *Ann Neurol, 36*(3), 348-355. doi:10.1002/ana.410360305

Sian, J., Dexter, D. T., Lees, A. J., Daniel, S., Jenner, P., & Marsden, C. D. (1994). Glutathione-related enzymes in brain in Parkinson's disease. *Ann Neurol, 36*(3), 356-361. doi:10.1002/ana.410360306

Sofic, E., Lange, K. W., Jellinger, K., & Riederer, P. (1992). Reduced and oxidized glutathione in the substantia nigra of patients with Parkinson's disease. *Neurosci Lett, 142*(2), 128-130.

Squitti, R., Quattrocchi, C. C., Salustri, C., & Rossini, P. M. (2008). Ceruloplasmin fragmentation is implicated in 'free' copper deregulation of Alzheimer's disease. *Prion, 2*(1), 23-27.

Stranahan, A. M., & Mattson, M. P. (2010). Selective vulnerability of neurons in layer II of the entorhinal cortex during aging and Alzheimer's disease. *Neural Plast, 2010*, 108190. doi:10.1155/2010/108190

Sun, F., Anantharam, V., Zhang, D., Latchoumycandane, C., Kanthasamy, A., & Kanthasamy, A. G. (2006). Proteasome inhibitor MG-132 induces dopaminergic degeneration in cell culture and animal models. *Neurotoxicology, 27*(5), 807-815. doi:10.1016/j.neuro.2006.06.006

Sóti, C., & Csermely, P. (2000). Molecular chaperones and the aging process. *Biogerontology, 1*(3), 225-233.

Taguchi, K., Watanabe, Y., Tsujimura, A., & Tanaka, M. (2015). Brain region-dependent differential expression of alpha-synuclein. *J Comp Neurol*. doi:10.1002/cne.23901

Taipale, M., Jarosz, D. F., & Lindquist, S. (2010). HSP90 at the hub of protein homeostasis: emerging mechanistic insights. *Nat Rev Mol Cell Biol, 11*(7), 515-528. doi:10.1038/nrm2918

Taipale, M., Tucker, G., Peng, J., Krykbaeva, I., Lin, Z. Y., Larsen, B., . . . Lindquist, S. (2014). A quantitative chaperone interaction network reveals the architecture of cellular protein homeostasis pathways. *Cell, 158*(2), 434-448. doi:10.1016/j.cell.2014.05.039

Tan, J. M., Wong, E. S., Kirkpatrick, D. S., Pletnikova, O., Ko, H. S., Tay, S. P., . . . Lim, K. L. (2008). Lysine 63-linked ubiquitination promotes the formation and autophagic clearance of protein inclusions associated with neurodegenerative diseases. *Hum Mol Genet, 17*(3), 431-439. doi:10.1093/hmg/ddm320

Tanner, C. M., & Goldman, S. M. (1996). Epidemiology of Parkinson's disease. *Neurol Clin, 14*(2), 317-335.

Terman, A., & Brunk, U. T. (1998). Lipofuscin: mechanisms of formation and increase with age. *APMIS, 106*(2), 265-276.

Terman, A., & Brunk, U. T. (2004). Lipofuscin. *Int J Biochem Cell Biol, 36*(8), 1400-1404. doi:10.1016/j.biocel.2003.08.009

Terman, A., Gustafsson, B., & Brunk, U. T. (2006). Mitochondrial damage and intralysosomal degradation in cellular aging. *Mol Aspects Med, 27*(5-6), 471-482. doi:10.1016/j.mam.2006.08.006

Texel, S. J., Xu, X., & Harris, Z. L. (2008). Ceruloplasmin in neurodegenerative diseases. *Biochem Soc Trans, 36*(Pt 6), 1277-1281. doi:10.1042/BST0361277

Texel, S. J., Zhang, J., Camandola, S., Unger, E. L., Taub, D. D., Koehler, R. C., . . . Mattson, M. P. (2011). Ceruloplasmin deficiency reduces levels of iron and BDNF in the cortex and striatum of young mice and increases their vulnerability to stroke. *PLoS One, 6*(9), e25077. doi:10.1371/journal.pone.0025077

Thal, D. R., Rüb, U., Orantes, M., & Braak, H. (2002). Phases of A beta-deposition in the human brain and its relevance for the development of AD. *Neurology, 58*(12), 1791-1800.

Thiruchelvam, M., McCormack, A., Richfield, E. K., Baggs, R. B., Tank, A. W., Di Monte, D. A., & Cory-Slechta, D. A. (2003). Age-related irreversible progressive nigrostriatal dopaminergic neurotoxicity in the paraquat and maneb model of the Parkinson's disease phenotype. *Eur J Neurosci, 18*(3), 589-600.

Tofaris, G. K., Razzaq, A., Ghetti, B., Lilley, K. S., & Spillantini, M. G. (2003). Ubiquitination of alpha-synuclein in Lewy bodies is a pathological event not associated with impairment of proteasome function. *J Biol Chem, 278*(45), 44405-44411. doi:10.1074/jbc.M308041200

Torsdottir, G., Kristinsson, J., Snaedal, J., Sveinbjornsdottir, S., Gudmundsson, G., Hreidarsson, S., & Johannesson, T. (2010). Case-control studies on ceruloplasmin and superoxide dismutase (SOD1) in neurodegenerative diseases: a short review. *J Neurol Sci, 299*(1-2), 51-54. doi:10.1016/j.jns.2010.08.047

Torsdottir, G., Kristinsson, J., Snaedal, J., Sveinbjörnsdóttir, S., Gudmundsson, G., Hreidarsson, S., & Jóhannesson, T. (2010). Case-control studies on ceruloplasmin and superoxide dismutase (SOD1) in neurodegenerative diseases: a short review. *J Neurol Sci, 299*(1-2), 51-54. doi:10.1016/j.jns.2010.08.047

Torsdottir, G., Sveinbjornsdottir, S., Kristinsson, J., Snaedal, J., & Johannesson, T. (2006). Ceruloplasmin and superoxide dismutase (SOD1) in Parkinson's disease: a follow-up study. *J Neurol Sci, 241*(1-2), 53-58. doi:10.1016/j.jns.2005.10.015

Unnithan, A. S., Choi, H. J., Titler, A. M., Posimo, J. M., & Leak, R. K. (2012). Rescue from a two hit, high-throughput model of neurodegeneration with N-acetyl cysteine. *Neurochem Int, 61*(3), 356-368. doi:10.1016/j.neuint.2012.06.001

Uryu, K., Richter-Landsberg, C., Welch, W., Sun, E., Goldbaum, O., Norris, E. H., . . . Trojanowski, J. Q. (2006). Convergence of heat shock protein 90 with ubiquitin in filamentous alpha-synuclein inclusions of alpha-synucleinopathies. *Am J Pathol, 168*(3), 947-961.

Uttara, B., Singh, A. V., Zamboni, P., & Mahajan, R. T. (2009). Oxidative stress and neurodegenerative diseases: a review of upstream and downstream antioxidant therapeutic options. *Curr Neuropharmacol, 7*(1), 65-74. doi:10.2174/157015909787602823

Uversky, V. N. (2009). Intrinsic disorder in proteins associated with neurodegenerative diseases. *Front Biosci (Landmark Ed), 14*, 5188-5238.

Uversky, V. N., Li, J., & Fink, A. L. (2001). Metal-triggered structural transformations, aggregation, and fibrillation of human alpha-synuclein. A possible molecular NK

between Parkinson's disease and heavy metal exposure. *J Biol Chem, 276*(47), 44284-44296. doi:10.1074/jbc.M105343200

Venkateshappa, C., Harish, G., Mahadevan, A., Srinivas Bharath, M. M., & Shankar, S. K. (2012). Elevated oxidative stress and decreased antioxidant function in the human hippocampus and frontal cortex with increasing age: implications for neurodegeneration in Alzheimer's disease. *Neurochem Res, 37*(8), 1601-1614. doi:10.1007/s11064-012-0755-8

Voges, D., Zwickl, P., & Baumeister, W. (1999). The 26S proteasome: a molecular machine designed for controlled proteolysis. *Annu Rev Biochem, 68*, 1015-1068. doi:10.1146/annurev.biochem.68.1.1015

Volpicelli-Daley, L. A., Luk, K. C., & Lee, V. M. (2014a). Addition of exogenous alpha-synuclein preformed fibrils to primary neuronal cultures to seed recruitment of endogenous alpha-synuclein to Lewy body and Lewy neurite-like aggregates. *Nat Protoc, 9*(9), 2135-2146. doi:10.1038/nprot.2014.143

Volpicelli-Daley, L. A., Luk, K. C., & Lee, V. M. (2014b). Addition of exogenous α-synuclein preformed fibrils to primary neuronal cultures to seed recruitment of endogenous α-synuclein to Lewy body and Lewy neurite-like aggregates. *Nat Protoc, 9*(9), 2135-2146. doi:10.1038/nprot.2014.143

Volpicelli-Daley, L. A., Luk, K. C., Patel, T. P., Tanik, S. A., Riddle, D. M., Stieber, A., . . . Lee, V. M. (2011a). Exogenous alpha-synuclein fibrils induce Lewy body pathology leading to synaptic dysfunction and neuron death. *Neuron, 72*(1), 57-71. doi:10.1016/j.neuron.2011.08.033

Volpicelli-Daley, L. A., Luk, K. C., Patel, T. P., Tanik, S. A., Riddle, D. M., Stieber, A., . . . Lee, V. M. (2011b). Exogenous α-synuclein fibrils induce Lewy body pathology leading to synaptic dysfunction and neuron death. *Neuron, 72*(1), 57-71. doi:10.1016/j.neuron.2011.08.033

Walker, L. C., & LeVine, H. (2000). The cerebral proteopathies: neurodegenerative disorders of protein conformation and assembly. *Mol Neurobiol, 21*(1-2), 83-95. doi:10.1385/MN:21:1-2:083

Walker, L. C., Levine, H., Mattson, M. P., & Jucker, M. (2006). Inducible proteopathies. *Trends Neurosci, 29*(8), 438-443. doi:10.1016/j.tins.2006.06.010

Wang, C., Sadovova, N., Hotchkiss, C., Fu, X., Scallet, A. C., Patterson, T. A., . . . Slikker, W. (2006). Blockade of N-methyl-D-aspartate receptors by ketamine produces loss of postnatal day 3 monkey frontal cortical neurons in culture. *Toxicol Sci, 91*(1), 192-201. doi:10.1093/toxsci/kfj144

Waxman, E. A., & Giasson, B. I. (2008). Specificity and regulation of casein kinase-mediated phosphorylation of alpha-synuclein. *J Neuropathol Exp Neurol, 67*(5), 402-416. doi:10.1097/NEN.0b013e31816fc995

Westermark, G. T., Johnson, K. H., & Westermark, P. (1999). Staining methods for identification of amyloid in tissue. *Methods Enzymol, 309*, 3-25.

Whetten-Goldstein, K., Sloan, F., Kulas, E., Cutson, T., & Schenkman, M. (1997). The burden of Parkinson's disease on society, family, and the individual. *J Am Geriatr Soc, 45*(7), 844-849.

Winslow, A. R., Chen, C. W., Corrochano, S., Acevedo-Arozena, A., Gordon, D. E., Peden, A. A., . . . Rubinsztein, D. C. (2010). alpha-Synuclein impairs macroautophagy: implications for Parkinson's disease. *J Cell Biol, 190*(6), 1023-1037. doi:10.1083/jcb.201003122

Wisen, S., Bertelsen, E. B., Thompson, A. D., Patury, S., Ung, P., Chang, L., . . . Gestwicki, J. E. (2010). Binding of a small molecule at a protein-protein interface regulates the chaperone activity of hsp70-hsp40. *ACS chemical biology, 5*(6), 611-622. doi:10.1021/cb1000422

Wu, M. L., Ho, Y. C., & Yet, S. F. (2011). A central role of heme oxygenase-1 in cardiovascular protection. *Antioxid Redox Signal, 15*(7), 1835-1846. doi:10.1089/ars.2010.3726

Xie, C., Markesbery, W. R., & Lovell, M. A. (2000). Survival of hippocampal and cortical neurons in a mixture of MEM+ and B27-supplemented neurobasal medium. *Free Radic Biol Med, 28*(5), 665-672.

Xie, W., Li, X., Li, C., Zhu, W., Jankovic, J., & Le, W. (2010). Proteasome inhibition modeling nigral neuron degeneration in Parkinson's disease. *J Neurochem, 115*(1), 188-199. doi:10.1111/j.1471-4159.2010.06914.x

Yang, Z., & Klionsky, D. J. (2010). Mammalian autophagy: core molecular machinery and signaling regulation. *Curr Opin Cell Biol, 22*(2), 124-131. doi:10.1016/j.ceb.2009.11.014

Yao, J., Irwin, R. W., Zhao, L., Nilsen, J., Hamilton, R. T., & Brinton, R. D. (2009). Mitochondrial bioenergetic deficit precedes Alzheimer's pathology in female mouse model of Alzheimer's disease. *Proc Natl Acad Sci U S A, 106*(34), 14670-14675. doi:10.1073/pnas.0903563106

Yoritaka, A., Hattori, N., Uchida, K., Tanaka, M., Stadtman, E. R., & Mizuno, Y. (1996). Immunohistochemical detection of 4-hydroxynonenal protein adducts in Parkinson disease. *Proc Natl Acad Sci U S A, 93*(7), 2696-2701.

Zarranz, J. J., Alegre, J., Gómez-Esteban, J. C., Lezcano, E., Ros, R., Ampuero, I., . . . de Yebenes, J. G. (2004). The new mutation, E46K, of alpha-synuclein causes Parkinson and Lewy body dementia. *Ann Neurol, 55*(2), 164-173. doi:10.1002/ana.10795

Zeevalk, G. D., Razmpour, R., & Bernard, L. P. (2008). Glutathione and Parkinson's disease: is this the elephant in the room? *Biomed Pharmacother, 62*(4), 236-249. doi:10.1016/j.biopha.2008.01.017

Zhang, W., Phillips, K., Wielgus, A. R., Liu, J., Albertini, A., Zucca, F. A., . . . Zecca, L. (2011). Neuromelanin activates microglia and induces degeneration of dopaminergic neurons: implications for progression of Parkinson's disease. *Neurotox Res, 19*(1), 63-72. doi:10.1007/s12640-009-9140-z

Appendix

Western blotting					
Primary Antibody	Source	Company	Catalog #	Lot #	Dilution
α-tubulin	Mouse	Sigma-Aldrich	T5168	078K4781, 103M4773V	1:100,000
β-actin	Rabbit	LI-COR Biosciences	926-42210	C00422-02	1:1000
β-actin	Mouse	Sigma-Aldrich	A5441	030M4788	1:40k-50k
Beclin 1	Rabbit	Santa Cruz	SC-11427	K2706	1:400
Catalase	Mouse	Sigma-Aldrich	C0979	CAT-505	1:5000
Ceruloplasmin	Mouse	BD Biosciences	611488	80753	1:1000
CHIP	Rabbit	Cell Signaling Technology	2080	2	1:1000
GAPDH	Rabbit	Cell Signaling Technology	2118S	8	1:5k-10k
GFAP	Rabbit	Dako	Z0334	20001046	1:5000
HO1 (Hsp32)	Rabbit	Sigma-Aldrich	H4535	081M1122	1:300
Hip	Rabbit	Cell Signaling Technology	2723	1	1:1000
Hop	Rabbit	Cell Signaling Technology	4464	1	1:1000
Hsc70	Rat	Enzo Life Sciences	ADI-SPA-815-D	04231339	1:1000
Hsp25	Goat	Santa Cruz	sc-1048	D0312	1:1000
Hsp40	Rabbit	Cell Signaling Technology	4868	2	1:1000
Hsp60	Rabbit	Cell Signaling Technology	4870	2	1:1000
Hsp70	Mouse	Calbiochem	386032	D00126860	1:1000
Hsp70	Rabbit	Millipore	AB9920	2278553	1:5000
K48-linked Ubiquitin	Rabbit	Millipore	05-1307	2299608	1:2000
LC3B	Rabbit	Cell Signaling Technology	2775	4	1:1000
MAP2	Mouse	Sigma-Aldrich	M9942	069K4770	1:1000
PA28	Rabbit	Calbiochem	539146	D00092184	1:1000
PA700 10B	Rabbit	Calbiochem	539147	D00110930	1:1000
Ubiquitin conjugated proteins	Mouse	Santa Cruz Biotechnology	Sc-8017	D0412	1:500

Immunocytochemistry					
Primary Antibody	Source	Company	Catalog #	Lot #	Dilution
β-tubulin III	Rabbit	Cell Signaling Technology	5568	4	1:1000
GFAP	Rabbit	Dako	Z0334	20001046	1:1000
Glutathione	Rabbit	Millipore	AB5010	NG1870405	1:300
MAP2	Mouse	Sigma-Aldrich	M9942	069K4770	1:2000
81A (α-Syn^{pSer129})	Mouse	Gift from Dr. Kelvin Luk and Dr. Virginia Lee from the University of Pennsylvania			1:2000
Synaptophysin	Rabbit	Millipore	04-1019	JBC179485	1:200

Secondary Antibody	Company	Catalog #	Immunocytochemistry Dilution	Western blotting Dilution
Donkey anti-Mouse 680	LI-COR	926-32222	1:2000	1:10K-20K
Goat anti-Mouse 680	LI-COR	926-32220	1:2000	1:10,000
Donkey anti-Mouse 800	LI-COR	926-32212	1:2000	1:10K-20K
Goat anti-Mouse 800	LI-COR	926-32210	1:2000	1:10K-20K
Donkey anti-Goat 800	LI-COR	926-32214	N/A	1:20,000
Donkey anti-Rabbit 680	LI-COR	926-32223	1:2000	1:10K-20K
Donkey anti-Rabbit 800	LI-COR	926-32213	1:2000	1:10K-20K
Goat anti-Rabbit 680	LI-COR	926-32211	1:2000	1:10,000
Donkey anti-Mouse 488	Life Technologies	A21202	1:1000	N/A
Goat anti-Mouse 488	Life Technologies	A11001	1:2000	N/A
Goat anti-Rabbit 555	Life Technologies	A21429	1:1000	N/A
Goat anti-Mouse 555	Life Technologies	A21424	1:1000	N/A